JOURNAL OF RESEARCH of the National Bureau of Standards—A. Physics and Chemistry
Vol. 75A, No. 5, September–October 1971

Energy Levels, Wave Functions, Dipole and Quadrupole Transitions of Trivalent Gadolinium Ions in Sapphire

Paul H. E. Meijer

Institute for Basic Standards, National Bureau of Standards, Washington, D.C. 20234
and
Physics Department, Catholic University of America, Washington, D.C. 20017

Jacques Lewiner

Ecole Superieure de Physiqué et de Chimie, Laboratoire d Electricité Générale, Paris 5^{e}

(March 22, 1971)

A computation is made of energy levels, wave functions and transition matrix elements of the Gd^{3+} ion in Al_2O_3. The crystal field parameters are taken from Geschwind and Remeika's paramagnetic resonance experiments. The transition probabilities are given for dipole radiation in three polarization directions. For ultrasonic work we give the real and imaginary parts of the five matrix elements of the quadrupole transition. From these one can easily deduce the transition probabilities in any given direction.

The magnetic field directions are described by the angles θ and ϕ, the polar and azimuthal angles with respect to the crystalline c axis. The values of θ go from 0 to $\pi/2$ in six steps and two values of π are chosen, 0 and 2 $\pi/3$ for which the variation is largest. The magnetic field strengths are from 0 to 0.6 tesla (6000 gauss); beyond this value the spin can be considered as "free." Some consideration is given to the analytical behavior of the energy versus field diagram for the direction $\theta=\phi=0$.

Key words: Corundum; spin Hamiltonian; energy levels of Gd^{+++} in Al_2O_3; quadrupole transitions; transition probabilities; ultrasonic (paramagnetic) resonance; ultrasonic transition probabilities; wave functions of Gd^{+++}

1. Introduction

After the successful use of tables [1][1,2] for Fe^{3+} doped Al_2O_3 to predict possible field directions and strengths for double resonance we decided to investigate the Gd^{3+} doped material. It appeared at first that there were some uncertainties with regard to the selection rules for ultrasonic transitions which, it turned out were unfounded. One can with good certainty predict that the "points in H-space" are double, i.e., electron and acoustic paramagnetic resonance is possible with the usual quadrupolar selection rules for ultrasonic resonance.

The acoustic transition probabilities, which are of quadrupolar nature, are tabulated in a new way. The previous method was found too restrictive if the sound wave were different from a simple plane wave in x, y, or z direction.

The spin Hamiltonian is described in section 3. The angle θ is varied for 0 to $\pi/2$ in steps $\pi/12$ and the angle $\varphi=0$ and $2\pi/3$. Only the positions of θ in which the energy levels change markedly with the change in φ are listed for both values of φ.

As before the number of values of the magnetic fields [the range and the steps] was a matter of compromise. The largest value is chosen such that one is in the free spin region. This value was divided into about 10 equal steps for preparation of the tables. In reality, finer steps were used in order to obtain a smooth curve near the noncrossing points.

[1] Figures in brackets indicate the literature references at the end of this paper.

[2] In this reference the following corrections should be made: The reference under figure 1 should be [11]: The $<\frac{1}{2}|-|\frac{1}{2}>$ element in the matrix on page 244 should start with $-8D/3$; The coefficients in the 1.6 and 2.5 wave functions should be a/C and a/D; The expression for $\Delta_{\pm}$ should end with $a^2/9$; The last two coefficients should be C^2 and D^2, rather than C and D, on the left hand side; On the right half top line of p. 245, δg and $d|$ should be replaced by dg and $\mathbf{d}$; In the first table, second line in the $(-1/2)$ column should be $-.999$; In the second table, first line in the $(-\frac{1}{2})$ column should be -1.000.

2. The Ion

The Gd^{3+} ion is in a $(f^7)\,^8S_{7/2}$ ground state. It has in common with the Fe^{3+} ion that the shell is half filled and that the orbital momentum is zero (according to Hund's rule). In such cases the crystal field splittings are relatively small, since the electric field acts on the ion through higher states with $J=7/2$ and $L \neq 0$, rather than on the ground state directly, according to the general ideas of angular momentum in atomic physics. The actual interaction is very complex; there are at least eight different mechanisms proposed. Wybourne [3] calculated all of these for the lanthanum ethylsulphate lattice and still could not obtain agreement with the experimental data. There is no explicit calculation of the Gd^{3+} wave functions in Al_2O_3 available in the literature as far as we are aware.

The electric field is produced by the O^--ions surrounding the Al sites (the Al sites are the places where the Gd ions go), and is rather strong. Geschwind and Remeika [4], whose parameters we use, report that the resulting splitting is the largest observed for this ion (1.24 cm^{-1}).

The two Al sites have C_3 point symmetry, one being rotated by $2\pi/3$ with respect to the other. Both share the same z axis, which we let coincide with the c axis of the crystal. Contrary to expectations, the two sites were not equally occupied. Since this was assumed by Geschwind and Remeika to be due to a "fluctuation" in the crystal during the growth, we omit consideration of this effect, but one should be aware of this possibility if one compares the transition probabilities with the experiment.

3. The Spin Hamiltonian

The spin Hamiltonian can be considered as a linear combination of Stevens' operators [5], using Hutchings' tables [2]. The general expression for the Hamiltonian in the absence of a magnetic field is:

$$\mathscr{H} = \sum_{n=1}^{2l} \sum_{m=-n}^{n} B_n^m O_n^m. \tag{1}$$

The factors α, β, γ in Stevens' paper are effectively 1, since we deal with an indirect interaction. General symmetry considerations as described in section 2 of reference [1] lead to the absence of certain coefficients B; those remaining in the case of f-electrons are:

$m=0$ with $n=2, 4, 6$

$m=3$ with $n=4, 6$ and $m=n=6$.

One can try to obtain some a priori ideas about the value of these coefficients either by making a point charge calculation, which is usually not very reliable, or by simply trying to establish which coefficients will be dominant on the basis of the description of the surroundings. The latter method was used for Fe^{3+} and we assumed a predominantly cylindrical field with a small cubic field added to it. The field of cubic symmetry was oriented in such a way that its body diagonal lay along the c axis. There is no compelling reason to consider the field from this point of view, although it was done in the Fe^{3+} case, since the large diameter of the Gd^{3+} ion may distort the lattice and hence displace the O^- ions. Since these ions are held responsible for creating the electric field, this will have influence on the crystal field parameters. Moreover, the assymmetric occupation mentioned above seems to suggest that once one site is occupied the other is avoided, which seems to confirm the distortion.

Also a look at the coefficients determined by Geschwind and Remeika shows no hint of a cubic field. According to the transforms in Hutchings' paper (ref. [2] eq 6.15) the ratio of the coefficients of O_4^0 to O_4^4 should be $1: -20\sqrt{2}$, and the ratios of the coefficients of O_6^0 to O_6^3 to O_6^6 should be $1: 35\sqrt{2}/4: 7718$. None of the values is in this neighborhood. (Compare table 1.)

TABLE 1. *Crystal field parameters of* Gd^{3+} *in* Al_2O_3 *in* cm^{-1} *according to Geschwind and Remeika (ref.* [4]).

$3B_2^0$	$= (1032.9 \pm 2.0)\,10^{-4}$
$60B_4^0$	$= (26.0 \pm 1.0)\,10^{-4}$
$1260B_6^0$	$= (1.0 \pm 0.5)\,10^{-4}$
$3B_4^3$	$= (18.3 \pm 1.0)\,10^{-4}$
$36B_6^3$	$< (1.0)\,10^{-4}$
$1260B_6^6$	$= (5.0 \pm 0.5)\,10^{-4}$
g	$= 1.9912 \pm 0.0005$

The most general way to study the wave functions is to use group theory [6, 7]. For trigonal symmetry and $J=7/2$ we find, using the double group, the representations Γ_4 and Γ_5 three times each and Γ_6 once. (Compare with appendix I.) Luttinger and Kittel [8] following Bethe [6], obtained this decomposition for cubic symmetry and found Γ_6, Γ_7, and Γ_8, two two-fold and one four-fold degenerate level. Since the two-fold levels in zero field are at comparable distance in our case, this shows again that there is no trace of "cubicity" in the crystal field parameters.

4. The Zero Field Matrix

The zero magnetic field matrix is given in eq (2) with $H_{ij}=H_{ji}$

	7/2	5/2	3/2	1/2	−1/2	−3/2	−5/2	−7/2
7/2	H_{11}	0	0	H_{14}	0	0	H_{17}	0
5/2	0	H_{22}	0	0	H_{25}	0	0	H_{28}
3/2	0	0	H_{33}	0	0	0	0	0
1/2	H_{41}	0	0	H_{44}	0	0	H_{47}	0
−1/2	0	H_{52}	0	0	H_{55}	0	0	H_{58}
−3/2	0	0	0	0	0	H_{66}	0	0
−5/2	H_{17}	0	0	H_{74}	0	0	H_{77}	0
−7/2	0	H_{28}	0	0	H_{85}	0	0	H_{88}

$$H_{11}=H_{88}=21B_2^0+420B_4^0+1260B_6^0=0.7413$$

$$H_{22}=H_{77}=3B_2^0-780B_4^0-6300B_6^0=0.6899\ 10^{-1}$$

$$H_{33}=H_{66}=-9B_2^0-180B_4^0+11340B_6^0=-0.3168$$

$$H_{44}=H_{55}=-15B_2^0+540B_4^0-6300B_6^0=-0.4936 \qquad (2)$$

$$-H_{14}=H_{58}=6\sqrt{35}B_4^3+72\sqrt{35}B_6^3=0.2165\ 10^{-1}$$

$$-H_{25}=H_{47}=12\sqrt{5}B_4^3-232\sqrt{5}B_6^3=0.1637\ 10^{-1}$$

$$H_{17}=H_{28}=360\sqrt{7}B_6^6=0.3780\ 10^{-3}.$$

If the magnetic field is along the z direction ($\theta=0$) the matrix has only diagonal Zeeman terms and it decomposes in two 1 by 1 and two 3 by 3 matrices. The singlet states are associated with $|\pm 3/2>$. The bases for the other two are formed by the 3 linear combinations of $|7/2>$, $|\frac{1}{2}>$ and $|-5/2>$ and the 3 linear combinations of $|-7/2>$, $|-\frac{1}{2}>$ and $|5/2>$.

From the diagonal matrix elements of the crystal field it is easy to see that the $|\pm\frac{1}{2}>$ levels lie lowest, the $|\pm 3/2>$ are next, followed by the $|\pm 5/2>$ and the $|\pm 7/2>$ are highest. The result is that the $|7/2>$, which goes up in energy if the magnetic field along the (positive) z axis is introduced, can be considered to be isolated for all practical purposes. Consequently we also can consider the $|\frac{1}{2}>$, $|-5/2>$ linear combinations as independent of $|7/2>$. If we look at the 3 combinations of $|-7/2>$, $|-\frac{1}{2}>$ and $|5/2>$ it is clear, from the small magnitude of the H_{28} matrix element that we can consider these as two linear combinations of $|-7/2>$ and $|-\frac{1}{2}>$ with a small admixture of $|5/2>$ and a $|5/2>$ with a small admixture of $|-7/2>$ and $|-\frac{1}{2}>$. In this way we reduced the diagonalization calculation, in first approximation, to a problem that requires not more than a 2 by 2 diagonalization.

Using arbitrary labels (b stands for $g\mu B$), we have:

$$E_1 = H_{11}+(7/2)b$$
$$2E_{2,3} = H_{55}+H_{88}-4b\pm[(H_{55}-H_{88}+3b)^2+4H_{58}^2]^{1/2}$$
$$2E_{4,5} = H_{44}+H_{77}-2b\pm[(H_{44}-H_{77}+3b)^2+4H_{47}^2]^{1/2}$$
$$E_6 = H_{77}-(5/2)b$$
$$E_7 = H_{33}+(3/2)b$$
$$E_8 = H_{66}-(3/2)b$$

for the approximate eigenvalues, and

$$|1>=|7/2>+\ \ldots$$
$$|2>=\cos\alpha_1|-7/2>+\sin\alpha_1|-\tfrac{1}{2}>+\epsilon_{26}|6>_0$$
$$|3>=-\sin\alpha_1|-7/2>+\cos\alpha_1|-\tfrac{1}{2}>+\epsilon_{36}|6>_0$$
$$|4>=\cos\alpha_2|-5/2>+\sin\alpha_2|\tfrac{1}{2}>+\ \ldots$$
$$|5>=-\sin\alpha_2|-5/2>+\cos\alpha_2|\tfrac{1}{2}>+\ \ldots$$
$$|6>=|5/2>+\epsilon_{62}|2>_0+\epsilon_{63}|3>_0$$
$$|7>=|3/2>$$
$$|8>=|-3/2>$$

$$tg(2\alpha_1)=2H_{58}/(H_{55}-H_{88}+3b)$$
$$tg(2\alpha_2)+2H_{47}/(H_{44}-H_{77}+3b)$$

for the eigenfunctions. We inserted prematurely the admixtures occurring when the O_6^6 matrix elements are *not* ignored (see below).

The conclusions with respect to the energy level diagram for $\theta=0$ are the following. If the spin were free the arrangement of the zero magnetic field splitting is such that there are 12 potential crossing points (compare fig. 1). The functions $|7>$ and $|8>$, associated with $m=\pm 3/2$, will cross all other levels. Since they behave like free spins, the energy will be exactly a linear function of the field. The members of the $|1>$,

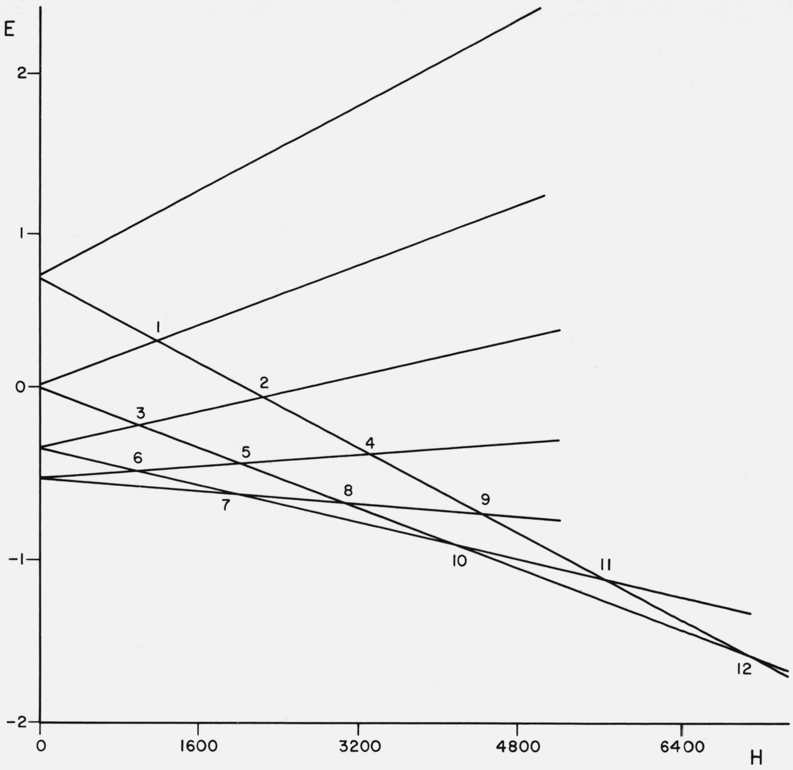

FIGURE 1. *Splitting of the levels on the basis of diagonal elements only.*

The crossing points 1–12 are discussed in the text.

$|4>$, $|5>$ combinations will cross the members of the $|2>$, $|3>$, $|6>$ set, in three points. The remaining three points are of the noncrossing type. Closest to the origin and highest in energy is the $|5/2>$, $|-7/2>$ intersection. This is associated with the small B_6^6 parameter, hence a "weak' noncrossing point. Next, in field, comes the $|1/2>$, $|-5/2>$ noncrossing point, which is associated with a relatively strong repulsion. Finally we have the $|-1/2>$, $|-7/2>$ noncrossing point which, although related to the stronger off-diagonal parameters B_4^3, is actually much less strongly repelled than is the case for the $|1/2>$, $|-5/2>$ interaction.

In these noncrossing points α goes from almost 0 to almost $\pi/2$. One can see from the first set of tables that the admixture angle α_1 in $|2>$ corresponds to only 0.08 radians at zero field and remains that way till the intersection with $|7/2>$ is approached. This means that the wave functions $|1>$ to $|4>$ are almost pure except in the crossing points, which facilitates the consideration of the intersections we left out in first approximation.

Returning to eq (2) the wave functions $|2>$, $|3>$ and $|6>$ have small admixtures indicated by ϵ_{ij}. The subscript 0 refers to the zeroth order wave functions. We ignore the fact that the other coefficients in the linear combination will slightly diminish when these admixtures are taken into account. The factors ϵ can be calculated either by perturbation theory or, if the main part of the wave function is rather pure, by a 2 by 2 diagonalization. Since (almost) all intersections are separated we can use the last method to determine the ϵ's.

To sum up: since each noncrossing is reasonably separated from the others, each can be calculated separately. The distance between the levels at such a point is determined by one particular off diagonal element. The repulsion is strongest at the point where 1/2 and $-5/2$ approach each other.

When the field is tilted ($\theta \neq 0$) the general tendency for the noncrossing points is to increase the gap. See figure 2. The crossing points become now noncrossing points also. If θ is about 45°, little is left of the original pattern. At this and higher angles the tables are most valuable.

The last figure of figure 2 ($\theta = \pi/2$) shows an interesting behavior. The levels for the 7/2 Kramers doublet "stick together" over a long distance in the H-direction. This is also true, but to a lesser degree for the 5/2 Kramers doublet, but barely for the $\pm 3/2$ combination and not at all for the $\pm 1/2$ level-pair. This behavior can be traced to general properties of the crystal field matrix.

If we ignore the off diagonal elements in eq (2) for the moment and if we imagine the magnetic field terms inserted (which lie on two lines parallel to and one step removed from the main diagonal) then 6th order perturbation theory is needed to remove the degeneracy between $+7/2$ and $-7/2$, 4th order for the $\pm 5/2$ levels, and 2nd order for the $\pm 3/2$ pair. The $\pm 1/2$ pair

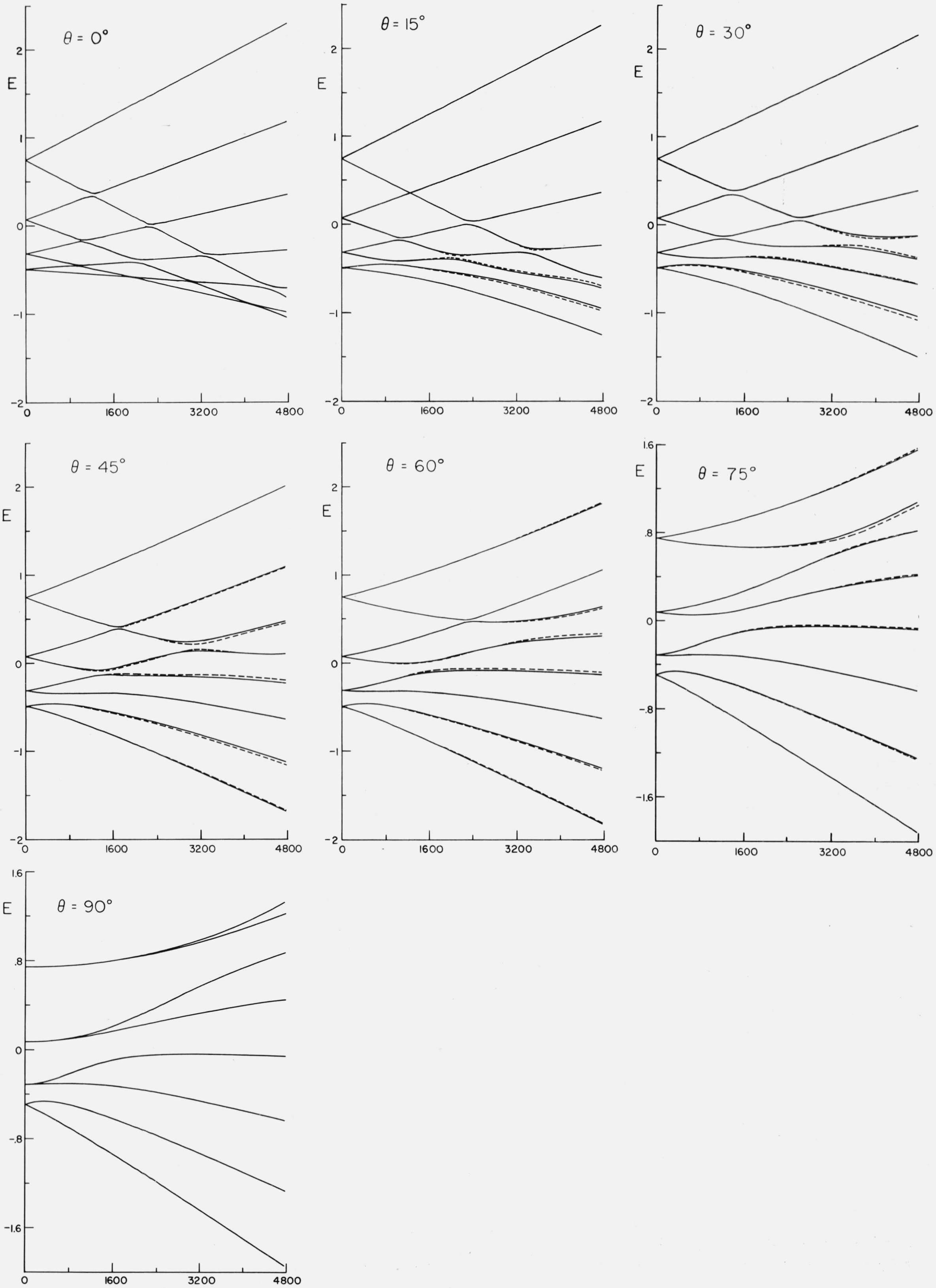

FIGURE 2. *Plot of the energy levels of* Gd^{3+} *in* Al_2O_3.

The solid line corresponds to $\varphi=0$, the dotted line to $\varphi=60°$. The energy is in cm^{-1} and the magnetic field in gauss (10^{-4} tesla). [Note that the scale for $\theta=75, 90°$ is slightly larger.]

429-270 O - 71 - 7

is degenerate and directly connected via a magnetic field term, hence acts like a linear Kramers term. A rough estimate gives that a field of about 10^3 to 10^4 G is needed to obtain a relative splitting of one percent in the 7/2 levels.

The off diagonal elements make it possible to obtain a splitting with lower order perturbation theory: a third order process via H_{14} and H_{47} and a magnetic field term or a second order process via H_{17} and magnetic field term. Each case is to be supplemented by similar terms. The weakness of the H_{17} coupling seems to make the third order process more favorable but symmetry considerations [4] show that the H_{14} etc. matrix elements are noneffective at $\theta=90°$. an estimate gives the second order process as requiring about the same field strengths to obtain a 1 percent relative energy difference.

In the range between 1000 and 3000 G all levels except the two lowest ran more or less horizontally for large θ. Hence it is possible to use this region in devices where insensitivity to the field strength is required.

The near degeneracy of the top levels in the $\theta=\pi/2$ figure could be used to study spin cross-relaxation as a function of the magnetic field strength: the field is initially set at a value of about 5000 G to separate the 7/2 levels by more than the line-width and one of the levels is saturated with respect to one of the lower levels by means of a pulse. Lowering the field to the range of coalescence (between 0 and 3000 G) and keeping it there during a period of time long (short) compared to the cross-relaxation time will (will not) allow transfer of energy via a phonon mode from one component of the Kramers doublet to another. When the field is quickly restored to its original value a signal of lower power is used to detect the occupation in the level. In order to know the amount of decay of occupation of the level through spin-lattice relaxation a control experiment has to be used. This consists of a saturation pulse followed by a detection pulse at the same time interval as the previous experiment without using the field cycle.

5. Transition Probabilities

The transition probabilities are calculated for all 28 pairs of wave functions. See table 1. For each pair the energy difference is indicated in GHz. First the matrix element of the dipolar transition is calculated and the absolute square is determined for each polarization direction.

These quantities are divided by $\frac{1}{4}(S+\frac{1}{2})^2$, the largest value the matrix elements squared can ever have for odd spin. The transition probabilities thus normalized were multiplied by 10^4 and written as properly rounded off integers.

Hence the tables give, for the dipole parts:

$$(P_\alpha)_{ij}=10^4\frac{|<i|S_\alpha|j>^2}{\frac{1}{4}(S+\frac{1}{2})^2}\qquad \alpha=x,y,z$$

and $S=7/2$.

For the quadrupole transition the real and imaginary parts of each of the symmetrized matrix elements $<i|(S_\alpha S_\beta)|j>$ are given rather than their absolute values. Since only five are linearly independent it is more convenient to use $x\pm iy$, z components rather then Cartesian components. In order to obtain the transition probability in a certain direction given by the polar coordinates θ_p, φ_p (the index p stands for polarization, in order to distinguish them from the polar angles used for the orientation of the magnetic field) one has to form the absolute square:

$$P_{\text{quad}}=10^{-8}|\sum_{\alpha\beta}P_{\alpha\beta}Y_1^\alpha Y_1^\beta|^2\qquad (\alpha,\beta=1,0,-1)$$

where $Y_1^z=\cos\theta_p$; $Y_1^\pm=\sin\theta_p\exp(\pm i\varphi_p)$ and $P_{\alpha\beta}$ is given by:

$$(P_{\alpha\beta})_{ij}=10^4\frac{\langle i|\{S_\alpha S_\beta\}|j\rangle}{(S+\frac{1}{2})\sqrt{(S+1\frac{1}{2})(S-\frac{1}{2})}}.$$

This quantity is also reduced by its maximum value (for odd spin) and for convenience written as an integer between 10^4 and zero. The curly brackets indicate that the expression has been symmetrized for $\alpha\neq\beta$:

$$\{S_\alpha S_\beta\}=(S_\alpha S_\beta+S_\beta S_\alpha)/2.$$

We thank J. Feeney for computer generated figures of the energy versus the field, and D. Martin for the drawing of the figures.

6. Appendix I

The trigonal double group has three extra irreducible representations compared to the single group

	E,R′	C_3,C_3'	D_2,D_2'
Γ_4	±1	±1	$\pm i$
Γ_5	±1	±1	$\mp i$
Γ_6	±2	∓1	0

The classes of elements E, C_3, D_2 correspond to the unit element, the two 3-fold rotations and the three 2-fold rotations. The elements with the prime are obtained when the rotation is pursued over an additional 360°; they correspond to the lower sign. Except for the unit element, there is some arbitrariness as to which are rotations less than 360° and which are more than 360°, depending on the direction of rotation (in Bethe's article [6] C corresponds to χ'' and C' to χ'; in Heine's work [9] C corresponds to AB, and C' to $\overline{AB}$.) The trigonal symmetry is the only case in which one deals with a one-dimensional double group representation;

TABLE 1. *Energy level differences, wave functions and transition probabilities for angles and field strengths indicated*

	ΔE	P_x	P_y	P_z	P_{11}		P_{10}		P_{00}		P_{-10}		P_{-1-1}	
	$\theta=0$ $\varphi=0$ H=0													
1–2	0.26804×10^{-04}	5328	5328	0	0	0	0	0	0	0	179	0	0	0
1–3	$-0.53255\times10^{+01}$	5017	5017	0	29	0	0	0	0	0	521	0	0	0
1–4	$-0.53255\times10^{+01}$	3	3	0	2777	0	0	0	0	0	14	0	0	0
1–5	$-0.16905\times10^{+02}$	2	2	0	0	0	−24	0	0	0	−8	0	−2405	0
1–6	$-0.16905\times10^{+02}$	0	0	10	0	0	0	0	−30	0	0	0	0	0
1–7	$-0.37059\times10^{+02}$	0	0	4	0	0	0	0	38	0	0	0	0	0
1–8	$-0.37059\times10^{+02}$	0	0	0	0	0	41	0	0	0	20	0	0	0
2–3	$-0.53255\times10^{+01}$	3	3	0	0	0	36	0	0	0	23	0	2777	0
2–4	$-0.53255\times10^{+01}$	5017	5017	0	0	0	−693	0	0	0	−173	0	−28	0
2–5	$-0.16905\times10^{+02}$	0	0	10	0	0	0	0	−30	0	0	0	0	0
2–6	$-0.16905\times10^{+02}$	2	2	0	2406	0	0	0	0	0	16	0	0	0
2–7	$-0.37059\times10^{+02}$	0	0	0	0	0	0	0	0	0	21	0	0	0
2–8	$-0.37059\times10^{+02}$	0	0	4	0	0	0	0	−37	0	0	0	0	0
3–4	0.0	0	0	0	0	0	0	0	0	0	0	0	0	0
3–5	$-0.11579\times10^{+02}$	4015	4015	0	81	0	0	0	0	0	−775	0	0	0
3–6	$-0.11579\times10^{+02}$	4	4	0	0	0	20	0	0	0	15	0	1	0
3–7	$-0.31733\times10^{+02}$	2	2	0	0	0	−11	0	0	0	−8	0	1644	0
3–8	$-0.31733\times10^{+02}$	0	0	0	49	0	0	0	0	0	0	0	0	0
4–5	$-0.11579\times10^{+02}$	4	4	0	0	0	0	0	0	0	−4	0	0	0
4–6	$-0.11579\times10^{+02}$	4015	4015	0	0	0	−1241	0	0	0	−465	0	81	0
4–7	$-0.31733\times10^{+02}$	0	0	0	0	0	0	0	0	0	0	0	−48	0
4–8	$-0.31733\times10^{+02}$	2	2	0	1644	0	0	0	0	0	−2	0	0	0
5–6	0.0	0	0	0	0	0	0	0	0	0	0	0	0	0
5–7	$-0.20154\times10^{+02}$	2345	2345	0	42	0	0	0	0	0	−829	0	0	0
5–8	$-0.20154\times10^{+02}$	0	0	0	0	0	0	0	0	0	0	0	0	0
6–7	$-0.20154\times10^{+02}$	0	0	0	0	0	0	0	1	0	0	0	0	0
6–8	$-0.20154\times10^{+02}$	2345	2345	0	0	0	−1422	0	0	0	−592	0	42	0
7–8	0.55395×10^{-04}	0	0	0	0	0	0	0	0	0	0	0	0	0
	$\theta=0$ $\varphi=0$ H=800													
1–2	$-0.22236\times10^{+01}$	5325	19	0	1169	0	18	0	0	0	87	0	0	0
1–3	$-0.30912\times10^{+01}$	5018	5018	0	0	0	−693	0	0	0	−173	0	1224	0
1–4	$-0.97895\times10^{+01}$	2	2	0	0	0	26	0	0	0	16	0	1445	0
1–5	$-0.12447\times10^{+02}$	6	5335	0	1267	0	−522	0	0	0	−63	0	0	0
1–6	$-0.23598\times10^{+02}$	0	0	5	15	0	0	0	−21	0	0	0	15	0
1–7	$-0.30361\times10^{+02}$	0	0	6	966	0	0	0	−45	0	0	0	−931	0
1–8	$-0.45986\times10^{+02}$	0	0	0	0	0	8	0	0	0	15	0	0	0
2–3	$-0.86756\times10^{+00}$	9	9	0	2775	0	0	0	0	0	−220	0	0	0
2–4	$-0.75659\times10^{+01}$	5010	5010	0	24	0	0	0	0	0	280	0	0	0
2–5	$-0.10224\times10^{+02}$	0	0	28	1470	0	0	0	−51	0	0	0	−591	0
2–6	$-0.21374\times10^{+02}$	1	1	0	0	0	−20	0	0	0	−14	0	−1266	0
2–7	$-0.28138\times10^{+02}$	1	1	0	0	0	68	0	0	0	465	0	24	0
2–8	$-0.43763\times10^{+02}$	0	0	3	0	0	0	0	32	0	0	0	−10	0
3–4	$-0.66983\times10^{+01}$	0	0	0	0	0	0	0	0	0	0	0	0	0
3–5	$-0.93560\times10^{+01}$	4009	22	0	0	0	−643	0	0	0	−249	0	134	0
3–6	$-0.20506\times10^{+02}$	2	2	0	13	0	0	0	0	0	−3	0	0	0
3–7	$-0.27270\times10^{+02}$	2	2	0	870	0	0	0	0	0	−3	0	0	0
3–8	$-0.42895\times10^{+02}$	0	0	0	0	0	7	0	0	0	0	0	−40	0
4–5	$-0.26577\times10^{+01}$	12	4994	0	0	0	191	0	0	0	−246	0	1	0
4–6	$-0.13808\times10^{+02}$	4016	4016	0	43	0	0	0	0	0	−776	0	0	0
4–7	$-0.20572\times10^{+02}$	0	0	0	−887	0	0	0	0	0	0	0	0	0
4–8	$-0.36197\times10^{+02}$	1	1	0	0	0	−17	0	0	0	−7	0	1644	0
5–6	$-0.11150\times10^{+02}$	0	0	0	0	0	0	0	0	0	−5	0	1169	0
5–7	$-0.17914\times10^{+02}$	2345	2345	0	0	0	−1421	0	0	0	−977	0	28	0
5–8	$-0.33539\times10^{+02}$	0	0	0	0	0	0	0	1	0	0	0	−12	0
6–7	$-0.67638\times10^{+01}$	0	0	0	11	0	0	0	0	0	0	0	−9	0
6–8	$-0.22389\times10^{+02}$	2344	2344	0	36	0	0	0	0	0	−829	0	0	0
7–8	$-0.15625\times10^{+02}$	0	0	0	0	0	−4	0	0	0	0	0	0	0

TABLE 1. *Energy level differences, wave functions and transition probabilities for angles and field strengths indicated*—Continued

	ΔE	P_x	P_y	P_z	P_{11}		P_{10}		P_{00}		P_{-10}		P_{-1-1}	
					$\theta=0$		$\varphi=0$		H=1600					
1–2	$-0.86008\times10^{+00}$	4995	4995	0	0	0	−693	0	0	0	−173	0	−44	0
1–3	$-0.44150\times10^{+01}$	5278	5278	0	−290	0	0	0	0	0	176	0	0	0
1–4	$-0.80276\times10^{+01}$	76	76	0	2388	0	0	0	0	0	41	0	0	0
1–5	$-0.14257\times10^{+02}$	1	1	0	0	0	20	0	0	0	13	0	2778	0
1–6	$-0.23669\times10^{+02}$	0	0	9	0	0	0	0	59	0	0	0	0	0
1–7	$-0.30295\times10^{+02}$	0	0	3	0	0	0	0	−16	0	0	0	0	0
1–8	$-0.54918\times10^{+02}$	0	0	0	0	0	0	0	0	0	11	0	0	0
2–3	$-0.35549\times10^{+01}$	76	76	0	0	0	170	0	0	0	64	0	2752	0
2–4	$-0.71675\times10^{+01}$	3942	3942	0	0	0	−1230	0	0	0	−461	0	381	0
2–5	$-0.13397\times10^{+02}$	0	0	0	0	0	0	0	0	0	0	0	0	0
2–6	$-0.22809\times10^{+02}$	4	4	0	−1642	0	0	0	0	0	5	0	0	0
2–7	$-0.29435\times10^{+02}$	1	1	0	0	0	0	0	0	0	−2	0	0	0
2–8	$-0.54058\times10^{+02}$	0	0	0	0	0	0	0	0	0	0	0	−35	0
3–4	$-0.36126\times10^{+01}$	0	0	223	0	0	0	0	−145	0	0	0	0	0
3–5	$-0.98417\times10^{+01}$	4927	4927	0	21	0	0	0	0	0	516	0	0	0
3–6	$-0.19254\times10^{+02}$	22	22	0	0	0	−194	0	0	0	−85	0	8	0
3–7	$-0.25880\times10^{+02}$	0	0	0	0	0	−17	0	0	0	−7	0	−2388	0
3–8	$-0.50503\times10^{+02}$	0	0	2	0	0	0	0	27	0	0	0	0	0
4–5	$-0.62291\times10^{+01}$	94	94	0	3	0	0	0	0	0	71	0	0	0
4–6	$-0.15641\times10^{+02}$	2324	2324	0	0	0	1410	0	0	0	587	0	−65	0
4–7	$-0.22268\times10^{+02}$	0	0	0	0	0	−1	0	0	0	0	0	−290	0
4–8	$-0.46890\times10^{+02}$	0	0	0	0	0	0	0	4	0	0	0	0	0
5–6	$-0.94120\times10^{+01}$	0	0	0	−75	0	0	0	0	0	0	0	0	0
5–7	$-0.16039\times10^{+02}$	4017	4017	0	45	0	0	0	0	0	−776	0	0	0
5–8	$-0.40661\times10^{+02}$	1	1	0	0	0	−8	0	0	0	−6	0	1644	0
6–7	$-0.66266\times10^{+01}$	0	0	0	0	0	0	0	1	0	0	0	0	0
6–8	$-0.31249\times10^{+02}$	0	0	0	0	0	0	0	0	0	0	0	0	0
7–8	$-0.24623\times10^{+02}$	2344	2344	0	31	0	0	0	0	0	−829	0	0	0
					$\theta=0$		$\varphi=0$		H=2400					
1–2	$-0.13671\times10^{+01}$	4992	4992	0	−62	0	0	0	0	0	−173	0	0	0
1–3	$-0.47937\times10^{+01}$	3931	3931	0	0	0	1229	0	0	0	461	0	409	0
1–4	$-0.81625\times10^{+01}$	87	87	0	0	0	−182	0	0	0	−68	0	2748	0
1–5	$-0.18350\times10^{+02}$	7	7	0	−1642	0	0	0	0	0	7	0	0	0
1–6	$-0.20095\times10^{+02}$	0	0	0	0	0	0	0	0	0	0	0	0	0
1–7	$-0.38365\times10^{+02}$	1	1	0	0	0	0	0	0	0	−1	0	0	0
1–8	$-0.65221\times10^{+02}$	0	0	0	0	0	0	0	0	0	0	0	−31	0
2–3	$-0.34266\times10^{+01}$	159	159	0	−2373	0	0	0	0	0	4	0	0	0
2–4	$-0.67954\times10^{+01}$	5193	5193	0	386	0	0	0	0	0	181	0	0	0
2–5	$-0.16983\times10^{+02}$	0	0	18	0	0	0	0	82	0	0	0	0	0
2–6	$-0.18728\times10^{+02}$	1	1	0	0	0	16	0	0	0	10	0	2777	0
2–7	$-0.36998\times10^{+02}$	0	0	2	0	0	0	0	−13	0	0	0	0	0
2–8	$-0.63854\times10^{+02}$	0	0	0	0	0	0	0	0	0	9	0	0	0
3–4	$-0.33688\times10^{+01}$	0	0	256	0	0	0	0	−156	0	0	0	0	0
3–5	$-0.13556\times10^{+02}$	2250	2250	0	0	0	−1406	0	0	0	−586	0	91	0
3–6	$-0.15301\times10^{+02}$	109	109	0	3	0	0	0	0	0	77	0	0	0
3–7	$-0.33571\times10^{+02}$	0	0	0	0	0	−2	0	0	0	0	0	−385	0
3–8	$-0.60427\times10^{+02}$	0	0	0	0	0	0	0	4	0	0	0	0	0
4–5	$-0.10188\times10^{+02}$	98	98	0	0	0	210	0	0	0	81	0	−13	0
4–6	$-0.11932\times10^{+02}$	4913	4913	0	18	0	0	0	0	0	515	0	0	0
4–7	$-0.30202\times10^{+02}$	0	0	0	0	0	−15	0	0	0	−6	0	−2374	0
4–8	$-0.57058\times10^{+02}$	0	0	2	0	0	0	0	24	0	0	0	0	0
5–6	$-0.17448\times10^{+01}$	0	0	0	0	0	0	0	0	0	0	0	−105	0
5–7	$-0.20015\times10^{+02}$	0	0	0	0	0	0	0	1	0	0	0	0	0
5–8	$-0.46871\times10^{+02}$	0	0	0	0	0	0	0	0	0	0	0	0	0
6–7	$-0.18270\times10^{+02}$	4017	4017	0	37	0	0	0	0	0	−776	0	0	0
6–8	$-0.45126\times10^{+02}$	1	1	0	0	0	−7	0	0	0	−5	0	1644	0
7–8	$-0.26856\times10^{+02}$	2344	2344	0	27	0	0	0	0	0	−829	0	0	0

TABLE 1. *Energy level differences, wave functions and transition probabilities for angles and field strengths indicated*—Continued

	ΔE	P_x	P_y	P_z	$P_{1\,1}$		$P_{1\,0}$		$P_{0\,0}$		$P_{-1\,0}$		$P_{-1\,-1}$	
					$\theta=0$		$\varphi=0$		H=3200					
1–2	$-0.26098\times10^{+01}$	3990	3990	0	0	0	1241	0	0	0	465	0	137	0
1–3	$-0.35847\times10^{+01}$	4999	4999	0	−109	0	0	0	0	0	−172	0	0	0
1–4	$-0.12580\times10^{+02}$	10	10	0	0	0	−60	0	0	0	−22	0	2775	0
1–5	$-0.13901\times10^{+02}$	23	23	0	−1639	0	0	0	0	0	12	0	0	0
1–6	$-0.26793\times10^{+02}$	0	0	0	0	0	0	0	0	0	0	0	0	0
1–7	$-0.47295\times10^{+02}$	1	1	0	0	0	0	0	0	0	−1	0	0	0
1–8	$-0.76384\times10^{+02}$	0	0	0	0	0	0	0	0	0	0	0	−27	0
2–3	$-0.97490\times10^{+00}$	47	47	0	0	0	−94	0	0	0	−30	0	−2396	0
2–4	$-0.99701\times10^{+01}$	0	0	29	0	0	0	0	−52	0	0	0	0	0
2–5	$-0.11291\times10^{+02}$	2304	2304	0	0	0	−1418	0	0	0	−591	0	161	0
2–6	$-0.24183\times10^{+02}$	12	12	0	1	0	0	0	0	0	26	0	0	0
2–7	$-0.44685\times10^{+02}$	0	0	0	0	0	0	0	0	0	0	0	−145	0
2–8	$-0.73774\times10^{+02}$	0	0	0	0	0	0	0	1	0	0	0	0	0
3–4	$-0.89952\times10^{+01}$	5296	5296	0	145	0	0	0	0	0	181	0	0	0
3–5	$-0.10316\times10^{+02}$	0	0	54	0	0	0	0	144	0	0	0	0	0
3–6	$-0.23208\times10^{+02}$	1	1	0	0	0	14	0	0	0	9	0	2772	0
3–7	$-0.43710\times10^{+02}$	0	0	2	0	0	0	0	−11	0	0	0	0	0
3–8	$-0.72799\times10^{+02}$	0	0	0	0	0	0	0	0	0	7	0	0	0
4–5	$-0.13209\times10^{+01}$	53	53	0	0	0	70	0	0	0	17	0	−8	0
4–6	$-0.14213\times10^{+02}$	5010	5010	0	17	0	0	0	0	0	520	0	0	0
4–7	$-0.34715\times10^{+02}$	0	0	0	0	0	−13	0	0	0	−5	0	−2401	0
4–8	$-0.63804\times10^{+02}$	0	0	1	0	0	0	0	22	0	0	0	0	0
5–6	$-0.12892\times10^{+02}$	0	0	0	0	0	0	0	0	0	0	0	−186	0
5–7	$-0.33394\times10^{+02}$	0	0	0	0	0	0	0	1	0	0	0	0	0
5–8	$-0.62483\times10^{+02}$	0	0	0	0	0	0	0	0	0	0	0	0	0
6–7	$-0.20502\times10^{+02}$	4017	4017	0	31	0	0	0	0	0	−776	0	0	0
6–8	$-0.49590\times10^{+02}$	1	1	0	0	0	−6	0	0	0	−4	0	1644	0
7–8	$-0.29089\times10^{+02}$	2344	2344	0	24	0	0	0	0	0	−829	0	0	0
					$\theta=0$		$\varphi=0$		H=4000					
1–2	$-0.38677\times10^{+00}$	3997	3997	0	0	0	1242	0	0	0	466	0	82	0
1–3	$-0.57437\times10^{+01}$	4868	4868	0	−287	0	0	0	0	0	−170	0	0	0
1–4	$-0.95097\times10^{+01}$	154	154	0	−1618	0	0	0	0	0	30	0	0	0
1–5	$-0.17036\times10^{+02}$	3	3	0	0	0	−36	0	0	0	−13	0	2778	0
1–6	$-0.33491\times10^{+02}$	0	0	0	0	0	0	0	0	0	0	0	0	0
1–7	$-0.56225\times10^{+02}$	0	0	0	0	0	0	0	0	0	−1	0	0	0
1–8	$-0.87547\times10^{+02}$	0	0	0	0	0	0	0	0	0	0	0	−25	0
2–3	$-0.53569\times10^{+01}$	113	113	0	0	0	−248	0	0	0	−98	0	−2367	0
2–4	$-0.91229\times10^{+01}$	2234	2234	0	0	0	−1400	0	0	0	−584	0	422	0
2–5	$-0.16650\times10^{+02}$	0	0	10	0	0	0	0	−31	0	0	0	0	0
2–6	$-0.33105\times10^{+02}$	4	4	0	0	0	0	0	0	0	15	0	0	0
2–7	$-0.55838\times10^{+02}$	0	0	0	0	0	0	0	0	0	0	0	−93	0
2–8	$-0.87160\times10^{+02}$	0	0	0	0	0	0	0	1	0	0	0	0	0
3–4	$-0.37660\times10^{+01}$	0	0	359	0	0	0	0	371	0	0	0	0	0
3–5	$-0.11293\times10^{+02}$	5152	5152	0	93	0	0	0	0	0	180	0	0	0
3–6	$-0.27748\times10^{+02}$	0	0	0	0	0	12	0	0	0	7	0	2736	0
3–7	$-0.50481\times10^{+02}$	0	0	1	0	0	0	0	−9	0	0	0	0	0
3–8	$-0.81803\times10^{+02}$	0	0	0	0	0	0	0	0	0	6	0	0	0
4–5	$-0.75266\times10^{+01}$	202	202	0	−15	0	0	0	0	0	−13	0	0	0
4–6	$-0.23982\times10^{+02}$	0	0	0	0	0	−1	0	0	0	0	0	−486	0
4–7	$-0.46715\times10^{+02}$	0	0	0	0	0	0	0	2	0	0	0	0	0
4–8	$-0.78037\times10^{+02}$	0	0	0	0	0	0	0	0	0	0	0	0	0
5–6	$-0.16455\times10^{+02}$	5018	5018	0	15	0	0	0	0	0	521	0	0	0
5–7	$-0.39189\times10^{+02}$	0	0	0	0	0	−12	0	0	0	−5	0	−2404	0
5–8	$-0.70511\times10^{+02}$	0	0	1	0	0	0	0	20	0	0	0	0	0
6–7	$-0.22734\times10^{+02}$	4018	4018	0	27	0	0	0	0	0	−776	0	0	0
6–8	$-0.54055\times10^{+02}$	0	0	0	0	0	−5	0	0	0	−4	0	1644	0
7–8	$-0.31322\times10^{+02}$	2344	2344	0	22	0	0	0	0	0	−829	0	0	0

TABLE 1. *Energy level differences, wave functions and transition probabilities for angles and field strengths indicated*—Continued

	ΔE	P_x	P_y	P_z	P_{11}		P_{10}		P_{00}		P_{-10}		P_{-1-1}	
							$\theta=0$ $\varphi=0$ H=4800							
1–2	$-0.18418\times10^{+01}$	3998	3998	0	58	0	0	0	0	0	466	0	0	0
1–3	$-0.66424\times10^{+01}$	2283	2283	0	0	0	−1396	0	0	0	−580	0	−464	0
1–4	$-0.10062\times10^{+02}$	62	62	0	0	0	−274	0	0	0	−117	0	2360	0
1–5	$-0.23340\times10^{+02}$	0	0	5	0	0	0	0	−22	0	0	0	0	0
1–6	$-0.42032\times10^{+02}$	2	2	0	0	0	0	0	0	0	11	0	0	0
1–7	$-0.66997\times10^{+02}$	0	0	0	0	0	0	0	0	0	0	0	−70	0
1–8	$-0.10055\times10^{+03}$	0	0	0	0	0	0	0	0	0	0	0	0	0
2–3	$-0.48006\times10^{+01}$	188	188	0	−1612	0	0	0	0	0	−33	0	0	0
2–4	$-0.82206\times10^{+01}$	4834	4834	0	−317	0	0	0	0	0	170	0	0	0
2–5	$-0.21498\times10^{+02}$	2	2	0	0	0	−25	0	0	0	−9	0	2778	0
2–6	$-0.40190\times10^{+02}$	0	0	0	0	0	0	0	0	0	0	0	0	0
2–7	$-0.65156\times10^{+02}$	0	0	0	0	0	0	0	0	0	0	0	0	0
2–8	$-0.98710\times10^{+02}$	0	0	0	0	0	0	0	0	0	0	0	−22	0
3–4	$-0.34200\times10^{+01}$	0	0	434	0	0	0	0	409	0	0	0	0	0
3–5	$-0.16698\times10^{+02}$	173	173	0	14	0	0	0	0	0	47	0	0	0
3–6	$-0.35389\times10^{+02}$	0	0	0	0	0	2	0	0	0	1	0	538	0
3–7	$-0.60355\times10^{+02}$	0	0	0	0	0	0	0	−1	0	0	0	0	0
3–8	$-0.93910\times10^{+02}$	0	0	0	0	0	0	0	0	0	1	0	0	0
4–5	$-0.13278\times10^{+02}$	5182	5182	0	−69	0	0	0	0	0	−173	0	0	0
4–6	$-0.31969\times10^{+02}$	0	0	0	0	0	−9	0	0	0	−6	0	−2725	0
4–7	$-0.56935\times10^{+02}$	0	0	1	0	0	0	0	9	0	0	0	0	0
4–8	$-0.90490\times10^{+02}$	0	0	0	0	0	0	0	0	0	−5	0	0	0
5–6	$-0.18692\times10^{+02}$	5020	5020	0	14	0	0	0	0	0	521	0	0	0
5–7	$-0.43657\times10^{+02}$	0	0	0	0	0	−11	0	0	0	−4	0	−2404	0
5–8	$-0.77212\times10^{+02}$	0	0	1	0	0	0	0	18	0	0	0	0	0
6–7	$-0.24966\times10^{+02}$	4018	4018	0	24	0	0	0	0	0	−776	0	0	0
6–8	$-0.58520\times10^{+02}$	0	0	0	0	0	−5	0	0	0	−3	0	1644	0
7–8	$-0.33555\times10^{+02}$	2344	2344	0	20	0	0	0	0	0	−829	0	0	0
							$\theta=15$ $\varphi=0$ H=800							
1–2	$-0.31424\times10^{+01}$	818	6825	242	410	0	237	0	31	0	238	0	−956	0
1–3	$-0.42999\times10^{+01}$	3643	1296	28	940	0	562	0	85	0	114	0	290	0
1–4	$-0.10532\times10^{+02}$	229	318	1	−54	0	17	0	11	0	−153	0	2401	0
1–5	$-0.13475\times10^{+02}$	157	211	7	2118	0	302	0	35	0	129	0	28	0
1–6	$-0.24217\times10^{+02}$	2	1	4	−1	0	−4	0	19	0	13	0	−704	0
1–7	$-0.31423\times10^{+02}$	0	1	4	−335	0	−36	0	−39	0	−14	0	1	0
1–8	$-0.46509\times10^{+02}$	0	0	0	0	0	0	0	11	0	−11	0	−44	0
2–3	$-0.11575\times10^{+01}$	982	2181	394	−2058	0	206	0	111	0	−7	0	262	0
2–4	$-0.73898\times10^{+01}$	4367	4062	28	0	0	−11	0	−48	0	468	0	432	0
2–5	$-0.10332\times10^{+02}$	434	623	4	769	0	427	0	−13	0	172	0	−19	0
2–6	$-0.21074\times10^{+02}$	19	8	0	7	0	19	0	9	0	−66	0	2183	0
2–7	$-0.28280\times10^{+02}$	0	0	1	−554	0	30	0	−12	0	16	0	−1	0
2–8	$-0.43366\times10^{+02}$	0	0	2	1	0	−1	0	−26	0	−6	0	138	0
3–4	$-0.62324\times10^{+01}$	457	535	4	14	0	−36	0	15	0	−148	0	−1320	0
3–5	$-0.91748\times10^{+01}$	3272	3338	2	−839	0	1126	0	26	0	409	0	−101	0
3–6	$-0.19917\times10^{+02}$	9	7	1	−2	0	−5	0	−9	0	19	0	−663	0
3–7	$-0.27123\times10^{+02}$	6	0	1	−1510	0	−3	0	20	0	−1	0	−1	0
3–8	$-0.42209\times10^{+02}$	0	0	0	0	0	1	0	8	0	8	0	−86	0
4–5	$-0.29424\times10^{+01}$	5	4	13	16	0	18	0	−19	0	15	0	2	0
4–6	$-0.13685\times10^{+02}$	3977	4002	7	−57	0	2	0	−51	0	771	0	304	0
4–7	$-0.20890\times10^{+02}$	1	1	0	61	0	37	0	0	0	17	0	0	0
4–8	$-0.35977\times10^{+02}$	6	0	0	0	0	10	0	−5	0	41	0	−1631	0
5–6	$-0.10742\times10^{+02}$	2	2	0	0	0	0	0	−1	0	18	0	24	0
5–7	$-0.17948\times10^{+02}$	2354	2330	2	64	0	−1420	0	−44	0	−591	0	51	0
5–8	$-0.33034\times10^{+02}$	0	0	0	0	0	0	0	0	0	1	0	−33	0
6–7	$-0.72060\times10^{+01}$	0	0	0	4	0	0	0	1	0	0	0	0	0
6–8	$-0.22292\times10^{+02}$	2332	2352	2	35	0	2	0	37	0	−827	0	−119	0
7–8	$-0.15086\times10^{+02}$	0	0	0	0	0	0	0	0	0	0	0	0	0

TABLE 1. *Energy level differences, wave functions and transition probabilities for angles and field strengths indicated*—Continued

	ΔE	P_x	P_y	P_z	P_{11}		P_{10}		P_{00}		P_{-10}		P_{-1-1}	
					$\theta=15$ $\varphi=0$ H=1600									
1–2	$-0.42338\times10^{+01}$	8	5623	485	−797	0	−540	0	−179	0	−184	0	869	0
1–3	$-0.74006\times10^{+01}$	1792	639	16	418	0	211	0	61	0	−101	0	1637	0
1–4	$-0.11231\times10^{+02}$	244	516	20	1022	0	429	0	73	0	173	0	41	0
1–5	$-0.16711\times10^{+02}$	65	70	0	−40	0	−26	0	−12	0	103	0	−1569	0
1–6	$-0.26758\times10^{+02}$	2	11	4	690	0	107	0	45	0	251	0	263	0
1–7	$-0.32479\times10^{+02}$	3	2	2	2	0	3	0	−11	0	−21	0	567	0
1–8	$-0.56888\times10^{+02}$	0	0	0	0	0	1	0	7	0	−5	0	−61	0
2–3	$-0.31669\times10^{+01}$	1621	4984	451	302	0	−150	0	−82	0	−127	0	−1104	0
2–4	$-0.69973\times10^{+01}$	3649	2	18	521	0	−640	0	−134	0	−233	0	134	0
2–5	$-0.12478\times10^{+02}$	325	443	4	−2	0	−4	0	−24	0	203	0	−1658	0
2–6	$-0.22524\times10^{+02}$	17	52	1	−778	0	−181	0	15	0	−80	0	−259	0
2–7	$-0.28246\times10^{+02}$	3	2	1	3	0	8	0	−4	0	−41	0	882	0
2–8	$-0.52654\times10^{+02}$	0	0	0	1	0	1	0	11	0	−3	0	−39	0
3–4	$-0.38305\times10^{+01}$	438	1150	320	−1206	0	279	0	197	0	8	0	67	0
3–5	$-0.93107\times10^{+01}$	4462	4141	63	49	0	−15	0	−78	0	444	0	1142	0
3–6	$-0.19357\times10^{+02}$	48	61	2	474	0	279	0	−17	0	123	0	42	0
3–7	$-0.25079\times10^{+02}$	87	68	2	7	0	16	0	20	0	−120	0	2106	0
3–8	$-0.49487\times10^{+02}$	0	0	1	0	0	3	0	23	0	13	0	−222	0
4–5	$-0.54802\times10^{+01}$	142	139	22	−4	0	4	0	−2	0	−29	0	−907	0
4–6	$-0.15527\times10^{+02}$	2320	2169	15	−631	0	1366	0	110	0	607	0	40	0
4–7	$-0.21248\times10^{+02}$	11	11	0	−1	0	−1	0	−4	0	30	0	−139	0
4–8	$-0.45657\times10^{+02}$	0	0	0	0	0	0	0	−2	0	−5	0	71	0
5–6	$-0.10047\times10^{+02}$	4	4	0	31	0	−28	0	−9	0	−7	0	3	0
5–7	$-0.15768\times10^{+02}$	3871	3972	8	−47	0	0	0	−55	0	761	0	459	0
5–8	$-0.40177\times10^{+02}$	1	1	0	0	0	−7	0	7	0	−22	0	1624	0
6–7	$-0.57215\times10^{+01}$	0	0	0	1	0	2	0	1	0	2	0	28	0
6–8	$-0.30130\times10^{+02}$	0	0	0	0	0	0	0	0	0	0	0	2	0
7–8	$-0.24409\times10^{+02}$	2332	2351	5	−30	0	−2	0	−66	0	827	0	132	0
					$\theta=15$ $\varphi=0$ H=2400									
1–2	$-0.57187\times10^{+01}$	88	5325	586	−888	0	−606	0	−250	0	−265	0	1184	0
1–3	$-0.98883\times10^{+01}$	1189	69	9	−1157	0	−595	0	−141	0	−161	0	−902	0
1–4	$-0.12725\times10^{+02}$	189	643	17	−383	0	−155	0	−9	0	−202	0	1694	0
1–5	$-0.23153\times10^{+02}$	24	44	6	−915	0	−234	0	−56	0	−88	0	−134	0
1–6	$-0.23837\times10^{+02}$	13	73	2	−125	0	−42	0	−12	0	−78	0	1267	0
1–7	$-0.41711\times10^{+02}$	1	0	1	0	0	0	0	8	0	3	0	−217	0
1–8	$-0.68233\times10^{+02}$	0	0	0	0	0	0	0	−3	0	4	0	31	0
2–3	$-0.41696\times10^{+01}$	250	6137	573	−667	0	774	0	304	0	270	0	323	0
2–4	$-0.70065\times10^{+01}$	3823	1741	70	−62	0	331	0	74	0	−8	0	−170	0
2–5	$-0.17434\times10^{+02}$	129	309	3	1032	0	468	0	−12	0	218	0	−238	0
2–6	$-0.18118\times10^{+02}$	224	131	14	34	0	56	0	17	0	−146	0	2080	0
2–7	$-0.35992\times10^{+02}$	9	11	2	1	0	−2	0	15	0	−19	0	−621	0
2–8	$-0.62514\times10^{+02}$	0	0	0	0	0	0	0	−8	0	9	0	−59	0
3–4	$-0.28369\times10^{+01}$	687	1246	1121	−258	0	34	0	283	0	−57	0	1645	0
3–5	$-0.13265\times10^{+02}$	2114	1374	20	−610	0	1214	0	157	0	485	0	−48	0
3–6	$-0.13949\times10^{+02}$	417	606	19	−29	0	100	0	−11	0	272	0	−551	0
3–7	$-0.31822\times10^{+02}$	2	1	0	3	0	7	0	3	0	−40	0	943	0
3–8	$-0.58344\times10^{+02}$	0	0	0	0	0	1	0	10	0	3	0	−65	0
4–5	$-0.10428\times10^{+02}$	172	557	58	−661	0	429	0	129	0	210	0	77	0
4–6	$-0.11112\times10^{+02}$	4909	3493	100	−97	0	53	0	102	0	−405	0	−1113	0
4–7	$-0.28985\times10^{+02}$	40	33	1	−8	0	−13	0	−17	0	114	0	−2061	0
4–8	$-0.55508\times10^{+02}$	0	0	1	0	0	−2	0	−18	0	−12	0	244	0
5–6	$-0.68398\times10^{+00}$	4	3	297	−12	0	−19	0	162	0	−3	0	234	0
5–7	$-0.18558\times10^{+02}$	38	39	0	4	0	1	0	13	0	−75	0	6	0
5–8	$-0.45080\times10^{+02}$	0	0	0	0	0	1	0	0	0	8	0	−161	0
6–7	$-0.17874\times10^{+02}$	3900	3913	35	−33	0	−3	0	−115	0	752	0	497	0
6–8	$-0.44396\times10^{+02}$	11	3	0	1	0	−6	0	13	0	−74	0	1599	0
7–8	$-0.26522\times10^{+02}$	2315	2350	10	−27	0	−5	0	−91	0	821	0	273	0

TABLE 1. *Energy level differences, wave functions and transition probabilities for angles and field strengths indicated*—Continued

	ΔE	P_x	P_y	P_z	P_{11}		P_{10}		P_{00}		P_{-10}		P_{-1-1}	
					$\theta=15$	$\varphi=0$	H=3200							
1–2	$-0.71149\times10^{+01}$	95	5067	668	−967	0	−748	0	−348	0	−293	0	1310	0
1–3	$-0.11069\times10^{+02}$	1010	31	1	−655	0	−421	0	−111	0	−90	0	−1150	0
1–4	$-0.18019\times10^{+02}$	60	266	11	−359	0	−122	0	−8	0	−171	0	1563	0
1–5	$-0.20561\times10^{+02}$	70	65	5	−857	0	−334	0	−72	0	−113	0	−305	0
1–6	$-0.31639\times10^{+02}$	3	9	0	0	19	0	29	0	0	0	−11	0	709
1–7	$-0.51653\times10^{+02}$	0	0	0	−103	0	3	0	5	0	1	0	−69	0
1–8	$-0.80293\times10^{+02}$	0	0	0	0	0	0	0	2	0	−2	0	−6	0
2–3	$-0.39539\times10^{+01}$	111	5027	1058	−306	0	570	0	438	0	120	0	401	0
2–4	$-0.10905\times10^{+02}$	2424	952	28	−184	0	291	0	91	0	−61	0	849	0
2–5	$-0.13446\times10^{+02}$	395	1095	6	545	0	807	0	71	0	394	0	−399	0
2–6	$-0.24524\times10^{+02}$	45	11	0	0	37	0	174	0	18	0	−22	0	1739
2–7	$-0.44538\times10^{+02}$	0	0	1	−112	0	0	0	7	0	17	0	−159	0
2–8	$-0.73178\times10^{+02}$	0	0	0	3	0	1	0	5	0	−3	0	−5	0
3–4	$-0.69508\times10^{+01}$	1971	3772	554	74	0	162	0	160	0	90	0	2077	0
3–5	$-0.94921\times10^{+01}$	2362	421	47	−1174	0	966	0	266	0	359	0	−312	0
3–6	$-0.20570\times10^{+02}$	108	286	3	0	−110	0	−147	0	−13	0	62	0	−1695
3–7	$-0.40585\times10^{+02}$	0	0	0	565	0	11	0	−1	0	−28	0	219	0
3–8	$-0.69224\times10^{+02}$	0	0	0	−3	0	0	0	−6	0	1	0	−1	0
4–5	$-0.25414\times10^{+01}$	54	342	905	−143	0	5	0	455	0	67	0	636	0
4–6	$-0.13619\times10^{+02}$	4615	4198	84	0	497	0	633	0	141	0	−296	0	−1108
4–7	$-0.33634\times10^{+02}$	42	36	1	−2126	0	−44	0	−20	0	93	0	48	0
4–8	$-0.62273\times10^{+02}$	0	0	1	25	0	1	0	17	0	15	0	26	0
5–6	$-0.11078\times10^{+02}$	247	216	284	0	104	0	−163	0	112	0	22	0	707
5–7	$-0.31092\times10^{+02}$	45	45	1	452	0	158	0	17	0	129	0	−120	0
5–8	$-0.59732\times10^{+02}$	0	0	0	−5	0	−3	0	−1	0	−10	0	−8	0
6–7	$-0.20014\times10^{+02}$	3885	3911	51	0	916	0	1232	0	139	0	456	0	−282
6–8	$-0.48654\times10^{+02}$	13	5	0	0	7	0	−39	0	−14	0	−2	0	−3
7–8	$-0.28639\times10^{+02}$	2310	2346	15	2	0	12	0	113	0	17	0	25	0
					$\theta=15$	$\varphi=0$	H=4000							
1–2	$-0.80885\times10^{+01}$	179	4409	712	814	0	750	0	436	0	248	0	−1327	0
1–3	$-0.13768\times10^{+02}$	797	102	3	−480	0	−337	0	−106	0	−46	0	−1461	0
1–4	$-0.18698\times10^{+02}$	18	279	22	734	0	409	0	106	0	199	0	−533	0
1–5	$-0.24334\times10^{+02}$	34	34	1	−50	0	−26	0	−18	0	77	0	−1324	0
1–6	$-0.40013\times10^{+02}$	2	2	0	−1	0	−5	0	−3	0	21	0	−441	0
1–7	$-0.62184\times10^{+02}$	0	0	0	0	0	0	0	−2	0	0	0	91	0
1–8	$-0.92948\times10^{+02}$	0	0	0	0	0	0	0	1	0	0	0	−18	0
2–3	$-0.56793\times10^{+01}$	785	5711	945	173	0	−543	0	−423	0	−82	0	−208	0
2–4	$-0.10609\times10^{+02}$	1965	229	2	59	0	904	0	178	0	354	0	206	0
2–5	$-0.16246\times10^{+02}$	443	695	10	−44	0	−70	0	42	0	−212	0	1822	0
2–6	$-0.31925\times10^{+02}$	5	7	0	7	0	11	0	7	0	−61	0	1242	0
2–7	$-0.54095\times10^{+02}$	0	0	0	0	0	0	0	5	0	7	0	−166	0
2–8	$-0.84860\times10^{+02}$	0	0	0	0	0	0	0	−2	0	3	0	25	0
3–4	$-0.49299\times10^{+01}$	266	1497	830	1173	0	−643	0	−565	0	−228	0	−326	0
3–5	$-0.10566\times10^{+02}$	4078	3386	233	−130	0	118	0	24	0	−48	0	−935	0
3–6	$-0.26245\times10^{+02}$	105	129	1	8	0	6	0	32	0	−175	0	2160	0
3–7	$-0.48416\times10^{+02}$	0	0	0	−1	0	−2	0	4	0	24	0	−564	0
3–8	$-0.79180\times10^{+02}$	0	0	0	0	0	0	0	−6	0	2	0	28	0
4–5	$-0.56364\times10^{+01}$	566	562	413	−7	0	48	0	−218	0	73	0	−1002	0
4–6	$-0.21316\times10^{+02}$	119	124	1	0	0	3	0	31	0	−112	0	560	0
4–7	$-0.43486\times10^{+02}$	0	0	0	−1	0	−2	0	0	0	20	0	−445	0
4–8	$-0.74250\times10^{+02}$	0	0	0	0	0	0	0	−3	0	0	0	31	0
5–6	$-0.15679\times10^{+02}$	4704	4604	167	−19	0	25	0	112	0	−445	0	−946	0
5–7	$-0.37850\times10^{+02}$	42	37	1	−8	0	−12	0	−24	0	143	0	−2210	0
5–8	$-0.68614\times10^{+02}$	0	0	1	0	0	−2	0	−15	0	−15	0	271	0
6–7	$-0.22171\times10^{+02}$	3918	3951	66	−25	0	−10	0	−156	0	742	0	628	0
6–8	$-0.52935\times10^{+02}$	13	6	0	1	0	−4	0	17	0	−91	0	1594	0
7–8	$-0.30764\times10^{+02}$	2306	2344	20	−22	0	−9	0	−130	0	813	0	366	0

TABLE 1. *Energy level differences, wave functions and transition probabilities for angles and field strengths indicated*—Continued

	ΔE	P_x	P_y	P_z	P_{11}		P_{10}		P_{00}		P_{-10}		P_{-1-1}	
					$\theta=15$		$\varphi=0$		H=4800					
1–2	$-0.91589\times10^{+01}$	225	4122	734	781	0	772	0	488	0	222	0	−1267	0
1–3	$-0.15853\times10^{+02}$	695	28	2	590	0	426	0	108	0	114	0	1195	0
1–4	$-0.19563\times10^{+02}$	52	311	21	−310	0	−196	0	−39	0	−162	0	1232	0
1–5	$-0.30902\times10^{+02}$	18	24	1	12	0	9	0	11	0	−69	0	1123	0
1–6	$-0.48876\times10^{+02}$	1	1	0	1	0	4	0	4	0	−15	0	323	0
1–7	$-0.73219\times10^{+02}$	0	0	0	0	0	0	0	3	0	0	0	−73	0
1–8	$-0.10612\times10^{+03}$	0	0	0	0	0	0	0	0	0	1	0	14	0
2–3	$-0.66937\times10^{+01}$	90	5199	912	−156	0	858	0	561	0	211	0	109	0
2–4	$-0.10404\times10^{+02}$	2646	653	57	21	0	−447	0	−72	0	−218	0	−318	0
2–5	$-0.21743\times10^{+02}$	189	260	4	19	0	26	0	−36	0	177	0	−2014	0
2–6	$-0.39717\times10^{+02}$	1	2	0	−5	0	−8	0	−4	0	39	0	−849	0
2–7	$-0.64060\times10^{+02}$	0	0	0	0	0	0	0	−3	0	−3	0	100	0
2–8	$-0.96957\times10^{+02}$	0	0	0	0	0	0	0	2	0	−1	0	−21	0
3–4	$-0.37108\times10^{+01}$	345	1600	2024	418	0	−187	0	−819	0	111	0	−1023	0
3–5	$-0.15049\times10^{+02}$	1625	1544	44	−47	0	35	0	67	0	−125	0	316	0
3–6	$-0.33023\times10^{+02}$	14	20	0	7	0	6	0	14	0	−99	0	1592	0
3–7	$-0.57366\times10^{+02}$	0	0	0	0	0	0	0	3	0	12	0	−270	0
3–8	$-0.90263\times10^{+02}$	0	0	0	0	0	0	0	−3	0	2	0	17	0
4–5	$-0.11339\times10^{+02}$	3226	3159	404	−37	0	61	0	−87	0	−6	0	−1299	0
4–6	$-0.29312\times10^{+02}$	105	121	0	5	0	5	0	39	0	−172	0	1861	0
4–7	$-0.53655\times10^{+02}$	0	0	0	0	0	−2	0	2	0	23	0	−546	0
4–8	$-0.86552\times10^{+02}$	0	0	0	0	0	0	0	−5	0	1	0	27	0
5–6	$-0.17974\times10^{+02}$	4776	4732	191	−14	0	28	0	122	0	−449	0	−877	0
5–7	$-0.42317\times10^{+02}$	43	39	1	−9	0	−11	0	−26	0	152	0	−2239	0
5–8	$-0.75213\times10^{+02}$	0	0	1	0	0	−2	0	−13	0	−15	0	277	0
6–7	$-0.24343\times10^{+02}$	3911	3943	79	−21	0	−13	0	−170	0	737	0	662	0
6–8	$-0.57240\times10^{+02}$	13	6	0	1	0	−3	0	18	0	−96	0	1589	0
7–8	$-0.32897\times10^{+02}$	2302	2342	25	−20	0	−11	0	−146	0	810	0	400	0
					$\theta=30$		$\varphi=0$		H=800					
1–2	$-0.43092\times10^{+01}$	83	6587	473	−925	0	−366	0	−58	0	−298	0	1217	0
1–3	$-0.66386\times10^{+01}$	1967	262	13	1237	0	482	0	106	0	75	0	599	0
1–4	$-0.11792\times10^{+02}$	273	374	2	−93	0	4	0	24	0	−196	0	2016	0
1–5	$-0.15544\times10^{+02}$	82	125	7	−1667	0	−297	0	−41	0	−130	0	−18	0
1–6	$-0.25105\times10^{+02}$	6	3	3	3	0	6	0	−15	0	−31	0	858	0
1–7	$-0.33605\times10^{+02}$	0	1	3	388	0	55	0	35	0	23	0	−1	0
1–8	$-0.47115\times10^{+02}$	0	0	0	0	0	1	0	14	0	−8	0	−89	0
2–3	$-0.23294\times10^{+01}$	643	4046	720	1160	0	−317	0	−141	0	−76	0	−437	0
2–4	$-0.74833\times10^{+01}$	3482	2839	73	21	0	51	0	91	0	−403	0	−30	0
2–5	$-0.11235\times10^{+02}$	690	867	0	1101	0	602	0	29	0	250	0	−58	0
2–6	$-0.20795\times10^{+02}$	50	33	1	11	0	18	0	17	0	−122	0	1928	0
2–7	$-0.29296\times10^{+02}$	1	6	1	−811	0	−39	0	−15	0	−12	0	−2	0
2–8	$-0.42805\times10^{+02}$	0	0	2	0	0	4	0	25	0	13	0	−247	0
3–4	$-0.51539\times10^{+01}$	1250	1463	74	55	0	−44	0	42	0	−203	0	−1839	0
3–5	$-0.89058\times10^{+01}$	3281	2823	65	1288	0	−1014	0	−142	0	−347	0	128	0
3–6	$-0.18466\times10^{+02}$	51	45	3	11	0	10	0	23	0	−85	0	991	0
3–7	$-0.26966\times10^{+02}$	11	31	1	1339	0	187	0	−18	0	81	0	−3	0
3–8	$-0.40476\times10^{+02}$	0	0	0	0	0	2	0	10	0	17	0	−224	0
4–5	$-0.37519\times10^{+01}$	37	34	34	−416	0	2	0	40	0	−18	0	−2	0
4–6	$-0.13312\times10^{+02}$	3880	3921	26	56	0	0	0	100	0	−752	0	−611	0
4–7	$-0.21812\times10^{+02}$	3	2	0	−94	0	−67	0	2	0	−29	0	3	0
4–8	$-0.35322\times10^{+02}$	14	3	0	0	0	9	0	−14	0	72	0	−1593	0
5–6	$-0.95602\times10^{+01}$	4	3	0	0	0	0	0	−2	0	27	0	95	0
5–7	$-0.18060\times10^{+02}$	2357	2273	10	338	0	−1401	0	−88	0	−582	0	51	0
5–8	$-0.31570\times10^{+02}$	0	0	0	0	0	0	0	2	0	−1	0	42	0
6–7	$-0.85002\times10^{+01}$	0	0	0	8	0	0	0	2	0	0	0	0	0
6–8	$-0.22010\times10^{+02}$	2315	2353	6	−36	0	−3	0	−70	0	823	0	235	0
7–8	$-0.13510\times10^{+02}$	0	0	0	0	0	0	0	0	0	0	0	0	0

TABLE 1. *Energy level differences, wave functions and transition probabilities for angles and field strengths indicated*—Continued

$\theta=30$ $\varphi=0$ $H=1600$

	ΔE	P_x	P_y	P_z	$P_{1\,1}$		$P_{1\,0}$		$P_{0\,0}$		$P_{-1\,0}$		$P_{-1\,-1}$	
1–2	$-0.66335\times10^{+01}$	19	5475	717	−1213	0	−574	0	−171	0	−365	0	1431	0
1–3	$-0.11326\times10^{+02}$	992	36	0	847	0	366	0	130	0	−24	0	1348	0
1–4	$-0.16219\times10^{+02}$	47	308	17	1228	0	383	0	67	0	214	0	−488	0
1–5	$-0.19796\times10^{+02}$	71	45	0	−124	0	−51	0	−27	0	98	0	−1352	0
1–6	$-0.31595\times10^{+02}$	1	2	2	468	0	87	0	34	0	31	0	41	0
1–7	$-0.34693\times10^{+02}$	3	1	1	3	0	2	0	−9	0	−21	0	502	0
1–8	$-0.58473\times10^{+02}$	0	0	0	0	0	0	0	−8	0	4	0	71	0
2–3	$-0.46921\times10^{+01}$	256	6300	1066	225	0	−407	0	−154	0	−239	0	−282	0
2–4	$-0.95858\times10^{+01}$	2481	627	6	−513	0	−829	0	−181	0	−227	0	−162	0
2–5	$-0.13162\times10^{+02}$	563	924	26	66	0	56	0	−66	0	324	0	−1507	0
2–6	$-0.24961\times10^{+02}$	2	33	0	−1092	0	−176	0	2	0	−84	0	8	0
2–7	$-0.28060\times10^{+02}$	17	11	0	6	0	10	0	8	0	−93	0	1233	0
2–8	$-0.51839\times10^{+02}$	0	0	1	0	0	−2	0	−15	0	−6	0	177	0
3–4	$-0.48937\times10^{+01}$	905	2781	756	−1541	0	619	0	302	0	215	0	369	0
3–5	$-0.84702\times10^{+01}$	3895	2710	181	149	0	−109	0	−156	0	309	0	1264	0
3–6	$-0.20269\times10^{+02}$	104	93	10	830	0	428	0	−17	0	193	0	−52	0
3–7	$-0.23367\times10^{+02}$	128	115	5	19	0	16	0	43	0	−190	0	1747	0
3–8	$-0.47147\times10^{+02}$	1	0	1	0	0	−3	0	−13	0	−30	0	409	0
4–5	$-0.35765\times10^{+01}$	445	467	384	12	0	27	0	−34	0	−35	0	−1213	0
4–6	$-0.15376\times10^{+02}$	2312	1905	134	−791	0	1266	0	306	0	513	0	−77	0
4–7	$-0.18474\times10^{+02}$	114	117	3	−10	0	−1	0	−32	0	137	0	−358	0
4–8	$-0.42254\times10^{+02}$	1	0	0	0	0	2	0	0	0	23	0	−310	0
5–6	$-0.11799\times10^{+02}$	83	79	1	426	0	−138	0	−45	0	−47	0	5	0
5–7	$-0.14897\times10^{+02}$	3693	3715	78	−37	0	−9	0	−168	0	707	0	951	0
5–8	$-0.38677\times10^{+02}$	26	12	1	−1	0	6	0	−25	0	111	0	−1509	0
6–7	$-0.30982\times10^{+01}$	0	0	0	1	0	0	0	4	0	−8	0	76	0
6–8	$-0.26878\times10^{+02}$	0	0	0	0	0	0	0	0	0	0	0	21	0
7–8	$-0.23780\times10^{+02}$	2287	2343	20	32	0	11	0	130	0	−809	0	−409	0

$\theta=30$ $\varphi=0$ $H=2400$

	ΔE	P_x	P_y	P_z	$P_{1\,1}$		$P_{1\,0}$		$P_{0\,0}$		$P_{-1\,0}$		$P_{-1\,-1}$	
1–2	$-0.86794\times10^{+01}$	197	4856	800	−984	0	−620	0	−267	0	−362	0	1799	0
1–3	$-0.15333\times10^{+02}$	622	50	21	913	0	512	0	199	0	62	0	1259	0
1–4	$-0.19949\times10^{+02}$	12	163	8	590	0	265	0	47	0	190	0	−853	0
1–5	$-0.28462\times10^{+02}$	11	1	1	140	0	58	0	19	0	−25	0	710	0
1–6	$-0.30799\times10^{+02}$	14	33	3	671	0	215	0	50	0	93	0	−55	0
1–7	$-0.45138\times10^{+02}$	1	0	0	0	0	0	0	7	0	6	0	−203	0
1–8	$-0.70668\times10^{+02}$	0	0	0	0	0	1	0	5	0	−2	0	−35	0
2–3	$-0.66535\times10^{+01}$	119	6819	1280	29	0	−622	0	−282	0	−336	0	343	0
2–4	$-0.11269\times10^{+02}$	2063	84	14	−271	0	−503	0	−203	0	−4	0	−735	0
2–5	$-0.19783\times10^{+02}$	163	345	9	−130	0	−66	0	54	0	−274	0	1806	0
2–6	$-0.22119\times10^{+02}$	132	126	1	−866	0	−414	0	−47	0	−156	0	−166	0
2–7	$-0.36458\times10^{+02}$	7	4	0	−4	0	−5	0	−2	0	68	0	−878	0
2–8	$-0.61988\times10^{+02}$	0	0	0	1	0	3	0	12	0	4	0	−132	0
3–4	$-0.46159\times10^{+01}$	72	3458	1980	−809	0	326	0	391	0	72	0	1017	0
3–5	$-0.13129\times10^{+02}$	2213	1258	75	−49	0	192	0	179	0	−262	0	214	0
3–6	$-0.15466\times10^{+02}$	693	996	22	−4	0	901	0	145	0	417	0	−121	0
3–7	$-0.29805\times10^{+02}$	50	44	1	−12	0	−13	0	−34	0	155	0	−1496	0
3–8	$-0.55335\times10^{+02}$	1	0	0	0	0	4	0	11	0	24	0	−300	0
4–5	$-0.85133\times10^{+01}$	2072	2902	560	−168	0	43	0	−43	0	221	0	1772	0
4–6	$-0.10850\times10^{+02}$	1781	671	130	−1202	0	829	0	336	0	289	0	−254	0
4–7	$-0.25189\times10^{+02}$	167	166	6	16	0	12	0	59	0	−212	0	1273	0
4–8	$-0.50719\times10^{+02}$	1	0	0	0	0	−3	0	−3	0	−37	0	454	0
5–6	$-0.23366\times10^{+01}$	87	71	475	−533	0	25	0	258	0	−35	0	1	0
5–7	$-0.16676\times10^{+02}$	3629	3653	141	−26	0	−24	0	−222	0	674	0	1077	0
5–8	$-0.42205\times10^{+02}$	36	21	1	−2	0	3	0	−35	0	139	0	−1467	0
6–7	$-0.14339\times10^{+02}$	53	53	3	2	0	3	0	24	0	−73	0	−262	0
6–8	$-0.39869\times10^{+02}$	1	0	0	0	0	0	0	5	0	−16	0	161	0
7–8	$-0.25530\times10^{+02}$	2263	2328	38	29	0	17	0	179	0	−794	0	−542	0

TABLE 1. *Energy level differences, wave functions and transition probabilities for angles and field strengths indicated*—Continued

	ΔE	P_x	P_y	P_z	P_{11}		P_{10}		P_{00}		P_{-10}		P_{-1-1}	
					$\theta=30$	$\varphi=0$	$H=3200$							
1–2	$-0.10533\times10^{+02}$	109	4426	955	1144	0	729	0	339	0	401	0	−1640	0
1–3	$-0.18479\times10^{+02}$	484	7	0	750	0	414	0	178	0	20	0	1256	0
1–4	$-0.25635\times10^{+02}$	7	113	6	−368	0	−148	0	−8	0	−169	0	1011	0
1–5	$-0.31295\times10^{+02}$	17	9	2	450	0	175	0	52	0	48	0	246	0
1–6	$-0.37735\times10^{+02}$	5	5	0	3	0	3	0	9	0	−46	0	601	0
1–7	$-0.56169\times10^{+02}$	0	0	0	−65	0	−8	0	6	0	−5	0	−188	0
1–8	$-0.83462\times10^{+02}$	0	0	0	0	0	0	0	−3	0	2	0	33	0
2–3	$-0.79462\times10^{+01}$	125	6204	1507	208	0	718	0	410	0	326	0	−391	0
2–4	$-0.15103\times10^{+02}$	1566	221	26	−356	0	−450	0	−209	0	44	0	−1162	0
2–5	$-0.20762\times10^{+02}$	53	301	9	658	0	465	0	57	0	276	0	−468	0
2–6	$-0.27202\times10^{+02}$	76	71	2	29	0	−37	0	−49	0	165	0	−1542	0
2–7	$-0.45637\times10^{+02}$	3	37	0	−75	0	9	0	1	0	−67	0	577	0
2–8	$-0.72929\times10^{+02}$	0	0	0	0	0	0	0	8	0	2	0	−72	0
3–4	$-0.71566\times10^{+01}$	600	4833	1825	526	0	−395	0	−358	0	−145	0	−988	0
3–5	$-0.12816\times10^{+02}$	1842	207	14	−318	0	856	0	313	0	279	0	−76	0
3–6	$-0.19256\times10^{+02}$	581	731	32	66	0	−24	0	115	0	−320	0	1261	0
3–7	$-0.37691\times10^{+02}$	16	0	0	4	0	−33	0	−22	0	64	0	−1157	0
3–8	$-0.64983\times10^{+02}$	0	0	0	0	0	−5	0	−8	0	−15	0	148	0
4–5	$-0.56595\times10^{+01}$	401	934	1303	1140	0	−461	0	−589	0	−164	0	−308	0
4–6	$-0.12100\times10^{+02}$	3501	3047	427	−218	0	125	0	187	0	−248	0	−1337	0
4–7	$-0.30534\times10^{+02}$	156	454	7	−108	0	−31	0	−71	0	277	0	−1634	0
4–8	$-0.57827\times10^{+02}$	1	0	0	1	0	0	0	−3	0	−43	0	453	0
5–6	$-0.64402\times10^{+01}$	441	439	365	1	0	66	0	−64	0	−26	0	−1153	0
5–7	$-0.24875\times10^{+02}$	73	69	3	7	0	−19	0	−44	0	117	0	−627	0
5–8	$-0.52167\times10^{+02}$	1	0	0	0	0	0	0	3	0	83	0	404	0
6–7	$-0.18435\times10^{+02}$	3608	2772	208	171	0	19	0	−262	0	658	0	1171	0
6–8	$-0.45727\times10^{+02}$	42	28	2	3	0	−4	0	44	0	−158	0	1411	0
7–8	$-0.27293\times10^{+02}$	2243	2313	58	−25	0	−23	0	−219	0	768	0	597	0
					$\theta=30$	$\varphi=0$	$H=4000$							
1–2	$-0.12236\times10^{+02}$	128	4025	1010	−1101	0	−784	0	−420	0	−386	0	1561	0
1–3	$-0.21693\times10^{+02}$	418	74	7	−541	0	−324	0	−151	0	24	0	−1399	0
1–4	$-0.30150\times10^{+02}$	1	84	6	−384	0	−173	0	−21	0	−160	0	820	0
1–5	$-0.34976\times10^{+02}$	14	1	0	177	0	84	0	39	0	−23	0	591	0
1–6	$-0.47263\times10^{+02}$	2	2	0	0	0	5	0	6	0	−29	0	411	0
1–7	$-0.67641\times10^{+02}$	0	0	0	0	0	0	0	−3	0	−3	0	124	0
1–8	$-0.96724\times10^{+02}$	0	0	0	0	0	1	0	3	0	0	0	−24	0
2–3	$-0.94562\times10^{+01}$	372	5893	1614	250	0	716	0	494	0	293	0	−554	0
2–4	$-0.17914\times10^{+02}$	1194	13	0	421	0	598	0	268	0	61	0	1146	0
2–5	$-0.22740\times10^{+02}$	12	284	12	−243	0	−236	0	9	0	−271	0	1167	0
2–6	$-0.35026\times10^{+02}$	15	15	0	23	0	21	0	29	0	−105	0	1125	0
2–7	$-0.55405\times10^{+02}$	1	0	0	1	0	1	0	−1	0	−24	0	324	0
2–8	$-0.84488\times10^{+02}$	0	0	0	0	0	2	0	6	0	1	0	−55	0
3–4	$-0.84574\times10^{+01}$	192	4851	1961	−566	0	614	0	550	0	231	0	572	0
3–5	$-0.13284\times10^{+02}$	2310	598	88	160	0	−448	0	−251	0	−48	0	39	0
3–6	$-0.25570\times10^{+02}$	276	326	13	−9	0	−5	0	−104	0	290	0	−1678	0
3–7	$-0.45948\times10^{+02}$	7	5	0	−6	0	−7	0	−15	0	85	0	−925	0
3–8	$-0.75031\times10^{+02}$	0	0	0	0	0	−2	0	−8	0	−10	0	147	0
4–5	$-0.48261\times10^{+01}$	237	1627	3154	505	0	−66	0	−722	0	134	0	−1118	0
4–6	$-0.17113\times10^{+02}$	1617	1549	141	−18	0	66	0	183	0	−275	0	−162	0
4–7	$-0.37491\times10^{+02}$	48	46	2	12	0	12	0	49	0	−168	0	1339	0
4–8	$-0.66574\times10^{+02}$	1	0	0	0	0	3	0	4	0	29	0	−310	0
5–6	$-0.12287\times10^{+02}$	2548	2556	644	−5	0	105	0	87	0	−130	0	−1687	0
5–7	$-0.32665\times10^{+02}$	147	149	6	14	0	14	0	80	0	−231	0	1269	0
5–8	$-0.61748\times10^{+02}$	1	0	0	0	0	3	0	−1	0	44	0	−453	0
6–7	$-0.20378\times10^{+02}$	3600	3675	271	22	0	56	0	296	0	−624	0	−1256	0
6–8	$-0.49461\times10^{+02}$	45	33	2	−2	0	0	0	−50	0	173	0	−1422	0
7–8	$-0.29083\times10^{+02}$	2225	2301	79	−23	0	−32	0	−255	0	764	0	729	0

TABLE 1. *Energy level differences, wave functions and transition probabilities for angles and field strengths indicated*—Continued

	ΔE	P_x	P_y	P_z	P_{11}		P_{10}		P_{00}		P_{-10}		P_{-1-1}	
						$\theta=30$	$\varphi=0$	H=4800						
1–2	$-0.13864\times10^{+02}$	218	3808	1056	−978	0	−773	0	−470	0	−365	0	1646	0
1–3	$-0.24763\times10^{+02}$	323	28	1	503	0	344	0	176	0	−9	0	1305	0
1–4	$-0.33401\times10^{+02}$	2	51	5	290	0	133	0	11	0	149	0	−785	0
1–5	$-0.41630\times10^{+02}$	7	11	0	39	0	32	0	27	0	−46	0	630	0
1–6	$-0.57069\times10^{+02}$	1	1	0	2	0	7	0	4	0	−19	0	279	0
1–7	$-0.79455\times10^{+02}$	0	0	0	0	0	1	0	4	0	3	0	−82	0
1–8	$-0.11036\times10^{+03}$	0	0	0	0	0	0	0	−1	0	1	0	18	0
2–3	$-0.10899\times10^{+02}$	349	5550	1710	−295	0	−772	0	−567	0	−294	0	613	0
2–4	$-0.19538\times10^{+02}$	1008	73	19	−299	0	−469	0	−217	0	−19	0	−1113	0
2–5	$-0.27766\times10^{+02}$	92	252	11	−28	0	−47	0	65	0	−209	0	1487	0
2–6	$-0.43206\times10^{+02}$	10	10	0	16	0	19	0	26	0	−91	0	910	0
2–7	$-0.65591\times10^{+02}$	1	0	0	0	0	0	0	2	0	20	0	−247	0
2–8	$-0.96499\times10^{+02}$	0	0	0	0	0	−1	0	−4	0	0	0	47	0
3–4	$-0.86384\times10^{+01}$	219	3057	2210	−255	0	491	0	699	0	136	0	469	0
3–5	$-0.16867\times10^{+02}$	1772	2059	151	−24	0	143	0	197	0	−143	0	441	0
3–6	$-0.32307\times10^{+02}$	114	135	6	12	0	26	0	83	0	−238	0	1573	0
3–7	$-0.54692\times10^{+02}$	3	2	0	−5	0	−6	0	−10	0	61	0	−654	0
3–8	$-0.85600\times10^{+02}$	0	0	0	0	0	−2	0	−6	0	−7	0	101	0
4–5	$-0.82284\times10^{+01}$	1475	2404	2078	−27	0	−29	0	428	0	−157	0	1146	0
4–6	$-0.23668\times10^{+02}$	678	672	39	5	0	−34	0	−163	0	249	0	−997	0
4–7	$-0.46054\times10^{+02}$	14	12	1	9	0	8	0	31	0	−86	0	902	0
4–8	$-0.76961\times10^{+02}$	0	0	0	0	0	3	0	5	0	14	0	−147	0
5–6	$-0.15440\times10^{+02}$	3563	3719	788	7	0	99	0	149	0	−232	0	−1557	0
5–7	$-0.37825\times10^{+02}$	156	157	7	−15	0	−15	0	−95	0	280	0	−1721	0
5–8	$-0.68733\times10^{+02}$	2	1	0	0	0	−2	0	2	0	−50	0	515	0
6–7	$-0.22386\times10^{+02}$	3580	3695	327	−21	0	−69	0	−321	0	608	0	1286	0
6–8	$-0.53293\times10^{+02}$	46	36	2	4	0	2	0	58	0	−182	0	1412	0
7–8	$-0.30908\times10^{+02}$	2209	2293	101	−22	0	−41	0	−286	0	750	0	796	0
						$\theta=45$	$\varphi=0$	H=800						
1–2	$-0.52229\times10^{+01}$	21	6158	590	−1134	0	−396	0	−58	0	−338	0	1331	0
1–3	$-0.88335\times10^{+01}$	1440	91	8	−1303	0	−454	0	−118	0	−53	0	−767	0
1–4	$-0.12946\times10^{+02}$	200	317	3	168	0	18	0	−28	0	208	0	−1734	0
1–5	$-0.17914\times10^{+02}$	40	91	13	−1450	0	−278	0	−57	0	−123	0	−8	0
1–6	$-0.25639\times10^{+02}$	10	5	2	3	0	5	0	−12	0	−46	0	890	0
1–7	$-0.36193\times10^{+02}$	0	0	1	124	0	27	0	23	0	10	0	−2	0
1–8	$-0.47205\times10^{+02}$	0	0	1	0	0	−1	0	−15	0	5	0	124	0
2–3	$-0.36106\times10^{+01}$	372	5145	832	−711	0	386	0	132	0	162	0	362	0
2–4	$-0.77232\times10^{+01}$	3055	1956	104	−51	0	−104	0	−131	0	361	0	−188	0
2–5	$-0.12691\times10^{+02}$	616	805	1	1378	0	603	0	49	0	252	0	−78	0
2–6	$-0.20416\times10^{+02}$	99	74	1	18	0	18	0	29	0	−172	0	1797	0
2–7	$-0.30970\times10^{+02}$	7	3	1	−605	0	29	0	−10	0	15	0	−13	0
2–8	$-0.41982\times10^{+02}$	1	0	1	0	0	−4	0	−21	0	−22	0	354	0
3–4	$-0.41126\times10^{+01}$	1493	2011	303	131	0	−40	0	62	0	−183	0	−1935	0
3–5	$-0.90802\times10^{+01}$	3258	2800	93	−1050	0	1021	0	180	0	345	0	−132	0
3–6	$-0.16805\times10^{+02}$	170	162	8	−16	0	−10	0	−42	0	171	0	−968	0
3–7	$-0.27360\times10^{+02}$	19	2	7	−1490	0	−78	0	43	0	−49	0	−16	0
3–8	$-0.38372\times10^{+02}$	1	0	0	0	0	3	0	7	0	32	0	−398	0
4–5	$-0.49676\times10^{+01}$	157	148	59	752	0	−86	0	−64	0	−1	0	8	0
4–6	$-0.12693\times10^{+02}$	3686	3732	51	−52	0	−1	0	−139	0	717	0	926	0
4–7	$-0.23247\times10^{+02}$	0	0	3	315	0	92	0	−13	0	47	0	−1	0
4–8	$-0.34259\times10^{+02}$	24	9	1	−1	0	8	0	−23	0	98	0	−1520	0
5–6	$-0.77250\times10^{+01}$	5	5	0	−1	0	0	0	−4	0	30	0	160	0
5–7	$-0.18279\times10^{+02}$	2328	2234	104	464	0	−1352	0	−290	0	−542	0	54	0
5–8	$-0.29292\times10^{+02}$	0	0	0	0	0	0	0	−2	0	3	0	−43	0
6–7	$-0.10554\times10^{+02}$	0	0	0	39	0	8	0	0	0	6	0	0	0
6–8	$-0.21567\times10^{+02}$	2295	2350	12	37	0	8	0	101	0	−815	0	−340	0
7–8	$-0.11012\times10^{+02}$	0	0	0	0	0	0	0	0	0	1	0	−7	0

TABLE 1. *Energy level differences, wave functions and transition probabilities for angles and field strengths indicated*—Continued

	ΔE	P_x	P_y	P_z	P_{11}		P_{10}		P_{00}		P_{-10}		P_{-1-1}	
	$\theta=45$ $\varphi=0$ H=1600													
1–2	$-0.81526\times10^{+01}$	17	5561	778	1348	0	565	0	140	0	412	0	−1585	0
1–3	$-0.14483\times10^{+02}$	965	2	1	1076	0	425	0	154	0	−5	0	1302	0
1–4	$-0.20853\times10^{+02}$	0	109	2	−869	0	−224	0	−24	0	−191	0	891	0
1–5	$-0.23112\times10^{+02}$	28	0	2	−449	0	−121	0	−35	0	23	0	−840	0
1–6	$-0.36084\times10^{+02}$	2	0	1	35	0	10	0	−10	0	−13	0	414	0
1–7	$-0.37070\times10^{+02}$	1	3	2	397	0	81	0	32	0	33	0	11	0
1–8	$-0.58858\times10^{+02}$	0	0	0	0	0	−1	0	−9	0	3	0	76	0
2–3	$-0.63305\times10^{+01}$	43	6103	1461	11	0	508	0	166	0	347	0	−99	0
2–4	$-0.12700\times10^{+02}$	2115	8	2	−750	0	−641	0	−231	0	−12	0	−836	0
2–5	$-0.14959\times10^{+02}$	58	922	40	−430	0	−279	0	28	0	−359	0	1069	0
2–6	$-0.27932\times10^{+02}$	20	31	0	−1	0	14	0	−15	0	142	0	−1237	0
2–7	$-0.28917\times10^{+02}$	24	49	1	943	0	235	0	28	0	103	0	−25	0
2–8	$-0.50705\times10^{+02}$	1	0	1	0	0	5	0	15	0	21	0	−291	0
3–4	$-0.63698\times10^{+01}$	18	5760	1341	1070	0	−576	0	−215	0	−325	0	−769	0
3–5	$-0.86286\times10^{+01}$	3850	377	44	450	0	−435	0	−296	0	108	0	765	0
3–6	$-0.21601\times10^{+02}$	249	149	3	−52	0	33	0	91	0	−258	0	1510	0
3–7	$-0.22587\times10^{+02}$	188	206	0	869	0	519	0	35	0	221	0	18	0
3–8	$-0.44375\times10^{+02}$	3	1	0	0	0	−4	0	−4	0	−55	0	573	0
4–5	$-0.22588\times10^{+01}$	216	823	3148	−439	0	−42	0	217	0	−88	0	1229	0
4–6	$-0.15232\times10^{+02}$	1257	1145	188	36	0	70	0	165	0	−367	0	−197	0
4–7	$-0.16217\times10^{+02}$	1447	1359	58	595	0	−1069	0	−212	0	−445	0	55	0
4–8	$-0.38005\times10^{+02}$	42	31	1	4	0	−1	0	32	0	−136	0	857	0
5–6	$-0.12973\times10^{+02}$	2244	2593	71	−107	0	2	0	−202	0	521	0	1392	0
5–7	$-0.13958\times10^{+02}$	786	549	55	858	0	−618	0	−184	0	−224	0	70	0
5–8	$-0.35746\times10^{+02}$	38	25	2	−2	0	2	0	−39	0	130	0	−1106	0
6–7	$-0.98556\times10^{+00}$	1	1	25	59	0	73	0	−19	0	42	0	−2	0
6–8	$-0.22773\times10^{+02}$	2211	2293	40	34	0	19	0	185	0	−780	0	−647	0
7–8	$-0.21788\times10^{+02}$	1	1	0	1	0	0	0	4	0	−18	0	−24	0
	$\theta=45$ $\varphi=0$ H=2400													
1–2	$-0.10624\times10^{+02}$	44	4526	1019	1325	0	657	0	219	0	461	0	−1678	0
1–3	$-0.19292\times10^{+02}$	459	2	1	889	0	421	0	195	0	−3	0	1210	0
1–4	$-0.26471\times10^{+02}$	0	97	6	598	0	206	0	30	0	177	0	−728	0
1–5	$-0.32992\times10^{+02}$	20	2	1	198	0	77	0	35	0	−37	0	664	0
1–6	$-0.39353\times10^{+02}$	2	1	0	271	0	78	0	28	0	20	0	88	0
1–7	$-0.47408\times10^{+02}$	1	1	0	−1	0	0	0	6	0	20	0	−304	0
1–8	$-0.71312\times10^{+02}$	0	0	0	0	0	−1	0	−6	0	0	0	67	0
2–3	$-0.86685\times10^{+01}$	65	6529	1671	369	0	639	0	254	0	404	0	−518	0
2–4	$-0.15847\times10^{+02}$	1421	1	3	798	0	623	0	274	0	20	0	930	0
2–5	$-0.22368\times10^{+02}$	77	375	24	265	0	144	0	−47	0	298	0	−1322	0
2–6	$-0.28729\times10^{+02}$	1	62	2	651	0	209	0	7	0	118	0	−59	0
2–7	$-0.36784\times10^{+02}$	16	11	0	4	0	6	0	19	0	−102	0	903	0
2–8	$-0.60688\times10^{+02}$	1	0	0	1	0	5	0	11	0	16	0	−212	0
3–4	$-0.71788\times10^{+01}$	1	5761	1999	−650	0	622	0	350	0	284	0	662	0
3–5	$-0.13700\times10^{+02}$	2344	709	64	−63	0	328	0	296	0	−205	0	123	0
3–6	$-0.20061\times10^{+02}$	307	71	24	611	0	591	0	50	0	283	0	−224	0
3–7	$-0.28116\times10^{+02}$	95	87	4	−24	0	−20	0	−70	0	220	0	−1462	0
3–8	$-0.52019\times10^{+02}$	2	1	0	0	0	−4	0	−3	0	−47	0	448	0
4–5	$-0.65207\times10^{+01}$	840	2177	2124	−370	0	3	0	120	0	69	0	1510	0
4–6	$-0.12882\times10^{+02}$	1453	897	603	−811	0	874	0	573	0	282	0	0	0
4–7	$-0.20937\times10^{+02}$	564	596	44	25	0	19	0	145	0	−334	0	577	0
4–8	$-0.44841\times10^{+02}$	11	7	0	0	0	2	0	−19	0	93	0	−720	0
5–6	$-0.63613\times10^{+01}$	676	810	180	−1325	0	271	0	310	0	44	0	73	0
5–7	$-0.14416\times10^{+02}$	3096	3052	307	−8	0	−68	0	−301	0	526	0	1545	0
5–8	$-0.38320\times10^{+02}$	74	57	4	4	0	3	0	65	0	−192	0	1212	0
6–7	$-0.80549\times10^{+01}$	7	6	10	−4	0	12	0	−2	0	26	0	−494	0
6–8	$-0.31959\times10^{+02}$	1	1	0	0	0	−1	0	−6	0	12	0	29	0
7–8	$-0.23904\times10^{+02}$	2182	2270	80	−30	0	−33	0	−256	0	753	0	808	0

TABLE 1. *Energy level differences, wave functions and transition probabilities for angles and field strengths indicated*—Continued

$\theta=45$ $\varphi=0$ H=3200

	ΔE	P_x	P_y	P_z	P_{11}		P_{10}		P_{00}		P_{-10}		P_{-1-1}	
1–2	$-0.12879\times10^{+02}$	74	4197	1111	1272	0	709	0	280	0	473	0	−1728	0
1–3	$-0.23520\times10^{+02}$	351	4	1	785	0	412	0	212	0	−8	0	1217	0
1–4	$-0.32650\times10^{+02}$	1	49	2	−385	0	−143	0	−11	0	−150	0	725	0
1–5	$-0.41550\times10^{+02}$	7	0	1	−259	0	−95	0	−35	0	−1	0	−377	0
1–6	$-0.44746\times10^{+02}$	0	3	0	130	0	42	0	10	0	42	0	−268	0
1–7	$-0.59282\times10^{+02}$	0	0	0	1	0	0	0	−5	0	−10	0	182	0
1–8	$-0.84327\times10^{+02}$	0	0	0	0	0	2	0	5	0	0	0	−42	0
2–3	$-0.10641\times10^{+02}$	114	6156	1920	493	0	710	0	337	0	436	0	−750	0
2–4	$-0.19770\times10^{+02}$	1026	47	9	−616	0	−527	0	−292	0	47	0	−1174	0
2–5	$-0.28671\times10^{+02}$	1	203	10	−507	0	−263	0	5	0	−277	0	977	0
2–6	$-0.31867\times10^{+02}$	58	1	0	311	0	159	0	69	0	−49	0	781	0
2–7	$-0.46403\times10^{+02}$	7	4	0	−2	0	−2	0	−11	0	72	0	−633	0
2–8	$-0.71448\times10^{+02}$	0	0	0	0	0	−3	0	−8	0	−11	0	155	0
3–4	$-0.91298\times10^{+01}$	164	5587	2460	407	0	−528	0	−369	0	−259	0	−515	0
3–5	$-0.18031\times10^{+02}$	1775	46	14	−194	0	−668	0	−363	0	−16	0	−509	0
3–6	$-0.21226\times10^{+02}$	42	627	44	169	0	314	0	−42	0	375	0	−723	0
3–7	$-0.35762\times10^{+02}$	55	48	3	18	0	19	0	66	0	−186	0	1224	0
3–8	$-0.60807\times10^{+02}$	2	1	0	1	0	5	0	2	0	44	0	−370	0
4–5	$-0.89007\times10^{+01}$	44	4059	2336	−937	0	458	0	401	0	212	0	1141	0
4–6	$-0.12097\times10^{+02}$	2667	350	81	458	0	−535	0	−428	0	−42	0	902	0
4–7	$-0.26632\times10^{+02}$	354	372	28	23	0	25	0	153	0	−330	0	1063	0
4–8	$-0.51677\times10^{+02}$	9	5	0	0	0	2	0	−19	0	91	0	−676	0
5–6	$-0.31959\times10^{+01}$	15	785	4795	589	0	180	0	−650	0	286	0	−912	0
5–7	$-0.17732\times10^{+02}$	1469	1475	175	−9	0	−66	0	−262	0	380	0	744	0
5–8	$-0.42776\times10^{+02}$	39	31	3	4	0	4	0	55	0	−153	0	884	0
6–7	$-0.14536\times10^{+02}$	1760	1778	332	−7	0	−88	0	−253	0	311	0	1560	0
6–8	$-0.39581\times10^{+02}$	58	51	4	5	0	6	0	67	0	−170	0	810	0
7–8	$-0.25045\times10^{+02}$	2134	2227	127	−27	0	−50	0	−317	0	716	0	966	0

$\theta=45$ $\varphi=0$ H=4000

	ΔE	P_x	P_y	P_z	P_{11}		P_{10}		P_{00}		P_{-10}		P_{-1-1}	
1–2	$-0.15007\times10^{+02}$	110	3851	1208	1199	0	742	0	338	0	478	0	−1748	0
1–3	$-0.27541\times10^{+02}$	252	6	0	−657	0	−385	0	−224	0	23	0	−1190	0
1–4	$-0.38538\times10^{+02}$	1	38	2	303	0	127	0	9	0	139	0	−667	0
1–5	$-0.47300\times10^{+02}$	5	0	1	−179	0	−76	0	−31	0	1	0	−306	0
1–6	$-0.54707\times10^{+02}$	1	0	0	−29	0	−8	0	1	0	−30	0	274	0
1–7	$-0.71525\times10^{+02}$	0	1	0	−4	0	5	0	−4	0	−2	0	125	0
1–8	$-0.97771\times10^{+02}$	0	0	0	0	0	0	0	−2	0	0	0	23	0
2–3	$-0.12534\times10^{+02}$	179	5873	2060	−550	0	−741	0	−402	0	−434	0	886	0
2–4	$-0.23531\times10^{+02}$	805	58	10	583	0	510	0	311	0	−56	0	1287	0
2–5	$-0.32293\times10^{+02}$	1	126	8	−362	0	−213	0	12	0	−237	0	862	0
2–6	$-0.39700\times10^{+02}$	24	4	0	−36	0	−26	0	−52	0	131	0	−911	0
2–7	$-0.56518\times10^{+02}$	3	9	0	−45	0	−42	0	−6	0	16	0	−448	0
2–8	$-0.82764\times10^{+02}$	0	0	0	1	0	2	0	7	0	9	0	−77	0
3–4	$-0.10997\times10^{+02}$	235	5680	2658	288	0	−591	0	−442	0	−283	0	−293	0
3–5	$-0.19759\times10^{+02}$	1304	73	19	177	0	582	0	365	0	34	0	530	0
3–6	$-0.27166\times10^{+02}$	177	141	27	229	0	103	0	−135	0	381	0	−1299	0
3–7	$-0.43985\times10^{+02}$	25	202	1	−60	0	−101	0	−51	0	100	0	−1006	0
3–8	$-0.70230\times10^{+02}$	1	0	0	0	0	−2	0	2	0	34	0	−152	0
4–5	$-0.87625\times10^{+01}$	19	3188	2919	829	0	−426	0	−607	0	−83	0	−773	0
4–6	$-0.16170\times10^{+02}$	1965	435	294	462	0	−194	0	−347	0	250	0	174	0
4–7	$-0.32988\times10^{+02}$	191	1085	17	−132	0	−133	0	−139	0	259	0	−1230	0
4–8	$-0.59233\times10^{+02}$	6	3	0	−2	0	−11	0	−17	0	80	0	−240	0
5–6	$-0.74073\times10^{+01}$	951	345	2428	200	0	−168	0	215	0	−146	0	1291	0
5–7	$-0.24225\times10^{+02}$	541	1835	56	3	0	−45	0	−206	0	374	0	−292	0
5–8	$-0.50471\times10^{+02}$	14	11	1	−5	0	−15	0	−37	0	108	0	−351	0
6–7	$-0.16818\times10^{+02}$	2747	1856	626	−503	0	61	0	365	0	−332	0	−619	0
6–8	$-0.43063\times10^{+02}$	97	87	7	7	0	−2	0	99	0	13	0	1271	0
7–8	$-0.26245\times10^{+02}$	2091	2193	178	21	0	44	0	370	0	−678	0	−708	0

TABLE 1. *Energy level differences, wave functions and transition probabilities for angles and field strengths indicated*—Continued

	ΔE	P_x	P_y	P_z	$P_{1\,1}$		$P_{1\,0}$		$P_{0\,0}$		$P_{-1\,0}$		$P_{-1\,-1}$	
					$\theta=45$	$\varphi=0$	H=4800							
1–2	$-0.17058\times10^{+02}$	162	3634	1259	−1106	0	−755	0	−390	0	−467	0	1779	0
1–3	$-0.31438\times10^{+02}$	196	4	0	−569	0	−368	0	−235	0	32	0	−1176	0
1–4	$-0.43974\times10^{+02}$	0	26	2	−247	0	−113	0	−7	0	−126	0	601	0
1–5	$-0.53978\times10^{+02}$	3	0	0	−105	0	−51	0	−24	0	11	0	−299	0
1–6	$-0.65274\times10^{+02}$	0	0	0	−10	0	−3	0	0	0	−17	0	187	0
1–7	$-0.84024\times10^{+02}$	0	0	0	0	0	−1	0	−3	0	−3	0	80	0
1–8	$-0.11155\times10^{+03}$	0	0	0	0	0	0	0	−2	0	0	0	22	0
2–3	$-0.14380\times10^{+02}$	261	5620	2161	559	0	752	0	457	0	426	0	−982	0
2–4	$-0.26915\times10^{+02}$	650	68	11	502	0	479	0	319	0	−67	0	1317	0
2–5	$-0.36919\times10^{+02}$	9	82	5	212	0	124	0	−42	0	222	0	−970	0
2–6	$-0.48216\times10^{+02}$	11	5	0	44	0	31	0	40	0	−87	0	734	0
2–7	$-0.66965\times10^{+02}$	1	1	0	0	0	0	0	3	0	−34	0	318	0
2–8	$-0.94496\times10^{+02}$	0	0	0	0	0	−2	0	−5	0	−5	0	80	0
3–4	$-0.12536\times10^{+02}$	301	5391	2823	−167	0	598	0	521	0	271	0	214	0
3–5	$-0.22540\times10^{+02}$	1105	273	53	155	0	455	0	361	0	−63	0	668	0
3–6	$-0.33836\times10^{+02}$	106	163	14	18	0	15	0	−130	0	286	0	−1277	0
3–7	$-0.52586\times10^{+02}$	12	9	0	−9	0	−11	0	−39	0	114	0	−818	0
3–8	$-0.80116\times10^{+02}$	1	0	0	2	0	5	0	2	0	27	0	−214	0
4–5	$-0.10004\times10^{+02}$	338	3385	3308	−548	0	222	0	580	0	−14	0	1057	0
4–6	$-0.21300\times10^{+02}$	1287	1026	172	−15	0	200	0	350	0	−239	0	76	0
4–7	$-0.40050\times10^{+02}$	92	96	8	17	0	22	0	116	0	−248	0	1214	0
4–8	$-0.67580\times10^{+02}$	3	2	0	0	0	−2	0	14	0	−64	0	457	0
5–6	$-0.11296\times10^{+02}$	1681	2536	2207	−174	0	−220	0	64	0	−134	0	1818	0
5–7	$-0.30046\times10^{+02}$	445	456	46	−14	0	−52	0	−225	0	335	0	−617	0
5–8	$-0.57576\times10^{+02}$	12	8	1	0	0	−1	0	−38	0	110	0	−673	0
6–7	$-0.18749\times10^{+02}$	2829	3057	784	38	0	172	0	402	0	−348	0	−1850	0
6–8	$-0.46280\times10^{+02}$	104	96	9	7	0	16	0	117	0	−251	0	1036	0
7–8	$-0.27530\times10^{+02}$	2053	2170	232	27	0	90	0	414	0	−643	0	−1185	0
					$\theta=60$	$\varphi=60$	H=800							
1–2	$-0.50399\times10^{+01}$	4870	1803	568	−528	−1093	124	−358	60	−8	202	35	769	−1030
1–3	$-0.89308\times10^{+01}$	321	1038	2	1001	946	−153	354	−96	−32	−2	307	223	−761
1–4	$-0.12891\times10^{+02}$	404	350	4	−53	29	−5	−80	−15	−27	86	121	−309	−1665
1–5	$-0.17860\times10^{+02}$	65	63	2	1346	−188	88	157	4	0	19	77	−9	29
1–6	$-0.25601\times10^{+02}$	3	5	3	−7	13	7	9	−17	−4	41	24	430	−849
1–7	$-0.36151\times10^{+02}$	0	1	2	−252	189	−27	−10	3	−26	−8	0	−2	0
1–8	$-0.47168\times10^{+02}$	0	0	1	0	0	1	0	−6	−14	−7	9	−72	−52
2–3	$-0.38909\times10^{+01}$	3735	1455	932	−462	−373	−40	311	−137	−58	−46	83	2	−375
2–4	$-0.78515\times10^{+01}$	2261	2579	90	3	−82	63	−50	81	90	−303	−128	73	132
2–5	$-0.12820\times10^{+02}$	560	735	24	1253	−175	169	528	−32	−97	33	296	−35	−18
2–6	$-0.20561\times10^{+02}$	112	105	1	38	4	1	0	17	7	−124	−73	−544	1655
2–7	$-0.31112\times10^{+02}$	2	10	1	−589	508	−2	−46	1	−7	46	−41	−2	−2
2–8	$-0.42128\times10^{+02}$	1	0	1	0	0	−4	−7	7	22	−2	−2	246	270
3–4	$-0.39607\times10^{+01}$	1827	2032	290	−29	−53	25	−56	69	35	−225	−110	74	−1855
3–5	$-0.89294\times10^{+01}$	3109	3117	120	1229	287	−401	−912	149	120	−180	−294	11	103
3–6	$-0.16670\times10^{+02}$	123	138	12	−6	1	4	5	16	20	−93	−131	−680	748
3–7	$-0.27221\times10^{+02}$	42	32	4	1255	−421	32	180	−4	−42	−46	87	3	3
3–8	$-0.38237\times10^{+02}$	2	3	0	0	−2	−2	−7	5	10	−11	11	108	347
4–5	$-0.49688\times10^{+01}$	88	88	4	−691	−549	82	113	−8	0	72	30	−9	13
4–6	$-0.12709\times10^{+02}$	3842	3760	66	−27	65	−16	−48	117	−86	88	−736	823	−360
4–7	$-0.23260\times10^{+02}$	0	0	1	−158	−38	−11	−3	5	9	−5	−10	4	0
4–8	$-0.34276\times10^{+02}$	19	11	0	1	1	−7	−30	−6	−2	−22	−59	−160	1522
5–6	$-0.77407\times10^{+01}$	3	3	0	0	8	0	−12	0	−2	17	22	78	−40
5–7	$-0.18291\times10^{+02}$	2283	2319	39	−534	−215	45	1382	−170	−58	35	567	−4	−45
5–8	$-0.29308\times10^{+02}$	0	0	0	0	1	0	1	0	0	4	−2	18	−17
6–7	$-0.10551\times10^{+02}$	0	0	0	5	1	3	−4	0	0	0	0	0	0
6–8	$-0.21567\times10^{+02}$	2306	2341	13	38	0	12	2	53	90	−820	0	−164	−292
7–8	$-0.11016\times10^{+02}$	0	0	0	0	0	0	0	0	0	−3	0	0	−4

TABLE 1. *Energy level differences, wave functions and transition probabilities for angles and field strengths indicated*—Continued

$\theta=60 \quad \varphi=60 \quad H=1600$

	ΔE	P_x	P_y	P_z	P_{11}		P_{10}		P_{00}		P_{-10}		P_{-1-1}	
1–2	$-0.76147\times10^{+01}$	4025	1352	822	−1085	−881	338	−354	128	49	−14	18	241	−1524
1–3	$-0.14632\times10^{+02}$	206	610	4	173	−970	68	−76	109	−91	−53	127	−1218	435
1–4	$-0.21136\times10^{+02}$	76	34	0	−222	855	−168	−1	3	−2	−118	−74	−654	181
1–5	$-0.22603\times10^{+02}$	27	58	3	−315	−147	49	−25	32	22	43	−80	104	964
1–6	$-0.35955\times10^{+02}$	2	1	2	−2	−4	5	0	20	0	−22	−25	−271	414
1–7	$-0.36910\times10^{+02}$	2	3	1	−166	−396	46	−20	−20	1	20	−6	12	−10
1–8	$-0.58738\times10^{+02}$	0	0	0	1	0	0	−5	6	9	2	−7	35	72
2–3	$-0.70174\times10^{+01}$	4473	1509	1445	35	−50	312	−99	88	−156	366	−13	85	14
2–4	$-0.13521\times10^{+02}$	481	1363	12	−438	608	−216	250	−106	235	127	191	738	70
2–5	$-0.14988\times10^{+02}$	816	396	66	−251	−244	−82	131	−23	−8	−239	2	260	−1051
2–6	$-0.28341\times10^{+02}$	47	38	1	−3	−32	28	26	−26	12	39	83	1033	−735
2–7	$-0.29295\times10^{+02}$	37	53	0	−32	−931	89	−90	27	−15	−48	−45	−26	16
2–8	$-0.51123\times10^{+02}$	0	0	1	2	0	7	−2	−15	−10	2	5	−24	−303
3–4	$-0.65038\times10^{+01}$	4250	1535	1074	−493	−1071	−125	21	−233	17	56	401	459	−655
3–5	$-0.79706\times10^{+01}$	1597	3197	91	424	−104	358	170	61	264	157	−143	−640	−638
3–6	$-0.21323\times10^{+02}$	195	203	0	5	0	75	−14	43	36	−182	−22	142	1511
3–7	$-0.22278\times10^{+02}$	186	190	16	−799	−407	−4	−443	90	58	5	−253	−3	−14
3–8	$-0.44106\times10^{+02}$	3	2	1	0	0	−5	2	−1	16	−14	4	492	209
4–5	$-0.14668\times10^{+01}$	632	390	2718	−334	140	325	246	−31	−190	51	270	−1067	−836
4–6	$-0.14819\times10^{+02}$	870	830	35	8	4	14	14	91	77	−334	−59	−26	−112
4–7	$-0.15774\times10^{+02}$	1665	1653	55	−668	−275	107	854	−167	−136	−1	179	−8	−41
4–8	$-0.37602\times10^{+02}$	12	10	0	1	−1	−1	−1	0	5	−47	11	697	252
5–6	$-0.13353\times10^{+02}$	2745	2816	173	−10	47	−26	−97	168	−146	153	−610	1254	−418
5–7	$-0.14308\times10^{+02}$	449	383	10	−170	683	40	−79	63	−58	−323	12	−50	16
5–8	$-0.36135\times10^{+02}$	38	29	0	2	2	−1	−12	4	1	−26	−80	−230	1201
6–7	$-0.95488\times10^{+00}$	0	0	22	−11	−15	−101	−39	25	0	−61	−30	2	−1
6–8	$-0.22783\times10^{+02}$	2248	2302	47	35	0	30	9	100	168	−804	8	−302	−528
7–8	$-0.21828\times10^{+02}$	1	1	0	0	0	0	0	−1	−3	20	2	3	11

$\theta=60 \quad \varphi=60 \quad H=2400$

	ΔE	P_x	P_y	P_z	P_{11}		P_{10}		P_{00}		P_{-10}		P_{-1-1}	
1–2	$-0.97783\times10^{+01}$	3516	1236	972	1090	−813	−143	−85	30	−204	289	−274	1523	608
1–3	$-0.19321\times10^{+02}$	135	454	4	−884	−248	−204	157	120	120	2	315	331	1306
1–4	$-0.26751\times10^{+02}$	45	13	1	−528	−203	−34	−31	−8	−4	62	85	−99	−670
1–5	$-0.32624\times10^{+02}$	5	7	1	74	35	16	−2	−17	−10	41	8	−26	−624
1–6	$-0.38944\times10^{+02}$	2	4	1	91	364	24	8	10	−3	19	−6	−3	−1
1–7	$-0.47171\times10^{+02}$	1	0	1	−4	5	−8	0	3	17	−3	0	210	185
1–8	$-0.71116\times10^{+02}$	0	0	0	0	0	5	−1	−4	−5	1	−1	−15	−44
2–3	$-0.95424\times10^{+01}$	4809	1641	1765	−135	340	−183	225	−163	217	−230	49	−533	50
2–4	$-0.16973\times10^{+02}$	318	948	0	−302	560	−298	195	−150	243	−66	383	932	−26
2–5	$-0.22846\times10^{+02}$	181	133	7	102	−149	32	−21	−27	61	−42	165	1294	115
2–6	$-0.29166\times10^{+02}$	48	65	1	773	−69	189	−38	−23	−50	65	−94	7	−4
2–7	$-0.37393\times10^{+02}$	20	13	2	5	3	9	0	27	−3	35	−50	−668	609
2–8	$-0.61338\times10^{+02}$	0	0	0	0	1	−4	2	−9	11	4	17	201	−51
3–4	$-0.74303\times10^{+01}$	3671	1236	2166	280	584	270	−165	350	−31	93	100	−365	522
3–5	$-0.13304\times10^{+02}$	1205	1624	124	0	−1	−128	198	−260	52	130	381	141	−162
3–6	$-0.19624\times10^{+02}$	429	438	44	−241	416	−592	38	−100	185	−243	−29	7	5
3–7	$-0.27850\times10^{+02}$	162	158	2	30	19	11	4	60	43	−69	−161	163	1401
3–8	$-0.51795\times10^{+02}$	3	2	1	1	0	−6	7	−17	−1	30	21	212	−475
4–5	$-0.58734\times10^{+01}$	2335	1744	1440	−106	−280	17	−190	3	0	−31	−118	1090	−1454
4–6	$-0.12193\times10^{+02}$	1488	1489	190	488	−978	−1080	−18	−212	297	−387	9	32	−7
4–7	$-0.20420\times10^{+02}$	438	432	18	−33	−19	−29	9	−97	−83	176	177	−131	−691
4–8	$-0.44365\times10^{+02}$	10	8	0	0	0	2	−5	13	2	−58	−29	−215	610
5–6	$-0.63199\times10^{+01}$	245	232	28	−311	945	388	49	82	−95	111	19	−22	6
5–7	$-0.14547\times10^{+02}$	3144	3130	355	−7	4	−97	12	−206	−223	597	75	472	1537
5–8	$-0.38491\times10^{+02}$	62	55	0	5	4	−1	−5	22	7	−163	−70	−271	1198
6–7	$-0.82267\times10^{+01}$	2	2	0	−3	3	3	2	−1	2	1	35	−163	−77
6–8	$-0.32172\times10^{+02}$	0	0	0	0	0	0	0	0	0	1	−2	−14	−13
7–8	$-0.23945\times10^{+02}$	2199	2261	94	0	−31	17	33	−235	136	−13	796	−698	401

	ΔE	P_x	P_y	P_z	$P_{1\,1}$		$P_{1\,0}$		$P_{0\,0}$		$P_{-1\,0}$		$P_{-1\,-1}$	
					$\theta=60$	$\varphi=60$	H=3200							
1–2	$-0.11792\times10^{+02}$	3600	1223	947	−621	−1180	267	−512	253	−13	169	−259	917	−1446
1–3	$-0.23396\times10^{+02}$	159	465	4	848	−329	26	45	−31	−160	−105	266	−1108	−902
1–4	$-0.33076\times10^{+02}$	4	1	3	88	395	−13	−25	36	−9	−1	134	−551	458
1–5	$-0.41817\times10^{+02}$	0	1	1	188	163	−11	34	11	9	0	53	81	−260
1–6	$-0.43498\times10^{+02}$	0	0	0	102	−72	19	23	0	13	0	5	253	125
1–7	$-0.58936\times10^{+02}$	0	0	0	0	0	2	−2	8	4	2	−9	−10	110
1–8	$-0.84073\times10^{+02}$	0	0	0	0	0	1	1	0	5	2	0	9	9
2–3	$-0.11603\times10^{+02}$	4123	1480	2145	378	−137	−99	5	−44	−365	514	−110	540	416
2–4	$-0.21284\times10^{+02}$	252	718	2	153	545	141	−224	−294	92	−73	−420	927	−803
2–5	$-0.30024\times10^{+02}$	114	21	6	420	340	−84	−31	−13	−20	65	−135	−199	799
2–6	$-0.31706\times10^{+02}$	29	70	0	197	−152	−65	62	14	−82	−66	45	−790	−367
2–7	$-0.47144\times10^{+02}$	6	5	1	−2	0	3	17	−19	−11	18	10	−25	−649
2–8	$-0.72280\times10^{+02}$	0	0	0	1	0	3	4	1	−12	2	0	−139	−70
3–4	$-0.96804\times10^{+01}$	4246	1395	2509	−333	104	234	79	−44	−361	369	57	−345	−234
3–5	$-0.18421\times10^{+02}$	259	1266	1	136	−186	−52	156	161	−372	−186	314	−550	−81
3–6	$-0.20103\times10^{+02}$	652	279	102	−95	−118	72	211	−35	7	−251	−74	278	−669
3–7	$-0.35541\times10^{+02}$	73	70	1	7	−16	54	16	−40	50	−20	89	1225	−206
3–8	$-0.60677\times10^{+02}$	2	1	0	1	1	0	3	−16	−2	1	15	138	−388
4–5	$-0.87407\times10^{+01}$	3268	1018	1764	964	443	−292	−27	324	152	−606	−368	138	1083
4–6	$-0.10423\times10^{+02}$	1170	2281	302	238	−324	316	40	−90	338	167	−361	−1065	−73
4–7	$-0.25860\times10^{+02}$	382	394	17	24	5	55	−87	101	120	−196	5	376	1019
4–8	$-0.50997\times10^{+02}$	11	9	0	0	0	1	3	−6	18	−36	8	646	127
5–6	$-0.16818\times10^{+01}$	439	179	4634	460	−91	−702	−258	135	618	−319	−223	681	665
5–7	$-0.17120\times10^{+02}$	1180	1172	183	1	2	−23	55	−219	−60	250	186	−162	696
5–8	$-0.42256\times10^{+02}$	31	29	0	−3	1	0	0	−6	−26	75	24	−552	−513
6–7	$-0.15438\times10^{+02}$	2094	2045	348	6	−11	−96	−165	132	−248	307	−457	1563	0
6–8	$-0.40574\times10^{+02}$	49	46	0	3	6	3	−1	36	0	19	−92	−482	795
7–8	$-0.25136\times10^{+02}$	2154	2219	149	28	0	73	16	164	295	−767	51	−496	−828
					$\theta=60$	$\varphi=60$	H=4000							
1–2	$-0.13737\times10^{+02}$	3020	1073	1138	−1045	671	135	148	−17	324	−437	278	−1549	−767
1–3	$-0.27283\times10^{+02}$	100	256	20	284	627	118	−253	−196	−26	−109	−317	706	−1086
1–4	$-0.39089\times10^{+02}$	12	4	0	292	−101	−72	−45	5	22	6	−53	498	415
1–5	$-0.47142\times10^{+02}$	1	3	0	109	−131	8	25	1	−5	−7	11	−212	−53
1–6	$-0.53715\times10^{+02}$	1	0	0	35	−13	−13	−16	2	12	0	−1	253	172
1–7	$-0.71076\times10^{+02}$	0	0	0	0	−3	1	6	5	−7	0	−1	−98	9
1–8	$-0.97476\times10^{+02}$	0	0	0	0	0	−1	3	4	0	1	1	−6	18
2–3	$-0.13546\times10^{+02}$	4267	1552	2127	−497	205	115	15	47	417	−501	187	−735	−498
2–4	$-0.25352\times10^{+02}$	215	579	3	166	510	171	−273	−314	77	−103	−451	907	−900
2–5	$-0.33406\times10^{+02}$	65	9	4	279	261	−75	16	−6	−21	42	−209	−237	617
2–6	$-0.39978\times10^{+02}$	29	40	1	16	48	62	−33	−73	15	28	21	626	−811
2–7	$-0.57339\times10^{+02}$	2	1	1	11	0	−8	−3	17	7	−9	−30	42	467
2–8	$-0.83739\times10^{+02}$	1	0	0	0	1	−1	−2	0	11	1	1	106	36
3–4	$-0.11806\times10^{+02}$	4283	1452	2714	205	−86	−117	−65	37	443	−246	−42	281	176
3–5	$-0.19859\times10^{+02}$	153	865	8	−156	148	−109	−208	−146	364	−114	−170	420	90
3–6	$-0.26432\times10^{+02}$	509	389	79	−20	2	−22	87	−10	−141	179	−151	−971	−680
3–7	$-0.43793\times10^{+02}$	28	33	1	3	−2	18	−11	−28	44	−100	40	1031	−86
3–8	$-0.70193\times10^{+02}$	1	1	0	0	1	1	0	−14	−1	0	7	117	−300
4–5	$-0.80540\times10^{+01}$	2534	693	2161	816	488	−127	−317	545	237	−281	34	−116	834
4–6	$-0.14627\times10^{+02}$	2038	2221	452	52	55	33	−272	301	8	−214	−204	215	−748
4–7	$-0.31987\times10^{+02}$	149	118	1	1	−25	0	30	−87	−80	125	211	−275	−1294
4–8	$-0.58388\times10^{+02}$	5	3	0	0	0	0	0	4	−14	18	1	−525	−93
5–6	$-0.65728\times10^{+01}$	1106	1001	1802	−15	96	69	277	158	−82	2	0	−1260	1055
5–7	$-0.23933\times10^{+02}$	300	273	32	4	17	26	−37	146	54	−76	−209	−17	304
5–8	$-0.50334\times10^{+02}$	9	8	0	2	0	−2	0	3	19	−38	−12	396	292
6–7	$-0.17360\times10^{+02}$	3146	3092	727	1	28	−163	51	−302	−257	456	125	283	1643
6–8	$-0.43761\times10^{+02}$	103	101	1	−5	7	4	−1	25	−68	124	−7	−1066	−389
7–8	$-0.26400\times10^{+02}$	2124	2179	209	23	0	95	10	179	349	−748	88	−581	−930

429-270 O - 71 - 8

TABLE 1. *Energy level differences, wave functions and transition probabilities for angles and field strengths indicated*—Continued

	ΔE	P_x	P_y	P_z	$P_{1\,1}$		$P_{1\,0}$		$P_{0\,0}$		$P_{-1\,0}$		$P_{-1\,-1}$	
						$\theta=60$	$\varphi=60$	$H=4800$						
1–2	$-0.15652\times10^{+02}$	2855	1039	1216	−1248	−1527	−124	−8	−368	−65	−248	−396	408	−1131
1–3	$-0.31077\times10^{+02}$	76	207	4	219	−278	82	−216	40	202	−50	14	−579	−204
1–4	$-0.44544\times10^{+02}$	8	3	0	−51	4	−34	0	24	−7	−83	0	103	−306
1–5	$-0.53730\times10^{+02}$	0	1	0	−21	4	−19	37	−7	3	−20	6	−28	64
1–6	$-0.64316\times10^{+02}$	0	0	0	−20	−24	−12	−11	2	−8	−21	−11	−60	−18
1–7	$-0.83479\times10^{+02}$	0	0	0	0	4	−2	−3	2	−6	1	−1	20	−4
1–8	$-0.11123\times10^{+03}$	0	0	0	0	5	0	3	1	3	2	2	3	−1
2–3	$-0.15425\times10^{+02}$	4101	1550	2256	682	−348	372	−35	−7	−478	41	−176	496	313
2–4	$-0.28892\times10^{+02}$	205	480	6	−157	−463	−118	242	329	−48	88	335	−468	692
2–5	$-0.38077\times10^{+02}$	41	16	3	−131	−275	35	−54	−36	5	15	71	239	−408
2–6	$-0.48664\times10^{+02}$	9	11	1	273	−142	−114	−28	3	−43	−104	−39	259	135
2–7	$-0.67827\times10^{+02}$	1	1	0	6	11	11	−2	7	−13	5	0	−86	5
2–8	$-0.95582\times10^{+02}$	0	0	0	−24	16	8	7	3	8	10	6	−16	−4
3–4	$-0.13467\times10^{+02}$	4119	1589	2920	293	−163	−273	−195	70	524	−341	−10	272	123
3–5	$-0.22653\times10^{+02}$	371	736	36	−469	268	−16	−154	38	359	−43	71	251	195
3–6	$-0.33239\times10^{+02}$	222	175	13	18	−185	−108	177	161	20	−31	−90	−676	1044
3–7	$-0.52402\times10^{+02}$	14	26	1	0	14	−26	43	−36	−38	67	−39	−1	−424
3–8	$-0.80157\times10^{+02}$	1	0	0	40	42	26	−16	−11	5	34	−2	35	−156
4–5	$-0.91853\times10^{+01}$	2467	939	2934	−35	−235	−74	−209	613	13	−105	−332	−862	1682
4–6	$-0.19772\times10^{+02}$	1266	1371	530	−1364	880	−241	−319	−20	−238	−196	−55	−110	−112
4–7	$-0.38935\times10^{+02}$	198	106	4	−89	−94	142	−89	77	−96	67	−43	−55	10
4–8	$-0.66689\times10^{+02}$	4	3	0	−23	108	9	51	9	16	11	8	−250	−43
5–6	$-0.10587\times10^{+02}$	2207	1908	1141	1046	−704	64	167	12	36	373	106	1814	1018
5–7	$-0.29749\times10^{+02}$	279	133	8	90	90	−171	78	−91	120	−143	−16	−560	61
5–8	$-0.57504\times10^{+02}$	6	5	0	62	−141	−1	−43	−7	−14	−13	5	222	60
6–7	$-0.19163\times10^{+02}$	3137	2774	611	97	168	−64	−66	−325	−186	−207	144	171	537
6–8	$-0.46917\times10^{+02}$	52	49	2	−171	−248	184	−235	−63	−6	87	−122	−89	70
7–8	$-0.27755\times10^{+02}$	2099	2140	268	637	953	−449	1146	432	58	−432	−329	664	−920
						$\theta=60$	$\varphi=0$	$H=800$						
1–2	$-0.58580\times10^{+01}$	8	5889	668	−1253	0	−399	0	−45	0	−361	0	1397	0
1–3	$-0.10521\times10^{+02}$	1183	50	7	−1418	0	−435	0	−130	0	−35	0	−934	0
1–4	$-0.13823\times10^{+02}$	111	287	4	312	0	49	0	−26	0	211	0	−1363	0
1–5	$-0.20250\times10^{+02}$	17	54	6	0	−1171	0	−114	0	39	0	−55	0	41
1–6	$-0.25654\times10^{+02}$	23	23	1	34	0	1	0	7	0	83	0	−1056	0
1–7	$-0.38882\times10^{+02}$	0	0	1	196	0	−11	0	23	0	−14	0	5	0
1–8	$-0.46655\times10^{+02}$	0	0	1	0	0	3	0	17	0	−1	0	−156	0
2–3	$-0.46627\times10^{+01}$	245	6389	937	−325	0	379	0	108	0	252	0	233	0
2–4	$-0.79648\times10^{+01}$	2694	1040	86	−99	0	−143	0	−165	0	285	0	−107	0
2–5	$-0.14392\times10^{+02}$	429	377	0	0	1472	0	371	0	−49	0	227	0	−82
2–6	$-0.19796\times10^{+02}$	309	195	4	−26	0	−29	0	−53	0	242	0	−1715	0
2–7	$-0.33024\times10^{+02}$	0	1	1	−609	0	24	0	−15	0	−10	0	−7	0
2–8	$-0.40797\times10^{+02}$	1	0	1	0	0	7	0	20	0	29	0	−446	0
3–4	$-0.33021\times10^{+01}$	955	2007	809	291	0	82	0	49	0	−109	0	−1808	0
3–5	$-0.97297\times10^{+01}$	3106	2716	183	0	−831	0	1049	0	−241	0	497	0	−48
3–6	$-0.15133\times10^{+02}$	572	617	53	51	0	23	0	80	0	−285	0	595	0
3–7	$-0.28362\times10^{+02}$	7	23	4	−1346	0	72	0	24	0	66	0	1	0
3–8	$-0.36134\times10^{+02}$	4	1	0	1	0	−1	0	0	0	−54	0	616	0
4–5	$-0.64276\times10^{+01}$	549	564	63	0	1260	0	−465	0	105	0	−90	0	−5
4–6	$-0.11831\times10^{+02}$	2921	3342	15	96	0	−5	0	97	0	−652	0	−1170	0
4–7	$-0.25060\times10^{+02}$	1	2	2	506	0	−31	0	−15	0	−36	0	−2	0
4–8	$-0.32832\times10^{+02}$	2	0	1	−1	0	−7	0	22	0	−41	0	1433	0
5–6	$-0.54036\times10^{+01}$	1	1	1	0	0	0	5	0	−8	0	25	0	147
5–7	$-0.18632\times10^{+02}$	2427	2160	88	0	−623	0	1391	0	−262	0	594	0	−61
5–8	$-0.26404\times10^{+02}$	0	0	0	0	0	0	0	0	4	0	3	0	−3
6–7	$-0.13229\times10^{+02}$	0	0	0	5	0	−5	0	0	0	−9	0	0	0
6–8	$-0.21001\times10^{+02}$	2304	2359	19	39	0	10	0	128	0	−814	0	−298	0
7–8	$-0.77723\times10^{+01}$	0	0	0	0	0	0	0	1	0	−1	0	1	0

TABLE 1. *Energy level differences, wave functions and transition probabilities for angles and field strengths indicated*—Continued

	ΔE	P_x	P_y	P_z	$P_{1\,1}$		$P_{1\,0}$		$P_{0\,0}$		$P_{-1\,0}$		$P_{-1\,-1}$	
					$\theta=60$ $\varphi=0$ H=1600									
1–2	$-0.91318\times10^{+01}$	15	4897	942	1401	0	539	0	103	0	458	0	−1642	0
1–3	$-0.16718\times10^{+02}$	588	1	5	−1087	0	−431	0	−182	0	4	0	−1141	0
1–4	$-0.23541\times10^{+02}$	4	111	4	586	0	168	0	12	0	187	0	−896	0
1–5	$-0.27216\times10^{+02}$	25	7	3	590	0	171	0	46	0	39	0	312	0
1–6	$-0.36465\times10^{+02}$	5	2	1	−8	0	−2	0	−5	0	−43	0	516	0
1–7	$-0.42628\times10^{+02}$	1	3	1	323	0	79	0	27	0	33	0	2	0
1–8	$-0.57915\times10^{+02}$	0	0	0	1	0	3	0	11	0	2	0	−120	0
2–3	$-0.75863\times10^{+01}$	5	6709	1563	−292	0	−514	0	−118	0	−393	0	372	0
2–4	$-0.14409\times10^{+02}$	1695	63	17	709	0	488	0	258	0	−120	0	995	0
2–5	$-0.18084\times10^{+02}$	35	467	17	854	0	415	0	36	0	296	0	−530	0
2–6	$-0.27333\times10^{+02}$	79	54	1	−38	0	−20	0	−48	0	182	0	−1266	0
2–7	$-0.33496\times10^{+02}$	13	25	1	774	0	183	0	30	0	78	0	−1	0
2–8	$-0.48783\times10^{+02}$	2	1	1	0	0	−6	0	−10	0	−37	0	395	0
3–4	$-0.68230\times10^{+01}$	141	5792	1799	696	0	−373	0	−75	0	−291	0	−979	0
3–5	$-0.10497\times10^{+02}$	2649	222	18	354	0	−704	0	−347	0	−97	0	238	0
3–6	$-0.19747\times10^{+02}$	430	469	32	−16	0	−9	0	−128	0	342	0	−1106	0
3–7	$-0.25910\times10^{+02}$	131	160	0	−953	0	−465	0	−39	0	−203	0	5	0
3–8	$-0.41197\times10^{+02}$	11	5	0	1	0	−4	0	12	0	−90	0	728	0
4–5	$-0.36745\times10^{+01}$	343	1639	2409	−1428	0	104	0	317	0	−83	0	567	0
4–6	$-0.12924\times10^{+02}$	2503	2357	193	−5	0	−60	0	−269	0	503	0	1044	0
4–7	$-0.19087\times10^{+02}$	544	511	11	42	0	734	0	129	0	311	0	−31	0
4–8	$-0.34374\times10^{+02}$	63	46	4	5	0	1	0	56	0	−174	0	1136	0
5–6	$-0.92494\times10^{+01}$	796	822	124	15	0	26	0	139	0	−225	0	−1341	0
5–7	$-0.15413\times10^{+02}$	1740	1442	133	−1147	0	1008	0	296	0	389	0	−64	0
5–8	$-0.30699\times10^{+02}$	30	25	2	−3	0	−2	0	−38	0	105	0	−506	0
6–7	$-0.61632\times10^{+01}$	5	4	4	160	0	−5	0	−21	0	6	0	1	0
6–8	$-0.21450\times10^{+02}$	2170	2268	65	−33	0	−28	0	−232	0	758	0	782	0
7–8	$-0.15287\times10^{+02}$	0	0	0	0	0	0	0	0	0	5	0	20	0
					$\theta=60$ $\varphi=0$ H=2400									
1–2	$-0.11886\times10^{+02}$	24	4338	1118	1414	0	625	0	158	0	502	0	−1691	0
1–3	$-0.22070\times10^{+02}$	377	1	2	901	0	413	0	212	0	−22	0	1178	0
1–4	$-0.30996\times10^{+02}$	0	58	3	−549	0	−188	0	−30	0	−161	0	615	0
1–5	$-0.37435\times10^{+02}$	9	0	1	−248	0	−83	0	−29	0	7	0	−378	0
1–6	$-0.47705\times10^{+02}$	0	3	0	231	0	70	0	25	0	41	0	−136	0
1–7	$-0.48473\times10^{+02}$	2	0	1	99	0	28	0	5	0	−10	0	270	0
1–8	$-0.70023\times10^{+02}$	0	0	0	1	0	3	0	8	0	3	0	−83	0
2–3	$-0.10185\times10^{+02}$	58	6457	1920	518	0	582	0	163	0	468	0	−780	0
2–4	$-0.19111\times10^{+02}$	1088	3	0	−856	0	−601	0	−321	0	27	0	−1034	0
2–5	$-0.25550\times10^{+02}$	5	200	10	−469	0	−216	0	20	0	−268	0	877	0
2–6	$-0.35820\times10^{+02}$	38	9	1	590	0	206	0	55	0	27	0	410	0
2–7	$-0.36588\times10^{+02}$	9	34	1	239	0	77	0	−14	0	151	0	−786	0
2–8	$-0.58138\times10^{+02}$	1	0	0	0	0	−5	0	−7	0	−30	0	286	0
3–4	$-0.89263\times10^{+01}$	8	6130	2391	491	0	−518	0	−207	0	−325	0	−470	0
3–5	$-0.15365\times10^{+02}$	1760	138	52	−162	0	−516	0	−362	0	76	0	−159	0
3–6	$-0.25635\times10^{+02}$	10	374	12	633	0	442	0	5	0	348	0	−549	0
3–7	$-0.26403\times10^{+02}$	383	96	15	299	0	221	0	162	0	−194	0	1061	0
3–8	$-0.47953\times10^{+02}$	11	6	0	0	0	5	0	−17	0	99	0	−668	0
4–5	$-0.64388\times10^{+01}$	57	3033	2819	−851	0	114	0	222	0	−17	0	1297	0
4–6	$-0.16709\times10^{+02}$	2068	116	9	314	0	−866	0	−413	0	−160	0	165	0
4–7	$-0.17477\times10^{+02}$	298	1709	209	147	0	−301	0	110	0	−491	0	−79	0
4–8	$-0.39027\times10^{+02}$	44	34	2	−3	0	−3	0	−57	0	165	0	−872	0
5–6	$-0.10270\times10^{+02}$	133	2197	794	1298	0	−475	0	−258	0	−269	0	−771	0
5–7	$-0.11038\times10^{+02}$	2978	857	134	547	0	−335	0	−441	0	202	0	1706	0
5–8	$-0.32588\times10^{+02}$	100	90	8	7	0	10	0	89	0	−208	0	788	0
6–7	$-0.76796\times10^{+00}$	8	47	5535	−78	0	−348	0	346	0	−341	0	429	0
6–8	$-0.22318\times10^{+02}$	386	402	25	13	0	23	0	142	0	−303	0	−371	0
7–8	$-0.21550\times10^{+02}$	1695	1775	109	−27	0	−48	0	−291	0	628	0	978	0

TABLE 1. *Energy level differences, wave functions and transition probabilities for angles and field strengths indicated*—Continued

	ΔE	P_x	P_y	P_z	P_{11}		P_{10}		P_{00}		P_{-10}		P_{-1-1}	
					$\theta=60$ $\varphi=0$ H=3200									
1–2	$-0.14413\times10^{+02}$	47	3978	1237	1348	0	671	0	205	0	524	0	−1752	0
1–3	$-0.26936\times10^{+02}$	261	0	3	817	0	420	0	238	0	−14	0	1100	0
1–4	$-0.37946\times10^{+02}$	0	35	2	−405	0	−154	0	−23	0	−141	0	555	0
1–5	$-0.47445\times10^{+02}$	6	0	1	−193	0	−71	0	−25	0	4	0	−306	0
1–6	$-0.54799\times10^{+02}$	0	1	0	158	0	55	0	18	0	30	0	−78	0
1–7	$-0.60958\times10^{+02}$	1	0	0	8	0	0	0	−3	0	−12	0	165	0
1–8	$-0.82750\times10^{+02}$	0	0	0	1	0	2	0	6	0	2	0	−54	0
2–3	$-0.12523\times10^{+02}$	71	6120	2158	662	0	654	0	224	0	499	0	−946	0
2–4	$-0.23533\times10^{+02}$	783	6	1	−782	0	−564	0	−348	0	56	0	−1149	0
2–5	$-0.33032\times10^{+02}$	5	122	7	−417	0	−190	0	25	0	−255	0	905	0
2–6	$-0.40387\times10^{+02}$	20	5	1	407	0	169	0	51	0	28	0	278	0
2–7	$-0.46545\times10^{+02}$	8	6	0	21	0	6	0	−19	0	88	0	−584	0
2–8	$-0.68337\times10^{+02}$	1	0	0	−1	0	−5	0	−5	0	−23	0	210	0
3–4	$-0.11010\times10^{+02}$	56	6091	2800	247	0	−545	0	−265	0	−342	0	−255	0
3–5	$-0.20509\times10^{+02}$	1382	112	35	−331	0	−567	0	−418	0	97	0	−630	0
3–6	$-0.27863\times10^{+02}$	20	230	12	465	0	404	0	32	0	296	0	−401	0
3–7	$-0.34022\times10^{+02}$	100	74	7	57	0	49	0	112	0	−217	0	1059	0
3–8	$-0.55814\times10^{+02}$	7	3	0	2	0	5	0	−14	0	80	0	−508	0
4–5	$-0.94992\times10^{+01}$	162	4466	3118	−769	0	252	0	232	0	120	0	1217	0
4–6	$-0.16853\times10^{+02}$	1462	65	11	280	0	−764	0	−467	0	−175	0	205	0
4–7	$-0.23012\times10^{+02}$	496	646	80	22	0	5	0	233	0	−383	0	493	0
4–8	$-0.44804\times10^{+02}$	33	24	2	−1	0	−3	0	−59	0	158	0	−792	0
5–6	$-0.73543\times10^{+01}$	361	1535	2263	1332	0	−257	0	−578	0	18	0	−518	0
5–7	$-0.13513\times10^{+02}$	2285	1889	559	77	0	−218	0	−436	0	261	0	1603	0
5–8	$-0.35305\times10^{+02}$	151	141	14	9	0	19	0	130	0	−263	0	783	0
6–7	$-0.61583\times10^{+01}$	413	462	851	−21	0	−184	0	−58	0	−94	0	1240	0
6–8	$-0.27951\times10^{+02}$	90	91	9	7	0	16	0	93	0	−162	0	81	0
7–8	$-0.21792\times10^{+02}$	1911	2002	214	−26	0	−82	0	−393	0	611	0	1277	0
					$\theta=60$ $\varphi=0$ H=4000									
1–2	$-0.16812\times10^{+02}$	56	3726	1334	1327	0	708	0	240	0	540	0	−1746	0
1–3	$-0.31557\times10^{+02}$	198	2	1	719	0	400	0	251	0	−27	0	1072	0
1–4	$-0.44649\times10^{+02}$	1	23	1	−302	0	−119	0	−10	0	−127	0	528	0
1–5	$-0.56180\times10^{+02}$	4	0	1	−156	0	−63	0	−25	0	4	0	−261	0
1–6	$-0.63943\times10^{+02}$	0	1	0	−72	0	−27	0	−9	0	−22	0	112	0
1–7	$-0.73916\times10^{+02}$	0	0	0	3	0	0	0	−3	0	−8	0	110	0
1–8	$-0.95968\times10^{+02}$	0	0	0	0	0	−1	0	−3	0	−1	0	40	0
2–3	$-0.14745\times10^{+02}$	91	5807	2336	739	0	703	0	279	0	511	0	−1023	0
2–4	$-0.27837\times10^{+02}$	600	20	4	−715	0	−538	0	−368	0	74	0	−1209	0
2–5	$-0.39368\times10^{+02}$	2	90	7	−378	0	−182	0	20	0	−237	0	824	0
2–6	$-0.47131\times10^{+02}$	13	0	0	−214	0	−99	0	−46	0	24	0	−406	0
2–7	$-0.57104\times10^{+02}$	4	2	0	11	0	4	0	−12	0	61	0	−403	0
2–8	$-0.79156\times10^{+02}$	0	0	0	2	0	5	0	5	0	18	0	−152	0
3–4	$-0.13092\times10^{+02}$	114	6093	3020	103	0	−566	0	−309	0	−353	0	−94	0
3–5	$-0.24622\times10^{+02}$	1115	70	21	−394	0	−606	0	−452	0	74	0	−786	0
3–6	$-0.32385\times10^{+02}$	4	161	11	−272	0	−228	0	47	0	−291	0	686	0
3–7	$-0.42359\times10^{+02}$	36	25	2	36	0	31	0	81	0	−165	0	889	0
3–8	$-0.64410\times10^{+02}$	3	1	0	−2	0	−4	0	11	0	−61	0	382	0
4–5	$-0.11531\times10^{+02}$	117	4760	3522	−703	0	351	0	343	0	163	0	1004	0
4–6	$-0.19294\times10^{+02}$	1333	97	27	−81	0	579	0	495	0	18	0	−165	0
4–7	$-0.29267\times10^{+02}$	273	332	42	13	0	20	0	219	0	−345	0	793	0
4–8	$-0.51319\times10^{+02}$	22	15	1	1	0	4	0	57	0	−139	0	700	0
5–6	$-0.77630\times10^{+01}$	1	2012	3858	−938	0	0	0	544	0	−184	0	1057	0
5–7	$-0.17736\times10^{+02}$	1519	1350	362	23	0	−202	0	−443	0	276	0	928	0
5–8	$-0.39788\times10^{+02}$	107	100	11	−7	0	−20	0	−130	0	243	0	−755	0
6–7	$-0.99734\times10^{+01}$	1122	1326	1336	66	0	270	0	210	0	70	0	−1805	0
6–8	$-0.32025\times10^{+02}$	168	170	20	10	0	30	0	155	0	−242	0	268	0
7–8	$-0.22052\times10^{+02}$	1832	1929	316	26	0	119	0	458	0	−538	0	−1433	0

TABLE 1. *Energy level differences, wave functions and transition probabilities for angles and field strengths indicated*—Continued

	ΔE	P_x	P_y	P_z	$P_{1\,1}$		$P_{1\,0}$		$P_{0\,0}$		$P_{-1\,0}$		$P_{-1\,-1}$	
					$\theta=60$	$\varphi=0$	$H=4800$							
1–2	$-0.19133\times10^{+02}$	73	3540	1405	1282	0	731	0	274	0	547	0	−1757	0
1–3	$-0.36038\times10^{+02}$	156	2	0	−645	0	−384	0	−261	0	37	0	−1054	0
1–4	$-0.51138\times10^{+02}$	1	15	1	231	0	101	0	7	0	113	0	−477	0
1–5	$-0.64298\times10^{+02}$	2	0	0	−121	0	−47	0	−20	0	7	0	−215	0
1–6	$-0.74339\times10^{+02}$	0	0	0	−41	0	−18	0	−6	0	−16	0	105	0
1–7	$-0.87082\times10^{+02}$	0	0	0	2	0	−1	0	−3	0	−5	0	75	0
1–8	$-0.10959\times10^{+03}$	0	0	0	0	0	−1	0	−2	0	−1	0	29	0
2–3	$-0.16905\times10^{+02}$	126	5575	2475	−772	0	−722	0	−317	0	−519	0	1116	0
2–4	$-0.32005\times10^{+02}$	472	32	5	645	0	518	0	385	0	−83	0	1213	0
2–5	$-0.45165\times10^{+02}$	2	45	4	−339	0	−164	0	30	0	−238	0	764	0
2–6	$-0.55206\times10^{+02}$	8	0	0	−117	0	−60	0	−37	0	38	0	−418	0
2–7	$-0.67949\times10^{+02}$	2	1	0	8	0	5	0	−6	0	44	0	−299	0
2–8	$-0.90453\times10^{+02}$	0	0	0	2	0	5	0	5	0	14	0	−114	0
3–4	$-0.15100\times10^{+02}$	165	5988	3253	137	0	−584	0	−350	0	−329	0	−54	0
3–5	$-0.28260\times10^{+02}$	852	2	25	378	0	602	0	470	0	−80	0	846	0
3–6	$-0.38301\times10^{+02}$	14	101	9	205	0	166	0	−78	0	270	0	−870	0
3–7	$-0.51044\times10^{+02}$	19	12	1	−26	0	−15	0	−65	0	133	0	−755	0
3–8	$-0.73548\times10^{+02}$	2	1	0	3	0	7	0	−8	0	51	0	−309	0
4–5	$-0.13160\times10^{+02}$	176	4719	3766	794	0	−294	0	−389	0	−130	0	−1081	0
4–6	$-0.23201\times10^{+02}$	1060	257	55	1	0	−469	0	−509	0	85	0	56	0
4–7	$-0.35944\times10^{+02}$	147	177	24	−10	0	−23	0	−194	0	332	0	−877	0
4–8	$-0.58448\times10^{+02}$	14	9	1	0	0	−3	0	−50	0	134	0	−636	0
5–6	$-0.10041\times10^{+02}$	214	2550	3978	−748	0	−146	0	391	0	−252	0	1418	0
5–7	$-0.22784\times10^{+02}$	1048	958	237	0	0	−200	0	−443	0	273	0	489	0
5–8	$-0.45288\times10^{+02}$	74	68	9	−6	0	−22	0	−126	0	214	0	−689	0
6–7	$-0.12743\times10^{+02}$	1455	1904	1697	122	0	327	0	284	0	78	0	−1982	0
6–8	$-0.35247\times10^{+02}$	207	208	28	11	0	43	0	200	0	−279	0	353	0
7–8	$-0.22504\times10^{+02}$	1767	1887	427	31	0	158	0	510	0	−470	0	−1549	0
					$\theta=75$	$\varphi=0$	$H=800$							
1–2	$-0.62160\times10^{+01}$	2	3781	708	−840	0	−362	0	−25	0	−350	0	1308	0
1–3	$-0.11580\times10^{+02}$	1119	15	5	−1203	0	−416	0	−135	0	11	0	−1223	0
1–4	$-0.14355\times10^{+02}$	33	285	6	−501	0	−169	0	12	0	−213	0	935	0
1–5	$-0.22321\times10^{+02}$	25	2024	5	−1103	0	−432	0	−39	0	−87	0	−5	0
1–6	$-0.25093\times10^{+02}$	25	16	2	9	0	7	0	5	0	84	0	−998	0
1–7	$-0.41442\times10^{+02}$	0	1	1	−754	0	−63	0	−24	0	−19	0	253	0
1–8	$-0.45458\times10^{+02}$	0	0	1	2	0	−2	0	−17	0	0	0	195	0
2–3	$-0.53641\times10^{+01}$	64	6922	1051	−370	0	387	0	57	0	217	0	171	0
2–4	$-0.81394\times10^{+01}$	2773	301	41	137	0	292	0	199	0	−215	0	394	0
2–5	$-0.16105\times10^{+02}$	303	318	2	361	0	439	0	49	0	182	0	244	0
2–6	$-0.18877\times10^{+02}$	287	213	8	−41	0	−33	0	−66	0	249	0	−1445	0
2–7	$-0.35226\times10^{+02}$	1	7	1	640	0	68	0	21	0	244	0	77	0
2–8	$-0.39242\times10^{+02}$	3	1	1	0	0	−7	0	−16	0	−45	0	507	0
3–4	$-0.27753\times10^{+01}$	341	2498	1504	−673	0	1	0	−30	0	59	0	1301	0
3–5	$-0.10741\times10^{+02}$	2672	17	65	−231	0	603	0	192	0	270	0	−77	0
3–6	$-0.13513\times10^{+02}$	1003	1117	56	59	0	12	0	115	0	−390	0	349	0
3–7	$-0.29862\times10^{+02}$	26	40	1	582	0	216	0	−1	0	102	0	295	0
3–8	$-0.33878\times10^{+02}$	10	4	0	−1	0	4	0	−9	0	81	0	−855	0
4–5	$-0.79658\times10^{+01}$	1106	1285	180	−1399	0	286	0	158	0	−36	0	−12	0
4–6	$-0.10737\times10^{+02}$	2552	2676	42	−39	0	−10	0	−141	0	569	0	1426	0
4–7	$-0.27087\times10^{+02}$	30	33	0	666	0	222	0	13	0	96	0	110	0
4–8	$-0.31102\times10^{+02}$	18	7	2	−1	0	−5	0	33	0	−87	0	1228	0
5–6	$-0.27715\times10^{+01}$	6	6	5	0	0	5	0	5	0	43	0	−590	0
5–7	$-0.19121\times10^{+02}$	2303	2221	31	−711	0	1360	0	160	0	611	0	48	0
5–8	$-0.23137\times10^{+02}$	1	1	0	0	0	0	0	−4	0	1	0	87	0
6–7	$-0.16350\times10^{+02}$	0	0	0	−103	0	−24	0	0	0	−9	0	−6	0
6–8	$-0.20365\times10^{+02}$	2274	2348	24	−40	0	−12	0	−144	0	805	0	447	0
7–8	$-0.40156\times10^{+01}$	0	0	0	3	0	2	0	0	0	1	0	−1	0

TABLE 1. *Energy level differences, wave functions and transition probabilities for angles and field strengths indicated*—Continued

	ΔE	P_x	P_y	P_z	$P_{1\,1}$		$P_{1\,0}$		$P_{0\,0}$		$P_{-1\,0}$		$P_{-1\,-1}$	
					$\theta=75$ $\varphi=0$ H=1600									
1–2	$-0.96538\times10^{+01}$	4	4795	989	1478	0	507	0	57	0	475	0	−1619	0
1–3	$-0.18046\times10^{+02}$	548	1	4	−1121	0	−422	0	−187	0	20	0	−1128	0
1–4	$-0.24952\times10^{+02}$	3	82	2	569	0	160	0	12	0	177	0	−770	0
1–5	$-0.30955\times10^{+02}$	13	8	3	−570	0	−152	0	−38	0	−45	0	−187	0
1–6	$-0.35764\times10^{+02}$	6	3	1	29	0	9	0	5	0	53	0	−513	0
1–7	$-0.47804\times10^{+02}$	0	1	1	245	0	61	0	23	0	25	0	1	0
1–8	$-0.55656\times10^{+02}$	0	0	0	1	0	4	0	12	0	7	0	−152	0
2–3	$-0.83921\times10^{+01}$	1	6733	1694	−416	0	−486	0	−59	0	−430	0	479	0
2–4	$-0.15298\times10^{+02}$	1424	21	8	750	0	479	0	278	0	−118	0	915	0
2–5	$-0.21302\times10^{+02}$	62	292	10	−1013	0	−413	0	−49	0	−259	0	385	0
2–6	$-0.26110\times10^{+02}$	106	65	2	85	0	38	0	68	0	−195	0	1173	0
2–7	$-0.38151\times10^{+02}$	7	14	1	661	0	146	0	29	0	62	0	0	0
2–8	$-0.46002\times10^{+02}$	4	2	0	0	0	−7	0	−6	0	−55	0	475	0
3–4	$-0.69058\times10^{+01}$	69	5455	2088	645	0	−288	0	−23	0	−250	0	−826	0
3–5	$-0.12909\times10^{+02}$	2004	457	30	27	0	770	0	328	0	155	0	−36	0
3–6	$-0.17718\times10^{+02}$	570	738	64	0	0	−10	0	173	0	−398	0	785	0
3–7	$-0.29758\times10^{+02}$	76	99	0	−967	0	−379	0	−34	0	−166	0	5	0
3–8	$-0.37610\times10^{+02}$	27	16	0	1	0	−3	0	30	0	−134	0	854	0
4–5	$-0.60037\times10^{+01}$	866	2429	1488	1671	0	−319	0	−303	0	−35	0	−439	0
4–6	$-0.10812\times10^{+02}$	2643	2082	288	−69	0	117	0	337	0	−423	0	−1417	0
4–7	$-0.22853\times10^{+02}$	277	275	2	451	0	595	0	85	0	258	0	−20	0
4–8	$-0.30704\times10^{+02}$	114	92	8	7	0	6	0	83	0	−220	0	998	0
5–6	$-0.48086\times10^{+01}$	438	464	335	15	0	63	0	116	0	−67	0	−1291	0
5–7	$-0.16849\times10^{+02}$	2028	1739	149	1124	0	−1123	0	−323	0	−436	0	59	0
5–8	$-0.24700\times10^{+02}$	56	54	4	6	0	6	0	53	0	−127	0	203	0
6–7	$-0.12040\times10^{+02}$	25	21	6	−280	0	69	0	42	0	18	0	−3	0
6–8	$-0.19892\times10^{+02}$	2063	2167	85	38	0	37	0	264	0	−720	0	−948	0
7–8	$-0.78515\times10^{+01}$	0	0	0	0	0	0	0	0	0	3	0	18	0
					$\theta=75$ $\varphi=0$ H=2400									
1–2	$-0.12550\times10^{+02}$	11	4249	1167	1466	0	573	0	87	0	523	0	−1691	0
1–3	$-0.23710\times10^{+02}$	344	1	6	−1003	0	−433	0	−223	0	12	0	−1062	0
1–4	$-0.33505\times10^{+02}$	0	43	2	503	0	166	0	24	0	156	0	−589	0
1–5	$-0.41342\times10^{+02}$	4	1	1	273	0	81	0	22	0	12	0	226	0
1–6	$-0.47964\times10^{+02}$	1	1	0	−54	0	−19	0	−8	0	−32	0	258	0
1–7	$-0.55553\times10^{+02}$	0	1	0	−185	0	−53	0	−18	0	−21	0	−6	0
1–8	$-0.66821\times10^{+02}$	0	0	0	0	0	−3	0	−8	0	−5	0	102	0
2–3	$-0.11160\times10^{+02}$	10	6417	2057	−687	0	−561	0	−84	0	−503	0	822	0
2–4	$-0.20955\times10^{+02}$	960	3	2	911	0	557	0	337	0	−76	0	1049	0
2–5	$-0.28791\times10^{+02}$	0	100	2	638	0	252	0	1	0	245	0	−651	0
2–6	$-0.35414\times10^{+02}$	39	10	0	−144	0	−55	0	−52	0	112	0	−761	0
2–7	$-0.43003\times10^{+02}$	6	12	1	−510	0	−150	0	−30	0	−66	0	13	0
2–8	$-0.54271\times10^{+02}$	3	1	0	2	0	8	0	3	0	49	0	−360	0
3–4	$-0.97950\times10^{+01}$	12	5954	2829	324	0	−439	0	−105	0	−345	0	−340	0
3–5	$-0.17631\times10^{+02}$	1308	2	0	−418	0	−649	0	−416	0	9	0	−367	0
3–6	$-0.24254\times10^{+02}$	180	397	49	109	0	78	0	−141	0	350	0	−841	0
3–7	$-0.31843\times10^{+02}$	111	112	3	719	0	429	0	83	0	181	0	14	0
3–8	$-0.43111\times10^{+02}$	29	19	0	0	0	2	0	−42	0	144	0	−727	0
4–5	$-0.78364\times10^{+01}$	41	4289	2681	−1165	0	239	0	226	0	63	0	990	0
4–6	$-0.14459\times10^{+02}$	1845	865	165	96	0	−256	0	−424	0	313	0	556	0
4–7	$-0.22048\times10^{+02}$	467	460	25	−208	0	−745	0	−195	0	−326	0	51	0
4–8	$-0.33316\times10^{+02}$	122	104	10	−7	0	−12	0	−110	0	246	0	−858	0
5–6	$-0.66227\times10^{+01}$	913	1625	1534	252	0	160	0	215	0	−21	0	−1851	0
5–7	$-0.14212\times10^{+02}$	1664	1130	320	1333	0	−821	0	−466	0	−261	0	120	0
5–8	$-0.25479\times10^{+02}$	255	256	25	13	0	24	0	150	0	−278	0	225	0
6–7	$-0.75890\times10^{+01}$	202	168	199	−818	0	94	0	192	0	−22	0	−9	0
6–8	$-0.18857\times10^{+02}$	1801	1881	177	28	0	71	0	361	0	−599	0	−1287	0
7–8	$-0.11268\times10^{+02}$	4	4	1	0	0	−4	0	−15	0	22	0	140	0

TABLE 1. *Energy level differences, wave functions and transition probabilities for angles and field strengths indicated*—Continued

	ΔE	P_x	P_y	P_z	$P_{1\,1}$		$P_{1\,0}$		$P_{0\,0}$		$P_{-1\,0}$		$P_{-1\,-1}$	
					$\theta=75$		$\varphi=0$		H=3200					
1–2	$-0.15216\times10^{+02}$	22	3905	1291	1416	0	614	0	116	0	551	0	−1741	0
1–3	$-0.28921\times10^{+02}$	235	5	9	909	0	439	0	249	0	−3	0	978	0
1–4	$-0.41139\times10^{+02}$	0	25	1	−423	0	−156	0	−29	0	−135	0	473	0
1–5	$-0.51505\times10^{+02}$	4	1	1	−213	0	−72	0	−22	0	−6	0	−216	0
1–6	$-0.60565\times10^{+02}$	0	1	0	−81	0	−30	0	−13	0	−24	0	138	0
1–7	$-0.65039\times10^{+02}$	0	0	0	112	0	37	0	13	0	13	0	18	0
1–8	$-0.78766\times10^{+02}$	0	0	0	12	0	1	0	−4	0	−2	0	67	0
2–3	$-0.13705\times10^{+02}$	20	6024	2301	783	0	594	0	107	0	533	0	−981	0
2–4	$-0.25922\times10^{+02}$	682	3	1	−891	0	−566	0	−373	0	72	0	−1092	0
2–5	$-0.36288\times10^{+02}$	1	93	5	−507	0	−211	0	11	0	−242	0	716	0
2–6	$-0.45348\times10^{+02}$	20	1	0	−217	0	−81	0	−45	0	55	0	−508	0
2–7	$-0.49823\times10^{+02}$	2	6	0	314	0	106	0	21	0	57	0	−57	0
2–8	$-0.63550\times10^{+02}$	1	1	0	39	0	20	0	4	0	46	0	−270	0
3–4	$-0.12217\times10^{+02}$	18	6295	3027	132	0	−489	0	−133	0	−378	0	−129	0
3–5	$-0.22583\times10^{+02}$	1170	12	9	−507	0	−640	0	−467	0	65	0	−615	0
3–6	$-0.31643\times10^{+02}$	25	206	18	−293	0	−188	0	81	0	−328	0	832	0
3–7	$-0.36118\times10^{+02}$	54	30	0	522	0	306	0	76	0	108	0	96	0
3–8	$-0.49845\times10^{+02}$	23	6	0	59	0	33	0	46	0	−103	0	591	0
4–5	$-0.10366\times10^{+02}$	9	4863	3439	−870	0	260	0	177	0	137	0	995	0
4–6	$-0.19426\times10^{+02}$	1517	220	50	−9	0	479	0	514	0	−188	0	−6	0
4–7	$-0.23900\times10^{+02}$	199	345	33	−181	0	−602	0	−168	0	−310	0	52	0
4–8	$-0.37627\times10^{+02}$	63	120	13	−13	0	−52	0	100	0	−268	0	779	0
5–6	$-0.90600\times10^{+01}$	388	3009	2813	−748	0	−72	0	−85	0	24	0	1679	0
5–7	$-0.13534\times10^{+02}$	1496	426	239	1037	0	−658	0	−590	0	−157	0	427	0
5–8	$-0.27261\times10^{+02}$	538	267	25	106	0	−117	0	−292	0	319	0	−210	0
6–7	$-0.44743\times10^{+01}$	609	313	2234	1230	0	140	0	−513	0	350	0	28	0
6–8	$-0.18201\times10^{+02}$	1359	1788	514	160	0	132	0	381	0	−441	0	−1394	0
7–8	$-0.13727\times10^{+02}$	66	143	321	87	0	−117	0	71	0	−256	0	−551	0
					$\theta=75$		$\varphi=0$		H=4000					
1–2	$-0.17754\times10^{+02}$	16	3664	1407	1447	0	651	0	127	0	575	0	−1692	0
1–3	$-0.33881\times10^{+02}$	177	0	2	−804	0	−415	0	−262	0	22	0	−957	0
1–4	$-0.48397\times10^{+02}$	0	17	1	327	0	124	0	17	0	123	0	−438	0
1–5	$-0.61086\times10^{+02}$	3	0	1	−148	0	−52	0	−19	0	3	0	−199	0
1–6	$-0.71935\times10^{+02}$	0	0	0	−74	0	−29	0	−12	0	−21	0	97	0
1–7	$-0.77058\times10^{+02}$	0	0	0	41	0	13	0	3	0	1	0	49	0
1–8	$-0.91397\times10^{+02}$	0	0	0	0	0	−2	0	−4	0	−3	0	49	0
2–3	$-0.16127\times10^{+02}$	24	5770	2496	−881	0	−637	0	−136	0	−553	0	1054	0
2–4	$-0.30643\times10^{+02}$	513	4	1	864	0	569	0	402	0	−68	0	1089	0
2–5	$-0.43333\times10^{+02}$	1	59	4	−425	0	−180	0	16	0	−221	0	667	0
2–6	$-0.54181\times10^{+02}$	12	0	0	−232	0	−90	0	−42	0	25	0	−356	0
2–7	$-0.59304\times10^{+02}$	0	3	0	136	0	51	0	6	0	51	0	−170	0
2–8	$-0.73643\times10^{+02}$	1	0	0	2	0	6	0	1	0	29	0	−184	0
3–4	$-0.14516\times10^{+02}$	27	6196	3301	−16	0	−514	0	−159	0	−396	0	29	0
3–5	$-0.27206\times10^{+02}$	906	22	12	566	0	639	0	504	0	−80	0	765	0
3–6	$-0.38054\times10^{+02}$	2	137	11	382	0	239	0	−46	0	306	0	−705	0
3–7	$-0.43177\times10^{+02}$	34	0	0	−257	0	−154	0	−77	0	22	0	−369	0
3–8	$-0.57516\times10^{+02}$	9	5	0	6	0	4	0	−30	0	94	0	−443	0
4–5	$-0.12689\times10^{+02}$	34	5231	3808	707	0	−283	0	−180	0	−167	0	−877	0
4–6	$-0.23538\times10^{+02}$	1282	47	16	−122	0	−645	0	−581	0	72	0	−181	0
4–7	$-0.28661\times10^{+02}$	0	252	33	155	0	305	0	−22	0	327	0	−345	0
4–8	$-0.43000\times10^{+02}$	57	45	6	−5	0	−17	0	−111	0	199	0	−674	0
5–6	$-0.10848\times10^{+02}$	35	3659	3835	−1053	0	58	0	180	0	−8	0	1367	0
5–7	$-0.15972\times10^{+02}$	1451	30	3	471	0	−539	0	−647	0	1	0	679	0
5–8	$-0.30310\times10^{+02}$	280	285	47	−12	0	−46	0	−245	0	327	0	−335	0
6–7	$-0.51233\times10^{+01}$	18	967	5145	970	0	440	0	−408	0	525	0	−837	0
6–8	$-0.19462\times10^{+02}$	1019	1011	258	4	0	134	0	441	0	−360	0	−1027	0
7–8	$-0.14339\times10^{+02}$	696	706	320	6	0	143	0	345	0	−179	0	−1332	0

TABLE 1. *Energy level differences, wave functions and transition probabilities for angles and field strengths indicated*—Continued

	ΔE	P_x	P_y	P_z	$P_{1\,1}$		$P_{1\,0}$		$P_{0\,0}$		$P_{-1\,0}$		$P_{-1\,-1}$	
					$\theta=75$		$\varphi=0$		H=4800					
1–2	$-0.20210\times10^{+02}$	21	3495	1486	−1422	0	−673	0	−143	0	−588	0	1698	0
1–3	$-0.38687\times10^{+02}$	139	0	2	743	0	410	0	277	0	−24	0	925	0
1–4	$-0.55437\times10^{+02}$	0	11	1	274	0	110	0	14	0	111	0	−388	0
1–5	$-0.70260\times10^{+02}$	2	0	0	−116	0	−43	0	−16	0	3	0	−165	0
1–6	$-0.82639\times10^{+02}$	0	0	0	−53	0	−22	0	−9	0	−16	0	72	0
1–7	$-0.90423\times10^{+02}$	0	0	0	17	0	4	0	0	0	−1	0	41	0
1–8	$-0.10464\times10^{+03}$	0	0	0	0	0	−1	0	−2	0	−2	0	32	0
2–3	$-0.18477\times10^{+02}$	32	5549	2651	−920	0	−660	0	−156	0	−568	0	1121	0
2–4	$-0.35227\times10^{+02}$	401	5	1	−815	0	−561	0	−422	0	72	0	−1092	0
2–5	$-0.50050\times10^{+02}$	1	39	3	361	0	158	0	−17	0	202	0	−610	0
2–6	$-0.62430\times10^{+02}$	7	0	0	176	0	72	0	37	0	−21	0	291	0
2–7	$-0.70213\times10^{+02}$	0	1	0	−64	0	−26	0	0	0	−37	0	157	0
2–8	$-0.84427\times10^{+02}$	1	0	0	−1	0	−4	0	0	0	−20	0	129	0
3–4	$-0.16750\times10^{+02}$	41	6090	3510	117	0	525	0	177	0	407	0	−145	0
3–5	$-0.31573\times10^{+02}$	715	24	12	−582	0	−635	0	−529	0	87	0	−843	0
3–6	$-0.43952\times10^{+02}$	2	85	8	−323	0	−197	0	51	0	−271	0	656	0
3–7	$-0.51736\times10^{+02}$	17	1	0	136	0	83	0	63	0	−55	0	389	0
3–8	$-0.65950\times10^{+02}$	5	2	0	−7	0	−4	0	24	0	−72	0	332	0
4–5	$-0.14823\times10^{+02}$	49	5340	4079	590	0	−294	0	−199	0	−174	0	−765	0
4–6	$-0.27202\times10^{+02}$	983	53	19	−202	0	−638	0	−601	0	65	0	−278	0
4–7	$-0.34986\times10^{+02}$	17	138	19	119	0	155	0	−98	0	293	0	−490	0
4–8	$-0.49200\times10^{+02}$	34	24	3	−4	0	−16	0	−97	0	165	0	−575	0
5–6	$-0.12379\times10^{+02}$	27	3697	4295	−998	0	31	0	257	0	−71	0	1272	0
5–7	$-0.20163\times10^{+02}$	1055	195	56	177	0	−462	0	−626	0	76	0	534	0
5–8	$-0.34377\times10^{+02}$	184	188	35	−7	0	−42	0	−236	0	297	0	−410	0
6–7	$-0.77835\times10^{+01}$	76	1462	4584	777	0	481	0	−202	0	502	0	−1324	0
6–8	$-0.21997\times10^{+02}$	716	681	198	−4	0	144	0	445	0	−310	0	−700	0
7–8	$-0.14214\times10^{+02}$	996	1030	714	18	0	249	0	478	0	−118	0	−1642	0
					$\theta=90$		$\varphi=0$		H=800					
1–2	$-0.63044\times10^{+01}$	0	5747	719	1361	0	357	0	3	0	380	0	−1415	0
1–3	$-0.11958\times10^{+02}$	1131	1	3	−1299	0	−391	0	−136	0	56	0	−1236	0
1–4	$-0.14522\times10^{+02}$	0	279	7	−831	0	−198	0	−7	0	−209	0	863	0
1–5	$-0.23931\times10^{+02}$	43	0	6	650	0	122	0	20	0	−14	0	784	0
1–6	$-0.23987\times10^{+02}$	0	41	1	774	0	139	0	30	0	121	0	−639	0
1–7	$-0.43675\times10^{+02}$	0	0	1	−26	0	−9	0	−21	0	−5	0	225	0
1–8	$-0.43680\times10^{+02}$	0	0	1	225	0	45	0	20	0	19	0	26	0
2–3	$-0.56531\times10^{+01}$	0	7234	1125	165	0	−352	0	7	0	−350	0	−124	0
2–4	$-0.82179\times10^{+01}$	2762	0	4	−241	0	−383	0	−211	0	136	0	−174	0
2–5	$-0.17626\times10^{+02}$	12	555	10	962	0	272	0	−28	0	347	0	−1223	0
2–6	$-0.17682\times10^{+02}$	540	11	1	1212	0	364	0	84	0	−28	0	951	0
2–7	$-0.37370\times10^{+02}$	6	1	1	−69	0	1	0	11	0	55	0	−608	0
2–8	$-0.37376\times10^{+02}$	1	5	1	606	0	62	0	25	0	31	0	−69	0
3–4	$-0.25648\times10^{+01}$	0	2552	1927	−1032	0	39	0	3	0	0	0	1064	0
3–5	$-0.11973\times10^{+02}$	3509	41	10	16	0	−561	0	−224	0	180	0	105	0
3–6	$-0.12029\times10^{+02}$	42	3318	111	87	0	−647	0	−10	0	−548	0	0	0
3–7	$-0.31717\times10^{+02}$	24	20	1	123	0	26	0	−24	0	129	0	−1070	0
3–8	$-0.31723\times10^{+02}$	19	24	0	−1076	0	−178	0	−4	0	−63	0	−121	0
4–5	$-0.94086\times10^{+01}$	27	3643	195	1019	0	−405	0	2	0	−466	0	−1181	0
4–6	$-0.94643\times10^{+01}$	3734	27	19	1180	0	−502	0	−232	0	138	0	1019	0
4–7	$-0.29152\times10^{+02}$	39	14	3	110	0	25	0	38	0	−92	0	933	0
4–8	$-0.29158\times10^{+02}$	16	41	0	−924	0	−234	0	11	0	−116	0	113	0
5–6	-0.55638×10^{-01}	0	5	7435	−114	0	−213	0	0	0	−196	0	128	0
5–7	$-0.19744\times10^{+02}$	1085	1648	20	71	0	−89	0	106	0	−652	0	−400	0
5–8	$-0.19749\times10^{+02}$	1202	640	9	−326	0	870	0	115	0	288	0	−74	0
6–7	$-0.19688\times10^{+02}$	1151	676	7	24	0	−130	0	−107	0	450	0	365	0
6–8	$-0.19694\times10^{+02}$	1139	1577	23	−439	0	1047	0	113	0	490	0	8	0
7–8	-0.54681×10^{-02}	0	0	852	−2	0	47	0	0	0	47	0	−1	0

TABLE 1. *Energy level differences, wave functions and transition probabilities for angles and field strengths indicated*—Continued

$\theta=90 \quad \varphi=0 \quad H=1600$

	ΔE	P_x	P_y	P_z	P_{11}		P_{10}		P_{00}		P_{-10}		P_{-1-1}	
1–2	$-0.97481\times10^{+01}$	0	4781	1000	1526	0	457	0	5	0	478	0	−1584	0
1–3	$-0.18486\times10^{+02}$	544	0	4	1143	0	403	0	185	0	−38	0	1131	0
1–4	$-0.25443\times10^{+02}$	1	67	2	620	0	175	0	18	0	173	0	−648	0
1–5	$-0.33281\times10^{+02}$	17	0	3	−435	0	−98	0	−24	0	6	0	−428	0
1–6	$-0.34421\times10^{+02}$	2	9	0	−417	0	−120	0	−36	0	−71	0	227	0
1–7	$-0.52186\times10^{+02}$	0	6	0	−92	0	27	0	13	0	11	0	−188	0
1–8	$-0.52229\times10^{+02}$	0	1	0	−188	0	−46	0	−18	0	−19	0	2	0
2–3	$-0.87376\times10^{+01}$	1	6645	1737	411	0	406	0	−16	0	443	0	−569	0
2–4	$-0.15695\times10^{+02}$	1335	0	2	842	0	501	0	286	0	−90	0	758	0
2–5	$-0.23533\times10^{+02}$	3	309	12	−810	0	−277	0	19	0	−324	0	841	0
2–6	$-0.24672\times10^{+02}$	180	60	11	−779	0	−293	0	−91	0	−4	0	−585	0
2–7	$-0.42437\times10^{+02}$	8	4	0	−186	0	−75	0	0	0	−143	0	558	0
2–8	$-0.42480\times10^{+02}$	3	8	1	−557	0	−110	0	−25	0	−45	0	−12	0
3–4	$-0.69575\times10^{+01}$	14	5185	2146	−678	0	282	0	−29	0	202	0	830	0
3–5	$-0.14795\times10^{+02}$	2405	1	86	−449	0	−615	0	−368	0	96	0	−86	0
3–6	$-0.15935\times10^{+02}$	88	1360	101	79	0	−472	0	25	0	−420	0	435	0
3–7	$-0.33700\times10^{+02}$	98	216	3	150	0	180	0	−68	0	205	0	−848	0
3–8	$-0.33743\times10^{+02}$	12	25	0	−1002	0	−226	0	−7	0	−102	0	28	0
4–5	$-0.78375\times10^{+01}$	1	4631	1513	1303	0	−285	0	−11	0	−224	0	−1229	0
4–6	$-0.89773\times10^{+01}$	3690	21	58	1036	0	−461	0	−461	0	79	0	983	0
4–7	$-0.26742\times10^{+02}$	164	136	13	429	0	−18	0	105	0	−254	0	548	0
4–8	$-0.26785\times10^{+02}$	180	183	0	−731	0	−523	0	−59	0	−234	0	1	0
5–6	$-0.11398\times10^{+01}$	14	387	5605	−336	0	−387	0	26	0	−328	0	602	0
5–7	$-0.18905\times10^{+02}$	1155	2880	60	338	0	198	0	222	0	−534	0	−645	0
5–8	$-0.18948\times10^{+02}$	1046	971	59	−542	0	877	0	218	0	357	0	−62	0
6–7	$-0.17765\times10^{+02}$	827	926	41	−119	0	−107	0	−176	0	361	0	974	0
6–8	$-0.17808\times10^{+02}$	1154	987	83	−868	0	831	0	236	0	317	0	−5	0
7–8	-0.42942×10^{-01}	0	0	7	−11	0	−12	0	0	0	−56	0	27	0

$\theta=90 \quad \varphi=0 \quad H=2400$

	ΔE	P_x	P_y	P_z	P_{11}		P_{10}		P_{00}		P_{-10}		P_{-1-1}	
1–2	$-0.12652\times10^{+02}$	0	4235	1187	1583	0	510	0	2	0	526	0	−1588	0
1–3	$-0.24229\times10^{+02}$	343	0	2	1049	0	415	0	221	0	−28	0	1010	0
1–4	$-0.34356\times10^{+02}$	1	37	1	−510	0	−153	0	−15	0	−155	0	553	0
1–5	$-0.43280\times10^{+02}$	7	0	2	−273	0	−74	0	−22	0	5	0	−298	0
1–6	$-0.47209\times10^{+02}$	0	2	0	−162	0	−47	0	−15	0	−39	0	161	0
1–7	$-0.61821\times10^{+02}$	0	0	0	25	0	2	0	−5	0	−8	0	140	0
1–8	$-0.61976\times10^{+02}$	0	0	0	−125	0	−36	0	−14	0	−16	0	26	0
2–3	$-0.11577\times10^{+02}$	0	6303	2110	757	0	491	0	−7	0	502	0	−757	0
2–4	$-0.21704\times10^{+02}$	904	0	1	−1018	0	−558	0	−345	0	75	0	−938	0
2–5	$-0.30628\times10^{+02}$	1	150	7	−694	0	−251	0	9	0	−277	0	739	0
2–6	$-0.34557\times10^{+02}$	42	1	0	−454	0	−155	0	−61	0	17	0	−417	0
2–7	$-0.49169\times10^{+02}$	5	5	0	91	0	31	0	0	0	80	0	−423	0
2–8	$-0.49324\times10^{+02}$	4	4	1	−417	0	−104	0	−26	0	−30	0	−87	0
3–4	$-0.10127\times10^{+02}$	0	6253	2725	324	0	−368	0	0	0	−336	0	−331	0
3–5	$-0.19051\times10^{+02}$	1595	1	6	−520	0	−636	0	−444	0	93	0	−468	0
3–6	$-0.22980\times10^{+02}$	1	410	35	−440	0	−344	0	11	0	−342	0	473	0
3–7	$-0.37592\times10^{+02}$	69	20	1	156	0	62	0	76	0	−153	0	757	0
3–8	$-0.37747\times10^{+02}$	20	63	1	−750	0	−288	0	−29	0	−164	0	152	0
4–5	$-0.89237\times10^{+01}$	0	5074	2858	−1085	0	222	0	8	0	194	0	1122	0
4–6	$-0.12853\times10^{+02}$	2100	0	1	−467	0	498	0	514	0	−107	0	−477	0
4–7	$-0.27465\times10^{+02}$	152	326	31	−108	0	−98	0	142	0	−362	0	618	0
4–8	$-0.27620\times10^{+02}$	339	145	1	599	0	605	0	155	0	202	0	95	0
5–6	$-0.39292\times10^{+01}$	0	1415	4122	−1008	0	−295	0	9	0	−296	0	1040	0
5–7	$-0.18541\times10^{+02}$	1424	660	75	107	0	−228	0	−374	0	390	0	655	0
5–8	$-0.18696\times10^{+02}$	640	1213	173	−614	0	803	0	261	0	397	0	76	0
6–7	$-0.14612\times10^{+02}$	507	1257	204	277	0	−55	0	206	0	−391	0	−1235	0
6–8	$-0.14767\times10^{+02}$	1413	534	174	−1276	0	598	0	397	0	106	0	−285	0
7–8	$-0.15507\times10^{+00}$	0	1	2186	85	0	241	0	−2	0	238	0	−19	0

TABLE 1. *Energy level differences, wave functions and transition probabilities for angles and field strengths indicated*—Continued

	ΔE	P_x	P_y	P_z	P_{11}		P_{10}		P_{00}		P_{-10}		P_{-1-1}	
					$\theta=90$ $\varphi=0$ H=3200									
1–2	$-0.15330\times10^{+02}$	0	3895	1319	1561	0	543	0	6	0	558	0	−1612	0
1–3	$-0.29528\times10^{+02}$	240	1	4	979	0	426	0	245	0	−15	0	918	0
1–4	$-0.42249\times10^{+02}$	1	21	1	−427	0	−143	0	−19	0	−137	0	454	0
1–5	$-0.53224\times10^{+02}$	4	0	1	−205	0	−61	0	−18	0	1	0	−211	0
1–6	$-0.60466\times10^{+02}$	0	1	0	−104	0	−35	0	−13	0	−25	0	98	0
1–7	$-0.72422\times10^{+02}$	0	0	0	39	0	9	0	0	0	−3	0	84	0
1–8	$-0.72934\times10^{+02}$	0	0	0	−78	0	−26	0	−12	0	−13	0	35	0
2–3	$-0.14198\times10^{+02}$	0	5977	2364	896	0	523	0	−8	0	537	0	−906	0
2–4	$-0.26920\times10^{+02}$	647	0	1	−1020	0	−573	0	−384	0	69	0	−968	0
2–5	$-0.37894\times10^{+02}$	1	83	5	−591	0	−222	0	6	0	−243	0	631	0
2–6	$-0.45136\times10^{+02}$	17	0	0	−324	0	−110	0	−45	0	14	0	−309	0
2–7	$-0.57092\times10^{+02}$	2	4	0	143	0	49	0	5	0	69	0	−281	0
2–8	$-0.57604\times10^{+02}$	3	1	1	−264	0	−74	0	−21	0	−10	0	−123	0
3–4	$-0.12722\times10^{+02}$	0	6326	3111	86	0	−405	0	0	0	−380	0	−92	0
3–5	$-0.23696\times10^{+02}$	1129	0	3	−645	0	−657	0	−492	0	78	0	−605	0
3–6	$-0.30938\times10^{+02}$	0	184	16	−473	0	−293	0	12	0	−297	0	500	0
3–7	$-0.42894\times10^{+02}$	55	3	0	271	0	120	0	83	0	−88	0	552	0
3–8	$-0.43406\times10^{+02}$	4	44	2	−529	0	−226	0	−15	0	−162	0	240	0
4–5	$-0.10974\times10^{+02}$	0	5325	3515	−901	0	204	0	7	0	175	0	927	0
4–6	$-0.18217\times10^{+02}$	1385	0	0	−78	0	566	0	542	0	−78	0	−101	0
4–7	$-0.30172\times10^{+02}$	41	332	35	−228	0	−230	0	107	0	−386	0	533	0
4–8	$-0.30684\times10^{+02}$	309	40	0	482	0	516	0	205	0	106	0	202	0
5–6	$-0.72424\times10^{+01}$	1	2478	3787	−1152	0	−200	0	17	0	−214	0	1189	0
5–7	$-0.19198\times10^{+02}$	1591	211	38	234	0	−430	0	−534	0	246	0	521	0
5–8	$-0.19710\times10^{+02}$	216	1153	247	−443	0	654	0	202	0	413	0	134	0
6–7	$-0.11956\times10^{+02}$	199	1796	898	694	0	−50	0	166	0	−249	0	−1385	0
6–8	$-0.12467\times10^{+02}$	1936	208	221	−1400	0	447	0	617	0	−72	0	−670	0
7–8	$-0.51167\times10^{+00}$	3	26	7553	268	0	602	0	−15	0	595	0	−116	0
					$\theta=90$ $\varphi=0$ H=4000									
1–2	$-0.17883\times10^{+02}$	0	3661	1424	1558	0	567	0	6	0	580	0	−1603	0
1–3	$-0.34575\times10^{+02}$	176	1	4	943	0	437	0	264	0	0	0	816	0
1–4	$-0.49709\times10^{+02}$	4	13	0	−271	0	−87	0	7	0	−124	0	469	0
1–5	$-0.62902\times10^{+02}$	2	0	1	−156	0	−49	0	−16	0	1	0	−165	0
1–6	$-0.73140\times10^{+02}$	0	0	0	−82	0	−30	0	−12	0	−21	0	73	0
1–7	$-0.83802\times10^{+02}$	0	0	0	22	0	8	0	1	0	−2	0	52	0
1–8	$-0.85276\times10^{+02}$	0	0	0	−42	0	−14	0	−7	0	−8	0	25	0
2–3	$-0.16693\times10^{+02}$	6	5666	2529	1075	0	601	0	32	0	552	0	−891	0
2–4	$-0.31826\times10^{+02}$	482	57	30	−902	0	−527	0	−412	0	115	0	−1050	0
2–5	$-0.45020\times10^{+02}$	1	51	3	−512	0	−204	0	4	0	−217	0	545	0
2–6	$-0.55257\times10^{+02}$	10	1	0	−270	0	−86	0	−37	0	14	0	−260	0
2–7	$-0.65919\times10^{+02}$	0	2	0	93	0	39	0	8	0	42	0	−184	0
2–8	$-0.67393\times10^{+02}$	1	0	0	−151	0	−43	0	−14	0	−1	0	−94	0
3–4	$-0.15133\times10^{+02}$	12	6246	3278	−59	0	−411	0	−16	0	−401	0	81	0
3–5	$-0.28327\times10^{+02}$	842	52	22	−622	0	−690	0	−525	0	50	0	−747	0
3–6	$-0.38565\times10^{+02}$	12	107	9	−554	0	−339	0	−42	0	−289	0	504	0
3–7	$-0.49227\times10^{+02}$	31	3	0	238	0	153	0	67	0	−21	0	351	0
3–8	$-0.50700\times10^{+02}$	4	21	1	−364	0	−164	0	−22	0	−124	0	177	0
4–5	$-0.13194\times10^{+02}$	8	5422	3898	−853	0	158	0	−44	0	182	0	722	0
4–6	$-0.23432\times10^{+02}$	1084	8	2	94	0	584	0	588	0	−113	0	247	0
4–7	$-0.34093\times10^{+02}$	10	221	27	−180	0	−203	0	74	0	−286	0	531	0
4–8	$-0.35567\times10^{+02}$	156	6	0	368	0	358	0	177	0	38	0	215	0
5–6	$-0.10238\times10^{+02}$	0	2905	4054	−960	0	−101	0	24	0	−68	0	1106	0
5–7	$-0.20899\times10^{+02}$	1406	555	11	28	0	−545	0	−634	0	170	0	284	0
5–8	$-0.22373\times10^{+02}$	62	676	173	−262	0	405	0	134	0	371	0	79	0
6–7	$-0.10662\times10^{+02}$	65	2034	2312	678	0	61	0	112	0	−29	0	−1130	0
6–8	$-0.12136\times10^{+02}$	1935	75	174	−1183	0	369	0	776	0	−139	0	−684	0
7–8	$-0.14739\times10^{+01}$	5	155	8608	481	0	720	0	−24	0	721	0	−276	0

TABLE 1. *Energy level differences, wave functions and transition probabilities for angles and field strengths indicated*—Continued

	ΔE	P_x	P_y	P_z	P_{11}		P_{10}		P_{00}		P_{-10}		P_{-1-1}	
					$\theta=90$		$\varphi=0$		H=4800					
1–2	$-0.20358\times10^{+02}$	0	3490	1509	1551	0	585	0	6	0	597	0	−1592	0
1–3	$-0.39469\times10^{+02}$	140	1	3	−857	0	−425	0	−276	0	12	0	−812	0
1–4	$-0.56931\times10^{+02}$	0	10	1	318	0	121	0	19	0	112	0	−330	0
1–5	$-0.72326\times10^{+02}$	1	0	1	−126	0	−41	0	−14	0	1	0	−133	0
1–6	$-0.85017\times10^{+02}$	0	0	0	−61	0	−25	0	−10	0	−16	0	56	0
1–7	$-0.95752\times10^{+02}$	0	0	0	25	0	7	0	1	0	0	0	35	0
1–8	$-0.98890\times10^{+02}$	0	0	0	−22	0	−8	0	−4	0	−4	0	15	0
2–3	$-0.19111\times10^{+02}$	0	5521	2713	−1032	0	−559	0	10	0	−575	0	1051	0
2–4	$-0.36573\times10^{+02}$	381	0	0	981	0	593	0	436	0	−49	0	931	0
2–5	$-0.51968\times10^{+02}$	0	34	2	−456	0	−184	0	2	0	−196	0	482	0
2–6	$-0.64659\times10^{+02}$	6	0	0	−212	0	−74	0	−32	0	11	0	−211	0
2–7	$-0.75394\times10^{+02}$	0	1	0	106	0	41	0	8	0	41	0	−123	0
2–8	$-0.78532\times10^{+02}$	0	0	0	−81	0	−24	0	−8	0	0	0	−59	0
3–4	$-0.17462\times10^{+02}$	0	6141	3606	−174	0	−427	0	3	0	−410	0	168	0
3–5	$-0.32857\times10^{+02}$	664	0	3	759	0	682	0	555	0	−60	0	718	0
3–6	$-0.45547\times10^{+02}$	0	72	6	458	0	246	0	−18	0	261	0	−484	0
3–7	$-0.56282\times10^{+02}$	19	0	0	−228	0	−105	0	−61	0	33	0	−294	0
3–8	$-0.59420\times10^{+02}$	0	6	0	205	0	90	0	2	0	78	0	−135	0
4–5	$-0.15395\times10^{+02}$	0	5548	4200	634	0	−208	0	−10	0	−176	0	−660	0
4–6	$-0.28086\times10^{+02}$	898	0	2	−308	0	−679	0	−629	0	54	0	−270	0
4–7	$-0.38821\times10^{+02}$	2	137	17	304	0	265	0	−49	0	317	0	−429	0
4–8	$-0.41959\times10^{+02}$	62	2	0	−275	0	−245	0	−124	0	−27	0	−177	0
5–6	$-0.12691\times10^{+02}$	1	3960	4429	−1147	0	−78	0	31	0	−105	0	1181	0
5–7	$-0.23426\times10^{+02}$	1118	23	7	145	0	−566	0	−682	0	113	0	212	0
5–8	$-0.26564\times10^{+02}$	22	294	77	−15	0	398	0	92	0	311	0	−81	0
6–7	$-0.10735\times10^{+02}$	25	2433	3662	1118	0	238	0	73	0	160	0	−1366	0
6–8	$-0.13873\times10^{+02}$	1413	34	125	−996	0	340	0	802	0	−161	0	−665	0
7–8	$-0.31381\times10^{+01}$	3	402	7244	741	0	868	0	−17	0	852	0	−583	000

they will of course appear in pairs in order to preserve the Kramers doublet structure.

The character of the reducible representation of $\Gamma_{7/2}$ is $\pm 8, \mp 1, 0$. We find that Γ_6 is contained once, the pair of Γ_4 and Γ_5 is contained three times. In order to see which wave functions are associated with these representations, we construct the projection operators [10] $e^{(\mu)}$ using

$$e^{(\mu)}=(n_\mu/g)\sum_i \chi_i^* C_i$$

where n_μ is the dimension of the μth irreducible representation, g the order of the group and χ_i the character of the ith class. C_i is the sum over all representation matrices of the class i. For $\mu=6$ we find that $\langle k|e^{(6)}|k\rangle=1$ for 2 $k=\pm1, \pm5, \pm7$, and all other elements are zero. The general result is that any three pairs of linear combinations of these 6 basic functions will transform like Γ_6. The remaining two basic functions $|\pm3/2\rangle$ transform according to the pair Γ_4 and Γ_5.

7. References

[1] Lewiner, J., and Meijer, P. H. E., J. of Res. Nat. Bur. Stand. (U.S.), 73A (Phys. and Chem.), No. 2, 241–247 (Mar.–Apr. 1969).
[2] Hutchings, M. T., Solid State Physics **16**, 227 (1964).
[3] Wybourne, B. G., Phys. Rev. **148**, 317 (1966).
[4] Geschwind, S., and Remeika, J. P., Phys. Rev. **122**, 757 (1961).
[5] Stevens, K. W. H., Proc. Phys. Soc. (London) **A65**, 209 (1952).
[6] Bethe, H., Ann. der Phys. **3**, 133 (1929).
[7] Opechowski, W., Physica **7**, 552 (1940).
[8] Luttinger, J. M., and Kittel, C., Phys. Rev. **73**, 162 (1948). See also J. de Boer and R. Van Lieshout, Physica **15**, 569, 1949. R. Lacroix, Helv. Phys. Acta **30**, 374 (1957). (All references are for cubic field only.)
[9] Heine, V., Group Theory in Quantum Mechanics (Pergamon Press).
[10] Meijer, P. H. E., and Bauer, E., Group Theory, Amsterdam, North Holland Publishing Co., 1962.

(Paper 75A5–683)

JOURNAL OF RESEARCH of the National Bureau of Standards—Physics and Chemistry
Vol. 75A, No. 5, September–October 1971

Publications of the National Bureau of Standards*

Selected Abstracts

Ahearn, A. J., **Quantitative analysis of solids by spark source mass spectrometry** *(Proc. Intern. Conf. on Mass Spectroscopy, Kyoto, Japan, Sept. 6–13, 1969), Chapter in Recent Development in Mass Spectroscopy,* K. Ogata and T. Hayakawa, Eds., *pp. 150–157 (University of Tokyo, Press, Tokyo, Japan, 1970).*

Key words: Fluctuations; homogeneity; ion sensitive emulsion; mass spectrometry; precision; quantitative analysis; solids; spark source; trace elements.

In spark source mass spectrometry, the ion sample generally misrepresents the solid sample. Consequently, standard reference materials are needed for direct comparison with the unknown or for the determination of correction factors. The precision in measurement of matrix element ions, trace element ions and their ratio is dependent on the homogeneity of the ion sensitive emulsion used. Methods for testing emulsion uniformity and results on Q2 plates are presented. In some the nonuniformity is less than 5%; in others up to a 60% change in 8 cm has been detected. Under optimum conditions, matrix ions are measured with an RSD $\leq 5\%$ but with trace ions this precision is usually poorer. This means that the trace element contents of the recorded ion sample fluctuate. The trace ions in a spark source ion sample from NBS SRM Platinum 681 fluctuate but not independently. Ion microprobe and other tests should indicate whether the observed fluctuations arise in solid sample inhomogeneities or in fluctuations in the production and/or transmission of trace ions in SSMS.

Almer, H. E., **Methods of calibrating weights for piston gages,** *Nat. Bur. Stand. (U.S.), Tech. Note 577, 54 pages (May 1971) 55 cents, SD Catalog No. C13.46:577.*

Key words: Balance; buoyancy; calibration; standards; substitution weighing; transposition weighing; true mass; uncertainty; value.

Generally weights for piston gages have odd denominations that are often not readily calibrated by intercomparison methods. Therefore, these weights are frequently calibrated by direct comparison methods. This paper presents direct comparison methods for calibrating piston gage weights for use with both equal-arm balances and single-pan balances. Methods of estimating the uncertainty of the values obtained are given. Also included are methods of checking for blunders or gross errors.

Ausloss, P., Rebbert, R. E., Sieck, L. W., **Ion-molecule reactions in the radiolysis of ethane,** *J. Chem. Phys.* **54,** *No. 6, 2612–2618 (March 15, 1971).*

Key words: Charge transfer; deactivation; ethane; ion-molecule; reactions; mass spectrometry; radiolysis.

The reactions of ions generated in ethane irradiated with gamma rays have been studied by analyzing the neutral products formed in reactions with ethane and with other molecules. In experiments in the presence of added $(C_2D_5)_2CDCD_3$, for example, it is shown that the following reactions take place: $C_2H_5^+ + C_2H_6 \rightarrow (C_4H_{11}^+)^* \rightarrow$ *sec*-$C_4H_9^+ + H_2$; *sec*-$C_4H_9^+ + (C_2D_5)_2CDCD_3 \rightarrow$ *n*-$C_4H_9D + C_6D_{13}^+$. The intermediate $(C_4H_{11}^+)^*$ ion can be stabilized by collisions, and will then undergo an undetermined reaction (neutralization or proton transfer) to give *n*-C_4H_{10} as a product. The overall rate constant for reaction of the ethyl ion with ethane is shown to be $\geq 10^{-10}$ cm³/molecule-s. Similarly, it is demonstrated that the reaction: $C_2H_3^+ + C_2H_6 \rightarrow C_4H_9^+$ leads predominantly to the formation of *t*-butyl ions under these conditions: $C_4H_9^+ + (C_2D_5)_2CDCD_3 \rightarrow (CH_3)_3CD + C_6D_{13}^4$. Supplementary experiments performed in a photoionization mass spectrometer demonstrate that ethyl ions undergo a "resonance H_2^- transfer" reaction with ethane: $C_2H_4^+ + C_2D_6 \rightarrow CD_4^+ + C_2H_4D_2$, with a rate constant of 1.1×10^{-10} cm³/molecule-s. Similarly, the ethane parent ion reacts with ethylene: $C_2H_6^+ + C_2D_4^+ \rightarrow C_2H_4 + C_2H_2D$. A series of experiments carried out in the presence of added C_2D_4 demonstrate that the reactions of ethylene ions, such as: $C_2H_4^+ + C_2D_4 \rightarrow C_4D_4H_4^+$, can be conveniently studied in an ethane system.

Becker, D. A., LaFleur, P. D., **Production and certification of NBS biological standard reference materials,** *Proc. 4th Annual Conf. on Trace Substances in Environmental Health, June, 1970, pp. 433–435 (University of Missouri, Columbia, Mo. March 1971).*

Key words: Biological standards; blood standard; botanical standards; environmental samples; standard reference material; tissue standard; trace analysis.

The use of adequate standards is important in the trace element analyses of complex biological materials comprising many environmental and biomedical samples. Available biological materials for interlaboratory comparisons are almost exclusively "round-robin" type samples, and have failed to provide a well-characterized widely distributed and easily available standard. The NBS Office of Standard Reference Materials is in the process of acquiring, analyzing and certifying a series of biological standards. These standards, when issued, will include six botanical standards, a blood standard and a tissue standard.

Bennett, H. S., **Absorbing centers in laser materials,** *J. Appl. Phys.* **42,** *No. 2, 619–630 (Feb. 1971).*

Key words: Antimony; heat conduction; laser materials; Nd-doped glass; platinum; stress components; thermoelastic theory.

One of the severe problems encountered in high-power-solid-state laser systems is the thermal damage to laser rods and optical elements arising from metallic or dielectric inclusions; i.e., impurities with physical and optical properties which differ substantially from those of the host material. Such inclusions may absorb an appreciable amount of the incident radiation and thereby may produce major stresses within the host material. In this paper, the dependence of the maximum value of the tensile stress upon the size of the inclusion and upon the physical properties of the host is examined. The feasibility of using optical techniques to detect metallic and dielectric inclusions in laser materials before they cause damage also is studied. The computations suggest that the use of laser pulse widths of the order of microseconds or longer may be more promising for the detection of small incipient absorbing centers than the use of nanosecond pulse widths.

Bennett, H. S., ***F* centers in ionic crystals: Semicontinuum-polaron models and polarizable-ion models,** *Phys. Rev. B.* **3,** *No. 8, 2763–2777 (April 15, 1971).*

Key words: CaF_2; CaO; *F* center; internal Stark effect; KCl; optical phonons; polarizable ion model; semicontinuum polaron model.

The three lowest-lying *F* center states for KCl, CaO, and CaF_2 are calculated within the framework of five semicontinuum polaron models and one polarizable ion model. The movement of the nearest neighbor ions to the *F* center and the *F* electrons are treated in a self-consistent manner in these models. Exact solutions to these models for the states involved in the transitions of optical absorption and emission are obtained numerically. In addition the internal Stark effect due to noncubic phonons is estimated. The absorption, the emission energy, and the lifetime of the first excited state are evaluated for the six models. It is shown that a semicontinuum polaron model agrees best with the experimental results for KCl and that the polarizable ion model gives the best results for CaO and CaF_2. In addition the semicontinuum polaron model and the internal Stark effect predict that the relaxed state in KCl consists of a strong mixing of $2p$-like and $2s$-like states which are spatially diffuse.

Boyne, H. S., **Laser frequency stabilization techniques and applications,** *Proc. 24th Annual Frequency Control Symp., on Frequency Control, Atlantic City, N.J., April 27–29, 1970, pp. 233–339 (U.S. Army Electronics Command, Fort Monmouth, N.J., 1970), IEEE Trans. Instr. Meas.* **IM–20,** *No. 1, 19–22 (Feb. 1971).*

Key words: Frequency; laser; laser frequency measurement; stabilization; techniques; time standard.

A review of progress in laser stabilization techniques and laser frequency measurement is given. Methods for relating laser frequencies to the time standard and methods for absolute laser frequency stabilization are described. Experimental information on reproducibility and noise characteristics is reported. Application to frequency and wavelength standards is discussed.

Boyne, H. S., Hall, J. L., Barger, R. L., Bender, P. L., Ward, J., Levine, J., Faller, J., **Absolute strain measurements with a 30 meter vacuum interferometer,** *Proc. Conf. Laser Applications in the Geoscience, Huntington Beach, Calif., June 1969, pp. 215–225 (1970).*

Key words: Earth strain; earth tide; geophysics; laser strainmeter; seismograph.

We present details on the design and performance of a 30 meter interferometric strain gauge. We also discuss a practical method for recording absolute earth strain measurements by comparing length changes in the interferometer with an absolute wavelength standard.

Cezairliyan, A., **A high speed method of measuring thermal expansion of electrical conductors,** *Rev. Sci. Instr.* **42,** *No. 4, 540–541 (April 1971).*

Key words: High-speed measurements; high temperature; platinum; thermal expansion.

A transient method for the measurement of thermal expansion of electrical conductors is described. The method is based on detecting the change in radiance coming from a constant radiation source as a result of the expansion of the specimen placed between the radiation source and a radiation detecting system. The specimen can be pulse heated from room temperature to near its melting point in less than one second and pertinent experimental quantities can be measured with a time resolution of 0.4 ms and a full-scale signal resolution of one part in 8000. To check the method, preliminary experiments were performed on platinum in the temperature range 300 to 700 K. The estimated inaccuracy of the results is within 5 percent. The agreement of the results with those in the literature is within 3 percent.

Chappell, S. E., Humphreys, J. C., **Silicon detector measurements of energy deposition in aluminum by monoenergetic electrons** *(Proc. Annual Conf. Nuclear Space Radiation, La Jolla, Calif., July 1970), IEEE Trans. Nuclear Science* **NS–17,** *No. 6, 272–277 (Dec. 1970).*

Key words: Absorbed energy vs depth; absorbed-energy distributions; incident monoenergetic electrons; Monte Carlo calculations; simi-infinite aluminum medium; silicon detector.

The energy deposited at various depths in aluminum by incident monoenergetic electrons has been measured with a silicon semiconductor, transmission detector. Beams of monoenergetic electrons with incident energies of 0.50, 0.75, and 1.0 MeV were directed normally on a semi-infinite slab of aluminum in which a 0.196-mm silicon detector was positioned at various depths. The pulse-height distributions recorded with the detector were converted to absorbed-energy distributions from which the probability of energy absorption per incident electron in the specific layer, as well as the absorbed energy as a function of depth in the material, could be determined. The curves of absorbed energy as a function of depth obtained for aluminum at each energy were compared to those calculated by Berger and Seltzer, employing a Monte Carlo method. Good agreement is shown between calculations and measurements.

Collin, G. J., Ausloos, P., **Ion-molecule reactions in the condensed-phase radiolysis of hydrocarbon mixtures. III. Reactions of i-$C_4H_8^+$ and $tert$-$C_4H_9^+$ ions originating from neopentane,** *J. Am. Chem. Soc.* **93,** *No. 6, 1336*–1340 (March 24, 1971).

Key words: Ion-molecule reactions; neopentane; neutralization; radiolysis; unimolecular/fragmentation.

The liquid phase radiolysis of neopentane has been investigated in the presence of various hydrocarbons and electron scavengers. It is found that the neopentane parent ion dissociates to yield t-$C_4H_9^+$ and iso-$C_4H_8^+$ ions with optimum yields of ~2.4 and ~0.9, respectively. The iso-$C_4H_8^+$ ion reacts with various added alkanes by the H_2^- transfer mechanism: $C_4H_8^+ + RH_2 \rightarrow iso\text{-}C_4H_{10} + R^+$. The relative rates of reaction with different RH_2 additives have been determined, and show the same trends as those observed for these reactions in the gas phase. That is, the rate is seen to increase with an increase in the exothermicity of the reaction (as calculated from gas phase thermodynamic data). The effect of the ΔH of reaction is, however, more pronounced in the liquid than in the gas phase. The t-butyl ion reacts more slowly with alkane additive than does the isobutene ion, but reacts effectively with isobutene and combines with a negative ion from CCl_4 to form t-C_4H_9Cl. Neutralization of the t-butyl ion leads to the formation of isobutene and propylene.

Danos, M., Gibson, B. F., **Very high-momentum components in nuclei and far "subthreshold" production of quarks,** *Phys. Rev. Letters* **26,** *No. 8, 473–476 (Feb. 22, 1971).*

Key words: Coherent production; cosmic rays; high momentum components; many-body clusters; nuclei; quarks.

An estimate, valid for inelastic processes, of the probabilities of the high-momentum components in nuclei resulting from many-body correlations, together with data from Serpukhov, is used to derive upper limits for the quark-production cross section near the threshold.

Danos, M., Spicer, B. M., **Quartet structure in light nuclei,** *Z. Physik* **237,** *320–326 (1970).*

Key words: Collective correlations; four particle-four hole states; light nuclei; quartets; rotational states; vibrational states.

The nature of the low-lying even parity, even spin states of $4n$-nuclei are discussed in terms of the quartet scheme, and many of their properties can be given by it. These states are also the low-lying states important in the collective correlations model of the giant dipole resonance, and the quartet scheme thus provides a description of them.

DeVoe, J. R., Spijkerman, J. J., **Mössbauer spectrometry,** *Anal. Chem. Annual Reviews* **42,** *No. 5, 366R–388R (April 1970).*

Key words: Chemical applications; literature; Mössbauer spectroscopy; review.

A review of the literature on chemical applications of Mössbauer Spectrometry for 1968 and 1969 are presented. This is done primarily with a table of pertinent information on compounds and techniques. New developments in the field are also presented.

Dibeler, V. H., **Photoionization studies and thermodynamic properties of some halogen molecules,** *(Proc. Intern. Conf. on Mass Spectroscopy, Kyoto, Japan, Sept. 8–13, 1969), Chapter in Recent Development in Mass Spectroscopy,* K. Ogata and T. Hayakawa, Eds., *pp. 781–790 (University of Tokyo Press, Tokyo, Japan, 1970).*

Key words: Chlorine monofluoride; dissociative ionization; fluorine; heats of formation; hot bands; hydrogen fluoride; ion pairs; mass spectrometry; molecular ionization; photoionization; vacuum ultraviolet.

Mass spectra and ion yield curves for molecular and dissociative ionization processes are measured for fluorine, hydrogen fluoride, chlorine, and chlorine monofluoride by means of a combined vacuum uv monochromator and mass spectrometer. Ionization and dissociation energies and heats of formation of the molecules are obtained and compared with values derived from thermochemical and spectroscopic studies.

Fatiadi, A. J., **Determination of inososes with an alkaline solution of copper(II) oxalate-tartrate complex (the Somogyi reagent) and reaction mechanisms involved,** *Carbohydrate Res.* **17**, *419–430 (March 1971).*

Key words: Determination; electron-transfer; inosose; oxidation; quantitative; radical; reagent.

Four inososes have been analyzed with the Somogyi reagent and empirical equations for their quantitative determination were derived because reaction of the Somogyi reagent with inososes affords nonstoichiometric quantities of cuprous oxide, and each inosose has a different reducing power.
Results from spectrophotometric and e.s.r. studies of the mechanism of oxidation of inososes with the Somogyi reagent at 25 to 55° are in agreement with a one-electron transfer process; however, at 90 to 100°, extensive degradation of inososes by the Somogyi reagent occurs, doubtless caused by generation of transient radicals during the oxidation, as evidenced by results of a radical-scavenging experiment.

Fickett, F. R., **Resistivity of polycrystalline aluminum and copper in high magnetic fields:** *The effect of temperature and purity, Appl. Phys. Letters* **17,** *No. 12, 525–527 (Dec. 15, 1970).*

Key words: Aluminum; copper; magnetoresistance.

Data are presented on the resistivity of polycrystalline aluminum and copper at 40 kOe and at temperatures from 4 K to 30 K. Specimen purity varies over three decades of residual resistance ratio. For either metal, the actual resistivity measured in the field at a given temperature decreases with increasing specimen purity. This result is important for proposed high magnetic field applications of these metals.

Furcolow, W. H., Technical Standards Coordinator, **Clinical thermometers (Maximum-self-registering, mercury-in-glass),** *Nat. Bur. Stand. (U.S.), Prod. Stand. 39–70, 12 pages (May 1971) 15 cents, SD Catalog No. C13.20/2:39–70.*

Key words: Clinical thermometers; glass thermometers, clinical; mercury-in-glass thermometers; thermometers, self-registering, clinical.

This Voluntary Product Standard covers the requirements and methods of testing maximum-self-registering, mercury-in-glass thermometers of the types commonly used for measuring body temperatures, such as oral and rectal types in both regular and basal temperature scales. It is intended to serve as a nationally recognized basis for certification of compliance by manufacturers and for procurement purposes by consumers. The standard includes requirements for bulb and stem glasses, mercury, dimensions, temperature scale ranges, and graduations, and performance criteria for thermometer aging, hard shaking determination, and accuracy of scale reading.

Garner, E. L., Machlan, L. A., Shields, W. R., **Standard Reference Materials: Uranium isotopic standard reference materials,** *(Certification of uranium isotopic standard reference materials), Nat. Bur. Stand. (U.S.), Spec. Publ. 260–27, 162 pages (April 1971) $1.25, SD Catalog No. C13.10:260–27.*

Key words: Absolute isotopic abundance; ignition procedure; isotopic standards; mass spectrometry; stoichiometry; uranium.

An ignition procedure has been developed that will yield reproducible stoichiometry for U_3O_8. The effects of temperature, length of ignition, rate of cooling, pressure and type of atmosphere were investigated. This ignition procedure has been used for the blending of high purity ^{235}U and ^{238}U separated isotopes to prepare calibration standards for the determination of bias effects in the thermal emission mass spectrometry of uranium. Weight aliquoting was used to prepare calibration mixes with $^{235}U/^{238}U$ ratios of more than 10 and less than 0.1 and to add a ^{233}U spike for the determination of minor isotope abundances in the uranium isotopic standards by the isotope dilution technique.
A description of the unique features of the mass spectrometer instrumentation including the source, NBS collector and expanded scale recorder are given. Two specific analytical procedures were used for the isotopic analysis of uranium and are adaptable, within a general framework, to fit the particular ion current intensity requirements of a wide range of isotopic distributions. Mass discrimination due to evaporation and ionization on the filaments, and other parameters such as temperature, time, sample size, sample mounting, total sample composition, acidity, filament material, pressure, nonohmic response, R-C response and source memory were studied as part of the development effort to establish sound analytical procedures.
The absolute isotopic abundances of 18 uranium SRMs were determined by thermal emission mass spectrometry. The general approach was to determine absolute $^{235}U/^{238}U$ ratios by using calibration mixes to correct for filament bias. Then the absolute ^{234}U and ^{236}U were determined by ^{233}U isotope dilution. For SRM U–0002, isotope dilution was the only practical means of determining the low abundance of ^{235}U as well as the ^{234}U. The limits given for the isotopic composition of the uranium SRMs are at least as large as the 95 percent confidence limits for a single determination and include terms for inhomogeneities of the material as well as analytical errors.

Geltman, S., Burke, P. G., **Electron scattering by atomic hydrogen using a pseudo-state expansion II. Excitation of 2*s* and 2*p* states near threshold,** *J. Phys. B: Atom. Molec. Phys.* **3**, *No. 8, 1062–1072 (Aug. 1970).*

Key words: Close coupling calculation; electron scattering; pseudo-state expansion.

The pseudo-state modification of the close-coupling expansion is applied to the 2*s* and 2*p* excitation of atomic hydrogen by electron impact. Pseudo-states are used which assure the implicit inclusion of all important excited state polarizabilities. A detailed comparison is made with results obtained from other modifications of the close-coupling expansion and the eigenphase minimum principle is used to determine the best result for each partial cross section. Comparison of the theory and experiment in the first electron volt above the $n=2$ threshold shows very good agreement in the ratio $Q(1s-2s)/Q(1s-2p)$, but a 20% discrepancy exists between the individual cross section magnitudes when experiment is normalized to the Born approximation at higher energies.

Green, M. S., Cooper, M. J., Sengers, J. M. H. L., **Extended theromodynamic scaling from a generalized parametric form,** *Phys. Rev. Letters* **26**, *No. 9, 492–495 (March 1, 1971).*

Key words: Coexistence curve; critical point; liquid-gas phase transition; parametric form; scaling; thermodynamic properties.

The Josephson-Schofield parametric representation for lowest order thermodynamic scaling is generalized, introducing an additional critical exponent. Expansions around the critical point are deduced for the various thermodynamic properties of fluids and to lowest order, the asymptotic power law forms are recovered. Experiment indicates that the full symmetry of magnets prevails to lowest order in the fluids. The idea of Griffiths and Wheeler that there is a unique direction in the space of intensive variables is used to determine the new critical exponent. An exponent $1-\alpha'$ is suggested for the diameter of the coexistence curve. Experimental data on the vapor pressure, critical isotherm and coexistence curve are shown to support the predicted forms.

Harman, G. G., Kessler, H. K., **Application of capacitor microphones and magnetic pickups to the tuning and trouble shooting of microelectronic ultrasonic bonding equipment,** *Nat. Bur. Stand. (U.S.), Tech. Note 573, 24 pages (May 1971) 35 cents, SD Catalog No. C13.46:573.*

Key words: Capacitor microphone; flip-chip; magnetic pickup; microelectronic interconnections; spider bonding; ultrasonic bonding; wire bonding.

Microelectronic ultrasonic wire bonding equipment typically welds wires to integrated circuits at frequencies between 50 and 65 kHz. Mechanical vibrations at these frequencies are difficult to measure directly and malfunctions of the system may not be recognized. Two different methods of measuring these vibrations are described. The first method involves use of a capacitor microphone and a tapered tip and the second method use of a small magnetic pickup. Procedures are given for establishing a specific ultrasonic vibration amplitude, tuning the ultrasonic system to resonance, and diagnosing both mechanical and electrical problems in wire bonding equipment. Although these techniques and procedures were developed for ultrasonic wire bonding equipment, they are applicable to otherultrasonic welding systems of lead attachment, such as flip-chip, beam lead and spider bonding.

Hastie, J. W., Hauge, R. H., Margrave, J. L., **Infrared spectra and geometries of heavy metal halides: $SrCl_2$, $BaCl_2$, $EuCl_2$, EuF_2, $PbCl_2$, and UCl_2,** *High Temp Sci.* **3,** *No. 1, 56–71 (Jan. 1971).*

Key words: Heavy metal halides; infrared spectra; matrix isolation; molecular geometries.

The heavy metal dihalide species $SrCl_2$, $BaCl_2$, $EuCl_2$, EuF_2, $PbCl_2$, and UCl_2, generated under thermodynamic equilibrium conditions, have been isolated in matrices of solid, Ne, Ar, Kr, and N_2. Methods of production varied from simple Knudsen vaporization for $SrCl_2$, $BaCl_2$, and $PbCl_2$, and decomposition vaporization, i.e., $EuX_3(s) \rightarrow EuX_2(g) + 1/2\ X_2$ to oxidation-vaporization, i.e., $CaCl_2(g) + U(s) \rightarrow UCl_2(g) + Ca(g)$; $Cl_2(g) + U(s) \rightarrow UCl_2(g)$; and $2HCl(g) + U(s) \rightarrow UCl_2(g) + H_2$ Infrared spectra for these matrix-isolated species were obtained (33–4000 cm^{-1}) and the symmetric (ν_1) and the antisymmetric (ν_3) vibrations observed in each case. For the chlorides the extremely low intensity nature of the bending frequency (ν_2), the numerous extraneous low frequency absorptions associated with lattice modes of the solid matrices and the ever-present HCl impurities, resulted in a less reliable assignment of ν_2 values. In some cases measurement of the various naturally occurring Cl^{35}, Cl^{37} isotopic species allowed definite assignments of the stretching frequencies to be made and the following bond angles were calculated: $SrCl_2$ ($130 \pm 5°$), $EuCl_2$ ($135 \pm 5°$), and $PbCl_2$ ($96 \pm 3°$). Fermi interactions between ν_1 and ν_3 for the unsymmetrical isotopic species were also observable in these cases. From the relative intensities of ν_1 and ν_3 the following bond angle estimates were made: $BaCl_2$ ($120 \pm 10°$), EuF_2 ($110 \pm 15°$), and UCl_2 ($100 \pm 15°$). These bond angles were also in accord with a consistent set of force-constant data.

Kamper, R. A., Zimmerman, J. E., **Noise thermometry with the Josephson effect,** *J. Appl. Phys.* **42,** *No. 1, 132–136 (Jan. 1971).*

Key words: Josephson effect; noise; superconductivity; thermometry.

Thermal noise causes a random frequency modulation of the self-oscillation of a Josephson junction, and the temperature of the noise source can be determined by analysis of the generated signal. We discuss the theoretical limitations of thermometry with this principle, and describe a prototype thermometer which has recorded noise temperatures down to 0.075 K.

Kidnay, A. J., Hiza, M. J., **The purification of helium gas by physical adsorption at 76° K,** *AIChE J.* **16,** *No. 7, 949–954 (Nov. 1970).*

Key words: Breakthrough time; helium; mixture adsorption; nitrogen methane.

The physical adsorption isotherms for three methane-helium mixtures, two nitrogen-helium mixtures, and one methane-nitrogen-helium mixture were measured at 76 K and pressures of 2 to 65 atm on a coconut shell charcoal. The adsorption isotherms of the pure components, nitrogen, methane, and helium, were also determined over the appropriate pressure ranges.
Methods for predicting the mixture adsorption isotherms using only the pure component isotherms are discussed and are shown to be adequate for these systems.
The concentration versus time or breakthrough curves were also measured for both the binary and ternary mixtures at a number of different flow rates. Mass transfer coefficients for both the gas phase and the adsorbed phase were obtained from these breakthrough curves using the method proposed by Eagleton and Bliss (11).

Kieffer, L. J., **Low energy electron collision cross section data. Part II. Electronic excitation level and line cross sections,** *Atomic Data* **1,** *No. 2, 121–287 (Nov. 1969).*

Key words: Atom; cross section; electron; molecule.

This is the second part of a comprehensive compilation of low energy electron collision cross section data. The compilation is limited to experimental measurements and includes data for all atomic species and for those molecules which are important in aeronomy, astrophysics, and plasma physics. The data included were taken from literature published through December, 1968.

Kulin, G., Gurewitz, P. H., Editors, **Hydraulic Research in the United States 1970 – Including Contributions from Canadian Laboratories,** *Nat. Bur. Stand. (U.S.), Spec. Publ. 346, 354 pages (Mar. 1971) $2.50, SD Catalog No. C13.10:346.*

Key words: Fluid mechanics; hydraulic engineering; hydraulic research; hydraulics; hydrodynamics; model studies; research summaries.

Current and recently concluded research projects in hydraulics and hydrodynamics for the years 1969–1970 are summarized. Projects from more than 250 university, industrial, state and federal government laboratories in the United States and Canada are reported.

Lane, N. F., Geltman, S., **Differential elastic and rotational excitation cross sections for electron-H_2 scattering,** *Phys. Rev.* **184,** *No. 1, 46651 (Aug. 5, 1969).*

Key words: Close coupling calculation; differential cross sections; elastic scattering; electron; h_2 (hydrogen molecule); rotational excitation.

Differential elastic and rotational excitation cross sections for electron-h_2 scattering have been calculated in the close coupling approximation. The resulting elastic angular distributions are found to be in very good agreement with measurements. An apparent oscillation in the measured differential cross section for rotational excitation is not found in the calculation.

Lloyd, E. C., Editor, **Accurate characterization of the high-pressure environment.** *Proceedings of a Symposium held at the National Bureau of Standards, Gaithersburg, Maryland, October 14–18, 1968, Nat. Bur. Stand. (U.S.), Spec. Publ. 326, 343 pages (March 1971) $4.50, SD Catalog No. C13.10:326.*

Key words: Accurate measurement; equation-of-state; fixed points; high pressure; high-pressure equipment; instrumentation; pressure scale; shock wave technique; temperature.

The volume contains 38 papers prepared for the Symposium on Accurate Characterization of the High-Pressure Environment held on October 14–18, 1968, at Gaithersburg, Maryland, under the sponsorship of the National Bureau of Standards and the Geophysical Laboratory of the Carnegie Institution of Washington. The papers are presented with the discussions that occurred during the sessions. The book also includes reports of several informal committees of the conferees on choices of reference pressure materials and on other matters relevant to improved measurement and calibration. The Symposium was intended to provide an authoritative survey of problems and techniques presently in use or proposed for precise high-pressure measurement and for temperature measurement at high pressure.

McConnell, P. M., Daney, D. E., Kirgis, J. B., **Thermoelastic expansion and creep of polyethylene terephthalate and polypyromelitimide film and polyethylene terephthalate fibers from 20 to 295 K,** *J. Appl. Phys.* **41,** *No. 13, 5066–5070 (Dec. 1970).*

Key words: Longitudinal; polyethylene terephthalate; polypyromelitimide; relative creep; thermoelastic; transverse.

A quartz tube dilatometer was used to measure the lineal thermal expansion and creep of single lengths of polyethylene terephthalate (PETP) film, Mylar, polypyromelitimide (PPMI) film, Kapton, and PETP multi-fiber yarn. Dacron, while stressed under constant tension. Tensions below and above the conventionally defined yield strength were used and the sample temperature ranged from 20 to 295 K. Relative creep strain measurements, taken at the constant temperatures 77, 195, and 295 K, were found to obey the equation

$$\epsilon = \exp\left[-2.3 \exp(A'y)\right]$$

where y is a function of stress, time, and temperature and A' is a constant depending on the material. This equation was used to correct the thermoelastic expansion measurements for creep at the higher stresses. PETP multi-fiber yarn subjected to a slight tension was found to elongate during cooldown from 293 to 20 K. Higher stresses caused less elongation; i.e., the coefficient of expansion increased with stress. This result is believed to be due to changes in crystallanity at the higher stresses. A similar stress effect was found with PETP film but not with PPMI film. The thermoelastic expansivity of the film samples was also found to be sensitive to the thickness.

McLaughlin, W. L., Hussmann, E. K., Eisenlohr, H. H., Chalkley, L., **A chemical dosimeter for monitoring gamma-radiation doses of 1–100 krad,** *Intern. J. Appl. Radiation Isotopes* **22,** *135–140 (1971).*

Key words: Chemical dosimeter; disinfestation; dosimeter; dyes; gamma rays; insect sterilization; shelf-like extension; sprouting inhibition.

A simple chemical dosimeter is described for measuring gamma-ray doses useful for insect sterilization, seed-sprouting inhibition, and food shelf-life extension. The solutions, colorless before irradiation, assume a stable blue-violet color when irradiated to absorbed doses from 1 to 100 kilorads. The readout may be made either visually, colorimetrically, or spectrophotometrically. The optical density is linear with dose, and the response does not vary with dose rate.

Manning, J. R., **Correlation effects and activation energies for diffusion in alloys,** *(Proc. Conf. Atomic Transport in Solids and Liquids, Marstand, Sweden, June 1970), Z. Naturforsch.* **26A,** *No. 1, 69–76 (Jan. 1971).*

Key words: Activation analysis; concentrated alloys; correlation factor; diffusion; random alloy; vacancies.

The problems involved in calculating correlation factors for diffusion in dilute alloys can be contrasted to those arising in concentrated solid solutions. As one moves from the pure element to the dilute alloy to the concentrated alloy, the calculation becomes progressively more difficult. Because of the complex atom configurations which can occur in concentrated alloys, it usually is not possible to calculate correlation factors in these alloys exactly.

Several important simplifications are available in nondilute random alloys. A large reduction in complexity can be secured by using a random alloy model where each atom is treated as diffusing in a uniform matrix, with the matrix properties being determined by the composition and jump frequencies in the alloy. Resulting equations in this random alloy model can be expressed directly in terms of the experimentally measurable tracer diffusion coefficients with no unknown vacancy jump frequencies appearing. Also these equations have the advantage of being in simple analytic form and not requiring numerical methods to evaluate the correlation factors. These two features make possible the direct expression of the temperature dependence of the correlation factor in terms of the experimental activation energies.

Equations are found for $\Delta H/\Delta Q$ in random binary cubic alloys, where ΔH is the difference between the activation enthalpies for diffusion of the two species and ΔQ is the difference between the experimentally measured activation energies of the two species. This ratio is never less than unity and can be much larger than unity. Values are plotted for diamond, body-centered cubic and face-centered cubic structures. From the magnitude and composition dependence of $\Delta H/\Delta Q$, it is concluded that the temperature dependence of the correlation factor cannot by itself explain the difference between the activation energies measured from tracer diffusion and from internal friction in the non-dilute range.

Mason, H. L., Editor, **Innovative metrology—key to progress,** *Proceedings of the 1970 Standards Laboratory Conference, Nat. Bur. Stand. (U.S.), Spec. Publ. 335, 132 pages (Mar. 1971) $1.50, SD Catalog No. C13.10:335.*

Key words: Metrology management; National Conference of Standards Laboratories; physical measurement; Proceedings NCSL.

The biennial Standards Laboratory Conference of the National Conference of Standards Laboratories convened at the Gaithersburg facilities of the National Bureau of Standards June 15–17, 1970. The theme of the meeting, Innovative Metrology—Key to Progress, was amplified by 23 papers presented at technical sessions devoted to new technologies and applications, laboratory management and operations, new methods of optimizing calibration intervals, new ways of managing, and new international developments.

Meinke, W. W., **Standard reference materials for clinical measurements,** *Anal. Chem.* **43,** *28A–47A (May 1971).*

Key words: Clinical chemistry; organic SRMs; standard reference materials; spectrophotometry SRMs.

The NBS Program in Standard Reference Materials for Clinical Chemistry measurements is described. Each of the SRMs issued in this area in the last five years is discussed. Future directions of the program are also mentioned.

Murkerjee, P., Mysels, K. J., **Critical micelle concentrations of aqueous surfactant systems,** *Nat. Stand. Ref. Data Ser., Nat. Bur. Stand. (U.S.), 36, 227 pages (Feb. 1971) $3.75, SD Catalog No. C13.48:36.*

Key words: Association colloid; bibliography; CMC: colloid; colloidal electrolyte; critical concentration; critical micelle concentration; detergent; hydrophobic bonding; Kraft point; long chain compounds; micelle; paraffin chain salts; selected values; soap; solubilization; standard values; surface active agents; surface chemistry; surface tension; surfactant.

Critical micelle concentrations (CMC's), have been collected, organized and evaluated. The literature has been scanned for numerical values from 1926 up to and including 1966. In addition, over 800 values, hitherto available only in graphical form or implied in experimental data, have been extracted from the publications and are included. Close to 5,000 entries, based on 333 references,

429-270 O - 71 - 9

dealing with 720 compounds are tabulated in the main tables. Whenever available, the temperature, any additives present, the method of determination and the literature source are given for each CMC value and an indication of the apparent quality of the preparation and method used are included. A shorter table gives selected values which are believed to be particularly reliable, including highly accurate ones. Among these, concordant values from at least two independent laboratories are emphasized.
Included in the Introduction is a general discussion of the importance and significance of CMC values and of methods for their determination, as well as a summary of the procedures used in the collection, evaluation and presentation of these values in the present work. Extensive indexes are provided.

Phucas, C. B., Technical Standards Coordinator, **Package quantities of green olives,** *Nat. Bur. Stand. (U.S.), Prod. Stand. 40–70, 9 pages (May 1971) 10 cents, SD Catalog No. C13.20/2:40–70.*

Key words: Green olives, package quantities of; olives, green, package quantities of; package quantities of green olives.

This Voluntary Product Standard covers a range of package quantities that are recommended for green olives and establishes specific packaging requirements in terms of net drained weight. Methods of labeling products which comply with this Standard are provided.

Phucas, C. B., Technical Standards Coordinator, **Package quantities of instant mashed potatoes,** *Nat. Bur. Stand. (U.S.), Prod. Stand. 41–70, 8 pages (April 1971) 10 cents, SD Catalog No. C13.20/2:41–70.*

Key words: Instant mashed potatoes, package quantities of; mashed potatoes, instant, package quantities of; package quantities of instant mashed potatoes; potatoes, instant mashed, package quantities of.

This Voluntary Product Standard covers a range of package quantities based on servings and establishes the definition of a serving which is based on the weight of the reconstituted product.

Reitwiesner, G. W., **On computer performance measurement programming measuring indexing adroitness by isolating complex primes,** *Nat. Bur. Stand. (U.S.), Tech. Note 572, 25 pages (Apr. 1971) 35 cents, SD Catalog No. C13.46:572.*

Key words: Assessment; complex; composite; computer; criteria; evaluation; Gaussian primes; indexing; measurement; performance; prime; program; test.

This writing, describing a computer performance test program, is concerned not primarily with specific measurements, but rather with a procedure for making measurement regarding specific properties of computer operation.
The program is written in a particular problem-oriented programming language; therefore assessment perforce spans the effects of the computer hardware, of the programming language, and of the intervening compiler processes.
The objective of the test is to assess adroitness in certain indexing operations. Assessment is accomplished by measuring execution time of a recursive programming loop.
The test problem was chosen as a convenient artifice to use certain specific indexing-type operations in the programming employed for solution.
The test program performs a simple computation for which the solution is completely definitive, yet for which both the solution and the time for achieving it are variable under parameters whose values are introduced as program input data.

Robertson, B., Mitchell, W. C., **Equations of motion in nonequilibrium statistical mechanics. III. Open systems,** *J. Math. Phys.* **12,** *No. 3, 563–568 (March 1971).*

Key words: Equations of motion; nonequilibrium statistical mechanics; open systems; thermal transport.

A simple hypothesis on the effect of the interaction between a system and its surroundings is used to generalize nonequilibrium statistical mechanics to apply to open systems. Thermal driving of a system by its surroundings is defined in statistical mechanics by analogy with the first law of thermodynamics, which describes exchange of heat between the system and an external source. The assumption that an isolated system is thermally driven is used to derive a Liouville equation with an additional term that is linear in the ex-strength. This formalism is attractive because the source strength, which is assumed known, appears in the equations linearly just as in classical thermodynamics or hydrodynamics. A microscopic expression for the source strength is obtained by comparing the thermal driving formalism with an exact dynamical analysis of the system interacting with its surroundings.

Scharf, K., **Spectrophotometric measurement of ferric ion concentration in the ferrous sulphate (Fricke) dosemeter,** *Phys. Med. Biol.* **16,** *No. 1, 77–86 (1971).*

Key words: Chemical dosimeter; chemical dosimetry, ferrous sulfate; ferrous sulfate dosimeter; ferric ions; Fricke dosimeter; radiation dosimeter; radiation dosimetry; spectrophotometry; spectrophotometric measurements.

A systematic error in the spectrophotometric measurement of ferric ion concentrations in the ferrous sulphate dosemeter may be made by an incorrect evaluation of a non-linear spectrophotometric calibration curve. Methods are discussed for determining the radiation-produced change in molarity from the actual calibration curve, and a method of normalization of measured absorbances is suggested. Normalization factors, converting measured absorbances into normalized values, can either be calculated by choosing a reference value of the molar extinction coefficient, or can be determined by comparative absorbance measurements on two spectrophotometers, one of them to be a precision instrument. Normalized absorbances are proportional to molarity and may be considered to be free of errors due to instrumental parameters and inaccuracies in acidity and temperature of solutions, and of errors in molarity if derived by comparative measurements.

Sieck, L. W., Searles, S., Ausloos, P., **High-pressure photoionization mass spectrometry. Photoionization of propane at 11.6–11.8 eV. Formation and reactivity of the $(C_3H_8)_2^+$ dimer ion,** *J. Chem. Phys.* **54,** *No. 1, 91–95 (Jan. 1, 1971).*

Key words: Ion-molecule reaction; kinetics; mass spectrometry; photoionization; propane; radiation chemistry.

The major reaction path of the propane molecular ion with propane was found to be the formation of the dimer ion $(C_3H_8)_2^+$ via a termolecular mechanism;

$$C_3H_8^+ + C_3H_8 \xrightarrow{C_3H_8} (C_3H_8)_2^+ + C_3H_8$$

In addition, $C_3H_6^+$ and $C_3H_7^+$ were also found as minor reaction products at lower pressures. The reactions of the dimeric ions with ethylene and NO were also investigated. The charge exchange reaction

$$(C_3H_8)_2^+ + NO \rightarrow NO^+ + 2C_3H_8$$

was found in propane-NO mixtures, suggesting a recombination energy in excess of 9.24 eV. The formation of $C_3H_8NO^+$ was also detected at higher total pressures. The dimeric ion was also found to transfer H_2 to ethylene without affecting the structural integrity of the Carbon skeleton,

$$(C_3H_8)_2^+ + C_2H_4 \rightarrow C_6H_{14}^+ + C_2H_6$$

indicating that this species exhibits the chemical behavior of a saturated hydrocarbon ion.

Slattery, W. J., Editor, **An index of U.S. voluntary engineering standards,** *Nat. Bur. Stand. (U.S.), Spec. Publ. 329, 1,000 pages (Mar. 1971) $9.00, SD Catalog No. C13.10:329.*

Key words: Engineering standards, index of; index of standards, recommended practices, specifications, and test methods; Key-

Word-In-Context index of voluntary standards; standards; voluntary, index of.

This computer-produced Index contains the permuted titles of more than 19,000 voluntary engineering and related standards, specifications, test methods, and recommended practices, in effect as of December 31, 1969, published by some 360 U.S. technical societies, professional organizations, and trade associations. The title of each standard can be found under all the significant key words which it contains. These key words are arranged alphabetically down the center of each page together with their surrounding context. The date of publication or last revision, the standard number, and an acronym designating the standards-issuing organization appear as part of each entry. A list of these acronyms and the names and addresses of the organizations which they represent are found at the beginning of the Index.

Spiegel, V., Jr., Murphey, W. M., **Calculation of thermal neutron absorption in cylindrical and spherical neutron sources,** *Metrologia*, **7,** *No. 1, 34–38 (Jan. 1971).*

Key words: Manganous sulfate bath; neutron source absorption; neutron source calibration; thermal neutron absorption.

A calculation of the thermal neutron self-absorption for cylindrical or spherical neutron sources has been made. The calculations are confirmed by the experimentally measured difference in manganous sulfate bath activity for bare and cadmium-covered Pu-Be and Am-Be neutron sources. The calculation is done in single interaction approximation and assumes that the incident thermal neutron flux is isotropic. The source material may be fissionable and be covered by up to three cladding materials. A computer program has been written for the numerical calculations.

Tech, J. L., **A high-dispersion spectral analysis of the Ba II Star HD 204075 (ζ Capricorni),** *Nat. Bur. Stand. (U.S.), Monogr. 119, 174 pages (March 1971) $3.25, SD Catalog No. C13.44:119.*

Key words: Abundances of elements in stars; Ba II stars (ζ Capricorni); curve of growth; equivalent widths; identification of spectral lines; ionization in stars; oscillator strengths; temperature in stars; turbulence in stars.

A double differential curve of growth analysis, using both the sun and ϵ Virginis (G9 II–III) as comparison stars, has been performed for the Ba II star ζ Capricorni. The observational material consists of equivalent widths, central depths, and half-widths for 1100 spectral lines measured on direct-intensity tracings of plates obtained by J. L. Greenstein at the coudé focus of the 200-in telescope. The plates cover the spectral regions 3880–4825 Å and 5100–6720 Å at reciprocal dispersions of 2.3 and 3.4 Å/mm, respectively. Line identifications given in earlier lists for barium stars have been critically re-examined. Three lines have been attributed with reasonable certainty to dysprosium, which has not previously been observed in barium stars.
The atmospheric parameters derived for ζ Cap are:

θ_{exc} :	1.13	$[P_e]_{\zeta-\cdot}$:	-1.28
θ_{ion} :	0.99	$[P_e]_{\zeta-\epsilon}$:	$+0.13$
$\log 2\alpha$:	-2.5	$[k]_{\zeta-\cdot}$:	-1.10
v_{micro} :	3.5 km/s	$[k]_{\zeta-\epsilon}$:	-0.03
v_{macro} :	5.5 km/s		

Atmospheric abundances have been derived for 37 elements. The results obtained with respect to the two comparison stars are in good agreement. The barium star exhibits essentially solar abundances for most elements lighter than germanium, but overabundances by factors of about two are indicated for carbon and lithium. With the exception of europium, all observed elements heavier than germanium are found to be overabundant in ζ Cap. Improved NBS *gf*-values, converted to the system of line strengths in ϵ Vir, have yielded exceptionally well-defined curves of growth for several rare earths. Overabundances by factors of about eight or nine have been found for the *s*-processed rare earths, as well as for dysprosium, which is generally considered to be *r*-processed. The abundances derived for the rare earths are greater by about a factor of three than those derived for the same star by Warner (Mon. Not. Roy. Astron. Soc. **129,** 263 (1965)).

Thurber, W. R., **Determination of deep impurities in silicon and germanium by infrared photoconductivity,** *Nat. Bur. Stand. (U.S.), Tech. Note 570, 13 pages (Mar. 1971) 25 cents, SD Catalog No. C13.46:570.*

Key words: Deep impurities; germanium; infrared; photoconductivity; photoresponse; semiconductors; silicon.

The feasibility of using infrared photoresponse and photoconductivity measurements to study deep impurities in germanium and silicon is examined by reviewing the literature. It is concluded that photoconductivity is useful in detecting the presence of specific impurities because each impurity has a long wavelength cut off in response associated with its ionization energy. However, when there are several deep impurities in the same specimen, it is difficult to be certain of detecting each one because some have broad cut offs and many have nearly the same ionization energies. Photoconductivity as a general technique has serious limitations for determining the total concentration of deep impurities. The equations for determining impurity concentration from the magnitude of the photoconductivity signal depend on the relative influence of deep and shallow centers. Equations are derived for several situations and experimental results from the literature are discussed for each one. Only uncompensated centers are available for photoionization and therefore the total concentration can not be obtained directly. In some situations the response due to a deep center is independent of its concentration. Other techniques for studying deep impurities are discussed briefly.

Uzgiris, E. E., Hall, J. L., Barger, R. L., **Precision infrared Zeeman spectra of CH_4 studied by laser-saturated absorption,** *Phys. Rev. Letters* **26,** *No. 6, 289–293 (Feb. 8, 1971).*

Key words: Lasers; methane; saturated absorption; Zeeman effect.

Zeeman splitting of the methane 2947.912 cm^{-1} $F_1^{(2)}$ line was observed. The g factor of the rotational magnetic moment of methane was measured to be $g_J = +0.311 \pm 0.006$ and it was found that $g_J(v_3=1)$ is equal to $g_J(v_3=0)$. A Doppler-generated level crossing signal in saturated absorption was observed and is described.

Wagman, D. D., Evans, W. H., Parker, V. B., Halow, I., Bailey, S. M., Schumm, R. H., Churney, K. L., **Selected values of chemical thermodynamic properties—Tables for elements 54 through 61 in the Standard order of arrangement,** *Nat. Bur. Stand. (U.S.), Tech. Note 270–5, 49 pages (Mar. 1971) 55 cents, SD Catalog No. C13.46:270–5.*

Key words: Enthalpy; entropy; Gibbs energy of formation; hafnium compounds; heat of formation; niobium compounds; scandium compounds; tantalum compounds; titanium compounds; vanadium compounds; yttrium compounds; zirconium compounds.

Contains tables of values for the standard heats and Gibbs (free) energies of formation, entropies and enthalpies at 298.15 K and heats of formation at 0 K for compounds of vanadium, niobium, tantalum, titanium, zirconium, hafnium, scandium, and yttrium (elements 54–61 in the Standard Order of Arrangement). These tables are a continuation of the comprehensive revision of NBS Circular 500.

Wampler, R. H., **A report on the accuracy of some widely used least squares computer programs,** *J. Am. Stat. Assoc.* **65,** *No. 330, 549–565 (June 1970).*

Key words: Computer programs; curve fitting; Gram-Schmidt orthogonalization; Householder transformations; iterative refinement; least squares; linear equations; orthogonalization; orthogonal polynomials; regression; rounding error; stepwise regression.

Two linear least squares test problems based on fifth degree polynomials have been run on more than twenty different computer programs in order to assess their numerical accuracy. The programs tested, all in present-day use, included representatives from several statistical packages as well as some from the SHARE library. Essentially four different algorithms were used in the various programs to obtain the coefficients of the least squares fits. The tests were run on several different computers, in double precision as well as single precision. By comparing the coefficients reported, it was found that those programs using orthogonal Householder transformations or Gram-Schmidt orthonormalization were much more accurate than those using elimination algorithms. Programs using orthogonal polynomials (suitable only for polynomial fits) also proved to be superior to those using elimination algorithms. The most successful programs accumulated inner products in double precision and made use of iterative refinement procedures. In a number of programs, the coefficients reported in one test problem were sometimes completely erroneous, containing not even one correct significant digit.

Weber, L. A., **Density and compressibility of oxygen in the critical region,** *Phys. Rev. A.* **2,** *No. 6, 2379–2388 (Dec. 1970).*

Key words: Chemical potential; coexistence curve; compressibility; critical point; oxygen; PVT.

Density versus height profiles have been measured in the critical region of oxygen by means of capacitance techniques. Results are given for the liquid and vapor densities at coexistence, for compressibilities along the coexistence curve to within $t\equiv(T-T_c)/T_c=-6\times10^{-5}$, for compressibilities along the critical isotherm to within $(\rho-\rho_c)/\rho_c=5\times10^{-2}$, and for compressibilities along the critical isochore to within $t=2\times10^{-4}$. The data are analyzed in terms of power law descriptions and are shown to be in excellent agreement with recent scaling law analyses of data for other fluids.

Weber, L. A., **Some vapor pressure and P, V, T, data on nitrogen in the range 65 to 140 K,** *J. Chem. Thermodynamics* **2,** *No. 6, 839–846 (Nov. 1970).*

Key words: Density; liquids; nitrogen; phase boundary; PVT; saturation density; vapor pressure.

New data are presented for the vapor pressure of nitrogen from 65–126 K and for seven PVT isochores between 80 and 140 K. The isochores range in density from 0.85 to 2.6 times critical. The vapor pressure data are compared with existing literature, and an equation is given for the vapor pressure on the IPTS–68 temperature scale between the triple point and the critical point.

Weir, C. E., Piermarini, G. J., Block, S., **On the crystal structures of Cs II and Ga II,** *J. Chem. Phys.* **54,** *No. 6, 2768–2770 (March 15, 1971).*

Key words: Cesium; gallium; high-pressure; polymorph; single crystal; x-ray diffraction.

The structures of Cs II and Ga II have been confirmed by high pressure single crystal x-ray studies. Cs II is Face Centered Cubic with $a=6.465\pm0.015$ Å and Ga II is Body Centered Tetragonal with $a=2.808\pm0.003$ Å and $c=4.458\pm0.0003$ Å.

White, H. J., Jr., **Federal information processing standards index, January 1, 1971,** *Nat. Bur. Stand. (U.S.), Fed. Info. Process. Stand. Publ. (FIPS Pub) 12, 143 pages, $1.50, SD Catalog No. C13.52:12.*

Key words: American National Standards; computers, data elements and codes; data processing systems; Federal Information Processing Standards; management information systems; International Organization for Standardization; standards; U.S. Government.

This publication provides material concerning standardization activities in the area of information processing at the Federal, National and International levels. Also included are related policy and procedural guideline documents. A list of Federal Government participants involved in the development of Federal Information Processing Standards is provided.

Weiderhorn, S. M., Johnson, H., **Effect of pressure on the fracture of glass,** *J. Appl. Phys.* **42,** *No. 2, 681–684 (Feb. 1971).*

Key words: Deep submergence; fracture; fracture energy; glass; high pressure; strength.

The fracture surface energies of three glass compositions were measured as a function of ambient pressure and were found to be independent of pressure, to 20 kbar, suggesting no change in the fracture mechanism. The mechanical behavior of glass thus differs from that of plastics or metals which are observed to become stronger and more ductile with increasing pressure. The difference in fracture behavior is believed due to the fact that fracture of glass is essentially a volume conserving process in contrast to metals and plastics for which volume expansion occurs.

Yokel, F. Y., Mathey, R. G., Dikkers, R. D., **Strength of masonry walls under compressive and transverse loads,** *Nat. Bur. Stand. (U.S.), Bldg. Sci. Ser. 34, 74 pages (Mar. 1971) 70 cents, SD Catalog No. C.13.29/2:34.*

Key words: Brick; cavity walls; composite walls; compressive strength; concrete block; flexural strength; masonrv; mortar; slenderness effects; standards; structural stability; walls.

Ninety walls of 10 different types of masonry construction were tested under various combinations of vertical and transverse load. It is shown that the effect of vertical load and wall slenderness on transverse strength can be predicted by rational analysis. The analysis is based on established theory which has been extended to account for the properties of masonry. Similar methods of rational analysis have been adopted for the design of steel structures and are presently being considered for reinforced concrete structures.

Other NBS Publications

J. Res. Nat. Bur. Stand. (U.S.), 75 C Engineering & Instrumentation, No. 2 (April–June 1971), SD Catalog No. C13.22/sec. C:75/2. $1.25.

Armstrong, G. T., Gibbs energy versus free energy, Chem. Eng. News, Letter to the Editor, p. 3 (April 26, 1971).

Baker, M. A., Study of the adherence of porcelain enamel to aluminum-use of the electron microscope and electron microprobe, Proc. Porcelain Enamel Institute Technical Forum, University of Illinois, Urbana, Ill., Oct. 7–9, 1970, 32, 48–51 (Porcelain Enamel Institute, Washington, D.C., 1971).

Ballard, D. B., Yakowitz, H., Goldstein, J. I., Study of metal in the lunar soil, Proc. 4th Annual Scanning Electron Microscope Symp., ITT Research Institute, Chicago, Ill., April 29, 1971, Part 1, 169–176 (April 29, 1971).

Brower, W. S., Jr., Parker, H. S., Growth of single crystal cuprous oxide, J. Crystal Growth **8,** 227–229 (1971).

Bullis, W. M., Editor, Methods of measurement for semiconductor materials, process control, and devices, Quarterly Report July 1 to September 30, 1970, Nat. Bur. Stand. (U.S.), Tech, Note 571, 58 pages (Apr. 1971) 60 cents, SD Catalog No. C13.46:571.

Burdick, M. D., An instrumental procedure for evaluating adherence of porcelain enamel cover coats direct-to-steel, Proc. Porcelain Enamel Institute Technical Forum, University of Illinois,

Urbana, Ill., Oct. 7–9, 1970, 32, 160–167 (Porcelain Enamel Institute, Washington, D.C., 1971).
Carter, R. S., Editor, Reactor Radiation Division: Annual Progress Report for the Period Ending October 31, 1970, Nat. Bur. Stand. (U.S.), Tech. Note 567, 66 pages (Mar. 1971) 70 cents, SD Catalog No. C13.46:567.
Costrell, L., CAMAC instrumentation system-introduction and general description, (Proc. Nuclear Science Symp., New York, N.Y., Nov. 6, 1970), IEEE Trans. Nucl. Sci. **NS–18,** No. 2, 1–6 (April 1971).
Currie, L. A., Rodriguez-Pasqués, R. H., Photonuclear tritium yields at 90 MeV, Nucl. Phys. **A157,** 49–60 (1970).
Danos, M., Gillet, V., Evidence for quartet structure in medium and heavy nuclei, Physics Letters **34B,** No. 1, 24–26 (Jan. 18, 1971).
Dikkers, R. D., Marshall, R. D., Thom, H. C. S., Hurricane Camille—August 1969, Nat. Bur. Stand. (U.S.), Tech. Note 569, 71 pages (Mar. 1971) 70 cents, SD Catalog No. C.13.46:569.
DiMarzio, E. A., Guttman, C. M., Separation by flow and its application to gel permeation chromatography, J. Chromatog. **55,** 83–97 (1971).
Dziuba, R. F., Dunfee, B. L., Resistive voltage-ratio standard and measuring circuit, IEEE Trans. Instr. Meas. **IM–19,** No. 4, 266–277 (Nov. 1970).
Engen, G. F., A new method of characterizing amplifier noise performance, IEEE Trans. Instr. Meas. **IM–19,** No. 4, 344–349 (Nov. 1970).
Fickett, F. R., Clark, A. F., Longitudinal magnetoresistance anomalies, J. Appl. Phys. **42,** No. 1, 217–219 (Jan. 1971).
Franklin, A. D., Bennett, H. S., Editors, ARPA–NBS program of research on high temperature materials and laser materials, Reporting Period July 1 to December 31, 1970, Nat. Bur. Stand. (U.S.), Tech. Note 574, 44 pages (May 1971) 50 cents, SD Catalog No. C13.46:574.
Gadzuk, J. W., Plummer, E. W., Energy distribution for thermal field emission, Phys. Rev. B. **3,** No. 7, 2125–2129 (April 1, 1971).
Gadzuk, J. W., Plummer, E. W., Hot-hole-electron cascades in field emission from metals, Phys. Rev. Letters **26,** No. 2, 92–95 (Jan. 11, 1971).
Herron, J. T., Huie, R. E., Mass spectrometric studies of the reactions of singlet oxygen in the gas phase, Ann. N.Y. Acad. Sci. **171,** Article 1, 229–238 (Oct. 15, 1970).
Hustvedt, E. H., Conference Coordinator, Friend, M. L., Editor, Proceedings of joint meeting of government operations research users and producers, held at the National Bureau of Standards, Gaithersburg, Maryland, June 5–6, 1969, Nat. Bur. Stand. (U.S.), Spec. Publ. 347, 164 pages (May 1971) $1.25, SD Catalog No. C13.10:347.
Klein, M., Hanley, H. J. M., The *m*–6–8 potential function, J. Chem. Phys. **53,** No. 12, 4722–4723 (Dec. 15, 1970).
Laufer, A. H., Low-temperature chromatographic determination of ketene and methyl ketene, J. Chromatogr. Sci. **8,** 677–678 (Nov. 1970).
McDonald, D. G., Evenson, K. M., Wells, J. S., Cupp, J. D., High-frequency limit of the Josephson effect, J. Appl. Phys. **42,** No. 1, 179–181 (Jan. 1971).
Matarrese, L. M., Evenson, K. M., Improved coupling to infrared whisker diodes by use of antenna theory, Appl. Phys. Letters **17,** No. 1, 8–10 (July 1, 1970).
Moore, C. E., Annual report on spectroscopy, July 1, 1969–June 30, 1970, Bull. Am. Astron. Soc. **3,** No. 1, 154–155 (1971).
Mountain, R. D., Comment on Rotational diffusion of spherical-top molecules in liquids, J. Chem. Phys. **54,** No. 7, 3243 (April 1, 1971).
Nimeroff, I., Color-match classification by variable parameters, Color. Engr. **9,** No. 2, 13–17 (March–April 1971).
Olson, W. B., Papousek, D., High-resolution infrared spectra of ethanelike molecules and the barrier to internal rotation: The ν_9, ν_{13} band of dimethylacetylene, J. Mol. Spectry. **37,** No. 3, 527–534 (March 1971).
Pecker, J. C., Thomas, R. N., Personal libraries and publication policies, Atoms **25,** 37–38 (Jan. 1970).
Phucas, C. B., Technical Standards Coordinator, Package quantities of instant nonfat dry milk, Nat. Bur. Stand. (U.S.), Prod. Stand. 37–70, 9 pages (April 1971) 10 cents, SD Catalog No. C13.20/2:37–70.
Ramboz, J. D., A link-compensated ratio transformer bridge, Rev. Sci. Instr. **42,** No. 4, 522–524 (April 1971).
Ruegg, F. C., A circuit which expands the count storage capacity of a multichannel analyzer, Nucl. Instr. Methods **92,** 7–11, (1971).
Scott, W. W., Jr., New coaxial RF-DC ammeter, IEEE Trans. Instr. Meas. **IM–19,** No. 4, 318–323 (Nov. 1970).
Sixsmith, H., Giarratano, P., A miniature centrifugal pump, Rev. Sci. Instr. **41,** No. 11, 1570–1573 (Nov. 1970).
Tate, E. L., Improving library collections by weeding, Proc. U.S. Department of Interior, 1970 Departmental Library Workshop, Washington, D.C., Sept. 28–Oct. 2, 1970, pp. 54–61 (U.S. Department of Interior Office of Library Services, Washington, D.C., Feb. 1971).
Van Blerkom, D., Hummer, D. G., The normalized on-the-spot approximation for line transfer problems, J. Quant. Spectrosc. Radiat. Transfer Note 9, No. 11, 1567–1571 (Nov. 1969).
Wachtman, J. B., Jr., Standard materials for measurements on ceramics, Am. Ceram. Soc. Bull. **50,** No. 3, 242–247 (March 1971).
Wait, D. F., The precision measurement of noise temperature of mismatched noise generators, IEEE Trans. Microwave Theory Tech. **MTT–18,** No. 10, 715–724 (Oct. 1970).
Wallace, B., Brown, W. E., Stoichiometric composition of whitlockite, J. Dental Res. **50,** No. 2, 343–346 (March–April 1971).
Woelfel, J. B., Paffenbarger, G. C., Expanding and shrinking 7-year-old dentures: report of cases, J. Am. Dental Assoc. **81,** No. 6, 1342–1348 (December 1970).
Zimmerman, J. E., Recent Developments in superconducting devices, J. Appl Phys. **42,** No. 1, 30–71 (Jan. 1971).

**Publications for which a price is indicated are available by purchase from the Superintendent of Documents, U.S. Government Printing Office, Washington, D.C. 20402 (foreign postage, one-fourth additional). The NBS non-periodical series are also available from the National Technical Information Service (NTIS), Springfield, Va. 22151, which was formerly the Clearinghouse. Reprints from outside journals and the NBS Journal of Research may often be obtained directly from the authors.*

U.S. GOVERNMENT PRINTING OFFICE : 1971 OL—429-270